UCL
Université catholique de Louvain

de Duve INSTITUTE

Tumor-specific CD8 T cells in a primary human breast carcinoma: a detailed analysis

David Schröder

Thesis submitted in candidature for the degree of PhD in Biomedical and Pharmaceutical Sciences

Promoter: Professor Pierre Coulie

2016

President of the Jury:

Professor Thomas Michiels, PhD
de Duve Institute
Université catholique de Louvain

Members of the Jury:

Professor Jean-Pascal Machiels, MD, PhD
Cliniques Universitaires Saint-Luc
Université catholique de Louvain

Professor Pierre van der Bruggen, PhD
Ludwig Institute for Cancer Research
de Duve Institute
Université catholique de Louvain

Javier Carrasco, MD, PhD
Grand Hôpital de Charleroi

Nicolas van Baren, MD, PhD
Ludwig Institute for Cancer Research
Université catholique de Louvain

External Member:
Karen Willard-Gallo, PhD
Molecular Immunology Unit
Jules Bordet Institute

Promoter:

Professor Pierre Coulie, MD, PhD
de Duve Institute
Université catholique de Louvain

The only place success comes before work is in the dictionary.

Vince Lombard

Diese Doktorarbeit ist Monique gewidmet, meiner Heldin der Wirklichkeit.

Remerciements, Danksagungen

Je tiens à remercier particulièrement le Pr Pierre Coulie pour son immense aide, son support et pour ses conseils prodigués tout le long de ma thèse. Il a été un véritable pilier de ma recherche.

C'est grâce au Dr Javier Carrasco que j'ai pu gouter à nouveau à la recherche et je le remercie beaucoup pour ça. Il a suivi avec le Pr Coulie ma thèse de près et ces deux personnes ont été d'un grand soutien pour moi. J'apprécie fortement leur rigueur, leur sens critique, leur créativité et leur dévouement pour la science.

L'aide essentielle du Pr Martine Berlière et du Pr Christine Galant ne se manifeste pas directement dans ma thèse, mais leur aide et leur motivation ont rendu possible l'accès au matériel tumoral au long du projet de façon efficace. Je les remercie beaucoup.

Je remercie le Pr Jean-Pascal Machiels pour son support, ainsi que celui de son équipe (Pr François Duhoux, …).

Je suis également très reconnaissant envers le Dr Jean-Luc Canon pour son soutien et son enthousiasme concernant ma thèse. Je n'oublierai pas non plus nos discussions lors des congrès à Paris ou à San Antonio.

I want to thank Karen Willard-Gallo for her point of view of tumor immunology and the interesting discussion during the private thesis defense.

Je remercie le Dr Nicolas van Baren pour son expertise, son aide, sa convivialité et son humour.

Pour comprendre le futur, il faut connaître le passé. Outre ses critiques, ses suggestions et le covoiturage Bruxelles-Louvain-la-Neuve, le Pr Pierre van der Bruggen m'a expliqué le passé de l'institut. Merci pour de m'avoir fait découvrir ce côté historique.

Je remercie aussi beaucoup Danièle Godelaine. Nos discussions variées (mon projet, l'histoire de l'institut, la science, la médicine et la vie en général) ont été très enrichissantes.

Je remercie le Pr Thomas Michiels d'avoir accepté de présider mon jury de thèse.

Je remercie le Dr Paul Delrée et Pascal Vannuffel de l'institut de Pathologie et de Génétique (IPG) pour leur aide respective dans l'obtention des échantillons tumoraux et dans l'analyse d'instabilité microsatellites des tumeurs.

Au jour le jour, le travail avec mes collègues était du pur bonheur. Merci à vous, l'équipe de choc ! Ce fut un grand plaisir de travailler avec vous. Merci Nicolas pour les heures passées, et parfois tardives, au cell sorter. Merci Gérald pour

l'initiation à la culture cellulaire et la biologie moléculaire, ta patience avec ce 'bleu', tes conseils et tes critiques. Merci Orian pour ton aide à la console et ton expertise de biologie moléculaire. Et merci de m'avoir appris davantage sur la France et les rues à sens unique de Bruxelles. Merci Nathalie pour ton travail et ta persévérance là où le travail s'avérait répétitif ou difficile. J'en suis très reconnaissant. Merci Kevin pour ton bon travail. Vive les T et mort à l'hypoxie tumorale. Thanks Stine for your help with the MLPC and our discussions. It was a pleasure to work with you. Merci Catherine pour ton humour, ta franchise, tes bons conseils et ta rigueur dans la gérance d'Hapicel. Je n'ai perdu aucun clone congelé et tu sais combien nous en avons congelés. Merci Aurélie pour tout ton travail (IHC, PCR, quantification de cellules), ton sourire et ton dévouement. Merci Marjorie pour l'initiation aux techniques (PCR, la coupe de tissue congelé etc.) et tes blagues. Merci Tif' pour ton encouragement, tes questions et tes suggestions. Merci Suzanne pour ton aide le long de ces quatre années. Merci Marie-Sophie pour ta bonne humeur, ton sourire et ta confiance dans l'électroporation des B-EBV. Merci Charlotte pour ton encouragement et pour les bonbons. Merci Melissa pour ton aide à l'IHC. Merci Florence pour ton amitié, ton soutien dans la dernière ligne droite (dîner) et les discussions dans le bus. Danke Delia für die Witze und Lacher auf der Arbeit. Merci René pour les discussions à table, dans les couloirs, dans la voiture ou le bus entre Bruxelles et LLN.

Il y a encore plein d'autres personnes qui m'ont aidé dans mon projet. Je remercie respectivement Dr Aurore Lafosse, Vincent Stroobant et Didier Colau pour l'obtention de tissu mammaire sain, la synthèse de peptides et de tetramers. De plus, je pense à l'équipe de Sophie Lucas (Julie, Olivier, …), l'équipe de Pierre van der Bruggen (Nathlie, Claude, …), l'équipe de Benoit Van den Eynde (Nathalie, Wenbin, Luc, Joanna, …), l'équipe de Miikka Vikkula (Raphaël Helaërs, Pascal Brouillard, …) et l'équipe de support de l'institut Ludwig.

Christine, du hast während dieser vier Jahre viel Geduld aufbringen müssen für deinen zerstreuten David. Danke für deine Geduld, deine Kraft, deine Lacher und Hilfe. Mama und Papa, ihr habt mir viel beigebracht und auf den Weg mitgegeben um eine Doktorarbeit abzuschließen. Ich danke euch sehr dafür und für eure Unterstützung während der vier Jahre. Am Ende wurde es schwer, doch Anne und Guillaume haben sich extra um mich gekümmert. Danke vielmals für die gemeinsamen Abendessen und das WE im Endsprint. Danke Philipp und Freunde, dass ihr mich von meiner Arbeit abgelenkt habt und mich wieder auf den Boden der Realität brachtet.

Table of contents

Table of illustrations

List of abbreviations

APC	Allophycocyanin
APOBEC	Apolipoprotein B mRNA editing enzyme, catalytic polypeptide
CAR	Chimeric antigen receptor
CD	Cluster of differentiation
CDR3	Complementarity determining region 3
CTLA-4	Cytotoxic T lymphocyte-associated antigen 4
CTL	Cytolytic T lymphocyte
DC	Dendritic cell
DCIS	Ductal carcinoma *in situ*
EBV-B	EBV-transformed B cells
ER	Estrogen receptor
FACS	Fluorescence-activated cell sorting
FITC	Fluorescein isothiocyanate
GFP	Green fluorescent protein
GM-CSF	Granulocyte-macrophage colony-stimulating factor
HER2	Human epidermal growth factor receptor 2
HEV	High endothelial venule
HLA	Human leukocyte antigen
HPV	Human papillomavirus
hTERT	Human telomerase reverse transcriptase
IHC	Immunohistochemistry
IFNγ	Interferon gamma
IL	Interleukin
Indel	Small insertion or deletion
MHC	Major histocompatibility complex
MLPC	Mixed lymphocyte-peptide culture
MMR	DNA mismatch repair
MSI	Microsatellite instability
mTOR	Mammalian target of rapamycin
NK cells	Natural killer cells
NSCLC	Non-small cell lung cancer
PBMC	Peripheral blood mononuclear cells

PD-1	Programmed death-1
PD-L1	Programmed death-ligand 1
PE	Phycoerythrin
PI3K	Phosphoinositide 3-kinase
PR	Progesterone receptor
RT-PCR	Reverse transcription polymerase chain reaction
RT-qPCR	Real-time quantitative polymerase chain reaction
shRNA	Short hairpin RNA
SNV	Single nucleotide variant
STAT1	Signal transducer and activator of transcription 1
TCGA	The Cancer Genome Atlas
TCR	T cell receptor
TCRBV repertoire	Repertoire of the variable part of the TCR beta chain
TILs	Tumor-infiltrating lymphocytes
TLS	Tertiary lymphoid structures
TN	Triple-negative
TNFα	Tumor necrosis factor alpha
UTR	Untranslated region
WES	Whole-exome sequencing

1 Introduction

1.1 Cancer immunotherapy

Cancer immunotherapy is gaining momentum in routine oncology practice following the development of blocking anti-CTLA-4 and anti-PD-1 antibodies. Initially, these drugs showed a significant antitumor activity in a previously hard-to-treat cancer, metastatic melanoma. The anti-CTLA-4 antibody ipilimumab increased the survival rate in patients with advanced melanoma: patients receiving ipilimumab plus dacarbazine had a survival rate at 3 years of 21% versus 12% for those receiving dacarbazine alone (standard therapy)[1]. Anti-PD-1 antibodies such as pembrolizumab were also tested in patients with advanced melanoma and proved to be more effective and less toxic than ipilimumab (estimated 1-year survival rates of >68% with pembrolizumab versus 58% with ipilimumab)[2]. With either of these two drugs, several patients displayed long-lasting antitumor responses, observed neither with conventional treatments except surgery, nor with targeted treatments such as $BRAF^{V600E}$ inhibitors. These clinical studies were then extended to patients with other solid tumors. Anti-CTLA-4 antibodies showed no or small benefit[3], while anti-PD-1 and anti-PD-L1 antibodies were efficient drugs for non-small cell lung cancer (NSCLC), renal cell carcinoma, bladder cancer, Merkel cell carcinoma and mismatch repair-deficient digestive cancer[3-5].

Immunostimulatory antibodies such as the blocking anti-CTLA-4 and anti-PD-1 antibodies have brought cancer immunotherapy in the limelight and stimulated the interest of many investigators and pharmaceutical companies. We only start to successfully manipulating the immune system to target cancer, with the prospect of testing a wide set of combinations between immunostimulatory antibodies and other modalities of cancer immunotherapy, including adoptive T cell therapy and immunization against tumor-specific antigens.

1.1.1 Scientific foundations for immunotherapy in cancer

The major scientific foundations for cancer immunotherapy are the concepts that tumor cells bear antigens that can be recognized by tumor-specific T cells, that many cancer patients spontaneously mount such T cell responses, and that T cell activity can be enhanced *in vivo* by antibodies that recognize inhibitory or costimulatory receptors present on the T cell surface.

Tumor cells bear antigens that can be recognized by T cells, notably cytolytic CD8 T lymphocytes (CTL). These tumor antigens are peptides of 8-12 amino acids, presented by HLA class I molecules. Five different classes of tumor antigens have been described. The tumor antigens that are encoded by somatic non-synonymous mutations, cancer-germline genes (*e.g. MAGEC2*) or oncogenic viruses (*e.g.* HPV-infected head and neck cancer) have high tumor specificity. Some tissue-specific antigens (*e.g.* Melan-A present in melanomas and melanocytes) and overexpressed antigens (*e.g.* HER2) are tumor antigens of lower tumor specificity[6]. They might be called tumor-associated antigens. Thus several genetic mechanisms underlie the antigenicity of tumor cells.

Tumor-specific T cells can be found in the blood or in the tumor of patients with cancer. Naive T cells against a given HLA-peptide combination can be detected in the blood at frequencies around 4 $x10^{-7}$ of the CD8 T cells[7]. However tumor-specific T cells can be detected in the blood or tumors of melanoma patients, and more rarely of patients with other types of cancer, at much higher frequencies, indicating that these T cells have been clonally amplified. Moreover such tumor-specific T cells present in cancer patients can be activated *in vitro* without providing the costimulatory signals that are required to prime naive T cells. Collectively these results indicate that antitumor T cell responses occur spontaneously in at least some cancer patients. For example we studied antitumor T cells present in the blood of 6 patients with advanced melanoma. Several clones of tumor-specific CD8 T cells were found at frequencies of 6 x 10^{-5} to 2 x 10^{-3} among blood CD8 T cells[8,9]. This is 100-10,000 times higher than the frequency of naive CD8 T cells against a given HLA-peptide combination and demonstrates T cell amplification. An extensive analysis of one of these patients showed that the antitumor T cell population was polyclonal. Several anti-MAGEC2 clonotypes were present in the blood at frequencies of 2 x 10^{-6} to 4 x 10^{-5} among CD8 T cells (~10-100 times amplification)[10]. Most anti-MAGEC2 clonotypes were also found in a regressing cutaneous metastasis, where they were enriched ~10-100 times when compared to the blood (frequencies of 3 x 10^{-4} to 10^{-3} among all tumor-infiltrating CD8 T cells). Recently, amplified tumor-specifc T cells were also found in metastases of gastro-intestinal carcinomas (9 x 10^{-5} to 1 x 10^{-2} among all T cells)[11].

That at least some cancer patients spontaneously mount T cell responses against their tumor indicates that these tumors are not only antigenic, but also

immunogenic. The immunogenicity of human tumors is an important parameter for cancer immunotherapy because immunostimulatory antibodies blocking CTLA-4 are expected to favor T cell priming of naive T cells, while those that target the PD-1 pathway are expected to boost existing T cell responses.

Tumeh and colleagues used immunohistochemistry (IHC) and immunofluoresence to study immune parameters in tumor samples from patients with metastatic melanoma that responded or not to a blocking anti-PD-1 antibody (pembrolizumab)[12]. In patients who responded to pembrolizumab, the number of CD8 T cells increased in the invasive tumor margin and within the tumor parenchyma compared with the pre-treatment situation. This increase was not observed in the tumors of patients who did not respond to the treatment. The CD8 T cells in tumors of responders displayed increased staining for the proliferation marker Ki67 and for granzyme B. Thus the proliferation of potentially cytolytic CD8 T cells suggests an antitumor activity of CD8 T cells during therapy. Before treatment, CD8 TILs were already more numerous in the tumors of responders than in those of non-responders. PD-1^+ and PD-$L1^+$ cells were also enriched in tumors of responders. PD-1 (programmed death 1) is an inhibitory receptor expressed on activated T cells[13] and most tumor- or blood-derived tumor-specific CD8 T cells express PD-1 in patients with metastatic melanoma[14,15]. In the pretreatment tumors analysed by Tumeh *et al.*, PD-1 staining was present mostly on CD8 T cells, PD-L1 staining on tumor cells and stromal cells and PD-1^+ and PD-$L1^+$ cells were found in close proximity. PD-L1 expression was likely induced by IFNγ, which was secreted by CD8 T cells because CD8 TILs were stained for pSTAT1, more in responders than in non-responders. These observations suggest that blocking the PD-1 pathway is clinically effective in patients that have already mounted an antitumor T cell response. CD8 T cells are probably activated *in situ*, proliferate, express PD-1 and secrete IFNγ before an inhibition by IFNγ-induced PD-$L1^+$ neighboring cells (tumor or stromal cells). The anti-PD-1 antibody blocks this inhibition, resulting in tumor regression. The results do not exclude that new antitumor T cells could be primed during therapy.

Finally, the present successes of cancer immunotherapy owe much to the discovery of T cell surface receptors that inhibit T cell activation.

1.2 Breast cancer: Immunology and immunotherapy

1.2.1 Breast cancer classification

Most malign breast tumors are carcinomas, the others are sarcomas and lymphomas. There are several types of breast carcinomas. Ductal (or 'no special type', NST) is the most frequent type (70-80%) followed by 'special' types such as lobular, medullary, mucinous and tubular carcinomas[16].

This histopathological classification is complemented by the detection of estrogen receptor (ER), progesterone receptor (PR) and human epidermal growth factor receptor 2 (HER2). About 75-80% of breast carcinomas express the ER and PR. HER2 overexpression occurs in 15-20% of breast carcinomas and is caused mainly by the amplification of the encoding gene, *ERBB2*. All these receptors mediate tumor cell proliferation[17]. Therefore, patients with hormone receptor-positive or HER2-positive tumors are treated with hormone therapy or receptor-blocking anti-HER2 antibodies, respectively. Based on the expression of these receptors, breast carcinomas are categorized in 3 groups (Figure 1-1):

- ER^+ tumors (most of them are also PR^+)
- $HER2^+$ tumors (overexpression of HER2)
- Triple-negative tumors (TN) ($ER^-PR^-HER2^-$)

Patients with ER^+ tumors have a heterogeneous prognosis: poorly differentiated ER^+ tumors are agressive tumors while well differentiated ones have a good prognosis. $HER2^+$ and triple-negative tumors are often poorly differentiated and agressive. The triple-negative tumors are nowadays the tumors with the worst prognosis.

Within the above-mentioned subtypes, breast tumors remain heterogeneous in their biology, prognosis and response to treatment. Therefore, other classifications have been proposed, of which the most widely used is the 'intrinsic' subtype classification. Four 'intrinsic subtypes' (Luminal A, Luminal B, HER2-overexpressing and Basal-like) were initially defined using the expression profiles of a set of 496 'intrinsic' genes[18]. There are partial overlaps between the intrinsic subtypes, ER-PR-HER2 types and tumor grade (differentiation) (Figure 1-1). Luminal tumors are ER^+HER2^- and of 2 subtypes. Luminal A tumors are well differentiated (low tumor grade) or with a low tumor cell proliferation (low

proportion of Ki67^{+} tumor cells). Luminal B tumors are poorly differentiated (high tumor grade) or with high tumor cell proliferation (high proportion of Ki67^{+} tumor cells). HER2-overexpressing tumors are HER2^{+}ER$^{+/-}$. Basal-like tumors are the triple-negative tumors. The overlap of the classification based on IHC with that based on gene expression is not perfect: luminal tumors with intermediate tumor grade or proliferation can not be assigned to luminal A or luminal B subtype without gene expression analysis. The overlap is particularly imperfect for TN/basal-like tumor: 70-80% of TN tumors are basal-like tumors and up to 45% of basal-like tumors are not TN tumors[19].

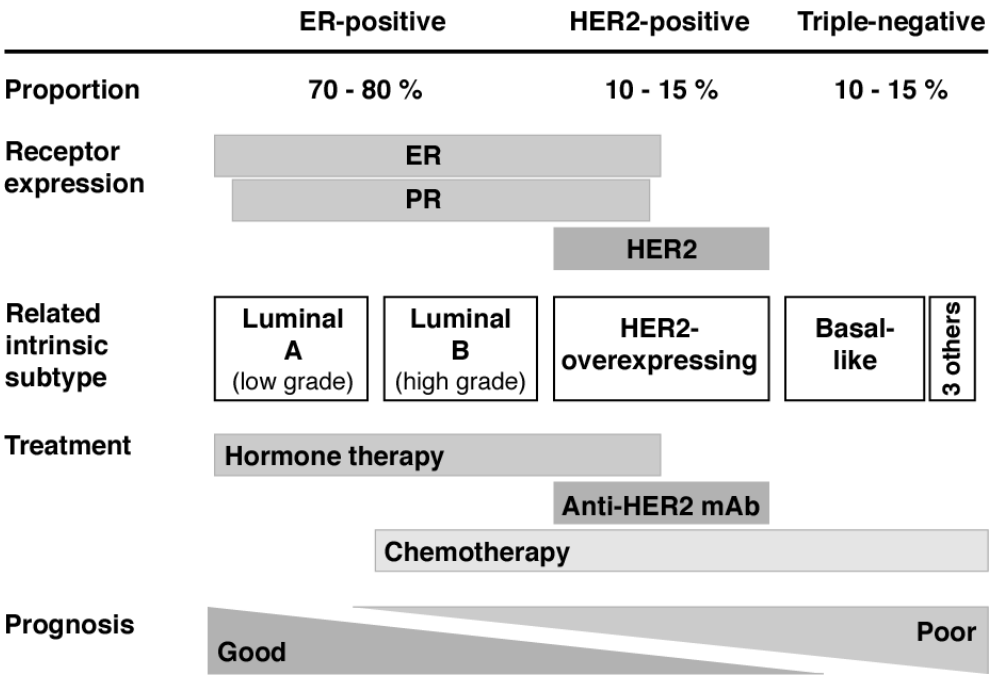

Figure 1-1. Classification of breast carcinomas.

Simplified version of the current classification of breast carcinomas. HER2-targeted therapies are mostly anti-HER2 monocolonal antibodies such as trastuzumab and pertuzumab. Figure adapted from http://www.pathophys.org/breast-cancer/[20]. Additional data from Dawson *et al.*, Carey *et al.* and Sotiriou and Pusztai[19,21,22].

1.2.2 Immune parameters of breast carcinomas

1.2.2.1 Lymphocyte infiltration

Ruffel *et al.* analysed by flow cytometry the composition of leukocytes in 14 untreated primary breast carcinomas. T cells ($CD3^+$) were the most frequent hematopoietic cells ($CD45^+$). On average, around 25% of leukocytes were $CD8^+$ T cells and around 40% were $CD4^+$ T cells. The ratio CD8/CD4 varied from 0.25 to 1.6 with a mean of 0.6. B cells ($CD19^+CD20^+$), macrophages ($CD14^{hi}CD11b^+HLA\text{-}DR^+$), dendritic cells ($CD14^{lo/-}CD11c^+HLA\text{-}DR^+$) and NK cells ($CD3^-CD56^+NKG2D^+$) were present at frequencies around 9%, 4%, 1% and 1%, respectively. Basophils, neutrophils or eosinophils represented ≤1% of the infiltrating leukocytes[23]. Similar results were obtained in another study, with 35 previously untreated primary breast tumors[24].

Many reports of the prognostic value of lymphocyte infiltration in primary breast tumors have been published since 1971, with conflicting results in the early studies[25,26]. Since 2010, several large-scale studies have observed a positive association between lymphocyte infiltration and clinical outcome in TN primary breast carcinomas. These studies have evaluated tumor-infiltrating lymphocytes (TILs) on hematoxylin and eosin (HE)-stained tumor sections. Most studies used the criteria of Denkert *et al.*[27] who defined intratumoral TILs as mononuclear cells within the tumor parenchyma or in direct contact to tumor cells. Stromal TILs were defined as mononuclear cells within the tumor stroma and without direct contact to tumor cells. Strictly speaking, these infiltrating 'lymphocyte-like' mononuclear cells are not necessarily lymphocytes[28]. Intratumoral TILs were quantified as the percentage of tumor area that is occupied by TILs, while stromal TILS were quantified as the percentage of stroma area that is covered by TILs. This quantification is robust and independent TIL evaluation by two pathologists is strongly correlated[29-32]. In most recent studies, only the stromal TILs are quantified because intratumoral TILs were shown to be correlated with stromal TILs and did not provide additional information. Moreover intratumoral TILs are less abundant and more difficult to detect[28].

Several studies have shown that the presence of TILs in primary breast carcinomas differed between tumor subtypes. TILs are associated with ER-negativity, high tumor grade and high tumor cell proliferation[30,31,33]. TN tumors, which are often high grade tumors, have the highest lymphocyte infiltration followed by $HER2^{+}ER^{-}$ and $HER2^{+}ER^{+}$ tumors, and by $ER^{+}HER2^{-}$ tumors which have the lowest lymphocyte infiltration (Figure 1-2). The variation of TIL numbers within each subtype is considerable.

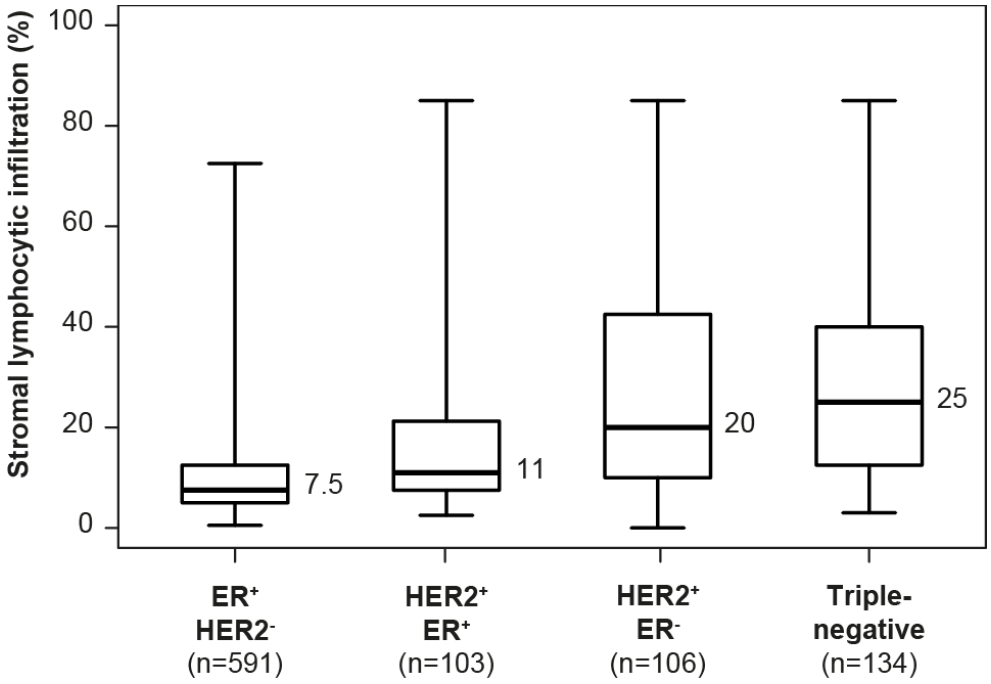

Figure 1-2. TIL distribution according to breast cancer subtypes.

Box-and-whisker plot of the stromal TIL distribution for $ER^{+}HER2^{-}$, $HER2^{+}$ and triple-negative primary tumors. $HER2^{+}$ tumors are divided into ER^{+} and ER^{-} tumors. Median percentage of stromal TILs is highlighted and represented by the inner line of the box. Outer lines of the box are 1rst and 3rd quartile. Minimum and maximum values are represented by the whiskers. Figure adapted from Loi *et al.*[30]

Over the last 3 years, 5 large studies (sample range: 134 to 897 tumors for each study) observed a positive association between TIL number and disease-free survival or overall survival in primary TN tumors, with or without adjuvant chemotherapy[29-31,33,34]. For each 10% increase of TILs in the tumor stroma, a 15-21% reduction of risk of death was observed. The prognostic value of TILs has also been observed for the residual tumor after neoadjuvant chemotherapy. Here also, TILs were positively associated with patient survival[35]. Finally, TILs were associated with response to neoadjuvant chemotherapy: the number of TILs in pre-treatment TN primary tumor biopsies was positively associated with the pathological complete tumor response following neoadjuvant chemotherapy[36].

TILs are predictive for therapy response also in $HER2^+$ primary breast tumors. Two studies showed that TILs in pre-treatment biopsies were associated with response to neoadjuvant therapy (chemotherapy with anti-HER2 antibody)[36,37]. The prognostic value of TILs in $HER2^+$ primary tumors treated with adjuvant therapy is less well documented. TILs were analysed in 4 clinical trials that compared several adjuvant treatment regimens. One study showed a prognostic value of TILs in all treatment arms[33]. In 3 other studies the prognostic value of TILs was limited to one treatment arm[30-32]. The reason for these differences is not understood.

For ER^+HER2^- primary tumors, no correlation has been observed between TILs and clinical outcome[30,31,33].

1.2.2.2 CD8 T cell infiltration

Two of the above-mentioned neoadjuvant trials studied the association of patient survival with T and B cell markers by IHC (CD3ε, CD20) or by RT-qPCR (*CD247* [CD3z], *IGKC, CD8A*)[27,36]. T as well as B cells were predictive for therapy response, and both were associated with TILs.

Whether CD8 T cells are associated with survival of patients with primary breast tumors has been evaluated in two large-scale retrospective analyses using IHC. $CD8\alpha^+$ had a prognostic value in TN and $HER2^+$ tumors or the whole population[38,39]. NK cells are also $CD8\alpha^+$ but their low frequency suggests that the CD8 T cells are associated with survival.

T cell marker	Tumor type	Time of analysis	Outcome	Prognostic value	HR (95% CI)*	Nbr	Ref
sTIL	TN	Before adj. CT	OS	Yes	0.79 (0.67-0.92)	481	[29]
			OS	Yes	0.83 (0.71-0.98)	256	[31]
			OS	Yes	0.85 (0.74-0.99)	199	[33]
			OS	Yes	0.79 (0.72- 0.86)	897	[34]
			DDFS	Yes	0.77 (0.61-0.98)	134	[30]
		After neoadj. CT (residual tumor tissue)	OS	Yes	0.86 (0.75-0.99)	278	[35]
		Before neoadj. CT (tumor biopsy)	pCR	Yes	1.17 (1.06-1.3)	314	[36]
sTIL	$HER2^{+}$	Before adj. CT (anthracycline) or not	OS	Yes	0.82 (0.69-0.96)	112	[33]
		Before adj. CT (anthracycline ± docetaxel)	OS	Trend in anthrac.-only arm	0.39 (0.08-1.94)‡	297	[31]
		Before adj. CT ± trastuzumab	DDFS	Trend in trastuzumab arm	0.82 (0.58-1.16)	209	[30]
		Before adj. CT ± trastuzumab	RFS	Yes in CT-only arm	0.79 (0.70-0.89)	945	[32]
		Before neoadj. CT on tumor (tumor biopsy)	pCR	Yes	1.28 (1.14-1.44)	266	[36]
			pCR	Yes	2.6 (1.26-5.39)**	387	[37]
sTIL	$ER^{+}HER2^{-}$	Before adj. CT	DDFS	No	0.93 (0.74-1.17)†	591	[30]
			OS	No	1.1 (1.0-1.3)†	1,078	[31]
			OS	No	1.01 (0.89-1.15)†	463	[33]

T cell marker	Tumor type	Time of analysis	Outcome	Prognostic value	HR (95% CI)*	Nbr	Ref
CD8	ER^-	Before adj. CT	BCSS	Yes	0.72 (0.62-0.84)$^{\Delta}$	3,591	[38]
	ER^+HER2^+	Before adj. CT	BCSS	Yes	0.73 (0.56-0.96)$^{\Delta}$	772	[38]
	All	Before adj. CT	BCSS	Yes	0.58 (0.41-0.82)$^{\int}$	1,334	[39]

Table 1-1. Summary of the prognostic value of T cell markers in primary breast tumors.

Adj., adjuvant; anthrac., anthracycline; BCSS, breast cancer–specific survival; CT, chemotherapy ; DFS, disease-free survival; DDFS, distant disease-free survival; IHC, immunohistochemistry; MFS, metastasis-free survival; Nbr, number of patients; neoadj., neoadjuvant; OS, overall survival; pCR, pathologic complete response; RFS, recurrence-free survival; sTILs, stromal TILs; 95% CI, 95% confidence intervals;
* for any 10% increase of TILs if not otherwise stated (HR are calculated in a multivariate analysis if not otherwise stated);
** patients are divided in 2 groups: high TIL (>5% of sTILs) or low TIL (≤5% of sTILs);
‡ patients are divided in 2 groups: high TIL (≥50% of sTILs or intratumoral TILs) or low TIL (<50% of sTILs and intratumoral TILs);
† HR of univariate analysis (multivariate analysis not performed);
$^{\Delta}$ cut-off of < or ≥1 stained cell per 0.6 mm tissue core biopsie (tissue microarrays);
$^{\int}$ cut-off of < or ≥2 stained cells per 0.6 mm tissue core biopsie (tissue microarrays)

1.2.2.3 Immune gene signatures

Immune gene signatures have been used in several studies that aimed to characterize the diversity of breast tumors.

Curtis *et al.* analysed the gene expression and copy number profiles of 1992 primary breast tumors (METABRIC tumor set) and identified an immune-related subgroup with favorable clinical outcome[40]. This subgroup (IntClust 4; 17% of the tumors) was characterized by few copy-number aberrations except for frequent deletions in the TCR alpha (*TRA*) and TCR gamma (*TRG*) loci. Deletions in these loci occur during the rearrangement of TCR gene segments in the thymus and are therefore present in mature T cells. Indeed, tumors of IntClust group 4 contained high numbers of TILs. *TRA* and *TRG* deletions were associated with the expression of immune genes, encoding proteins involved in T cell activation and proliferation, cell-mediated cytotoxicity, antigen presentation and leukocyte activation. Interestingly, this immune-related subgroup contained not only TN and $HER2^+$ tumors, but also tumors of all the different intrinsic subtypes.

Dedeurwaerder *et al.* explored the DNA methylation profiles of primary breast tumors[41]. In some tumors they observed a hypomethylation signature of several immune genes and this signature was positively associated with TILs. They assessed the prognostic value of the signature in a public data set of more than 700 untreated breast tumors. The survival analysis was performed with a signature of 55 genes that had the strongest inverse correlation between DNA methylation and gene expression in their own set of tumors. In the public data set, the expression profile of 32 out of the 55 genes had a prognostic value. Within the 32 genes, 11 immune genes were associated with better clinical outcome and high lymphocyte infiltration in the tumors (*CD3D*, *CD3G*, *ICOS*, *LCK*, *UBASH3A*, *CD6*, *LAX1*, *SIT1*, *CCL5*, *HCLS1*, *CD79B*). DNA methylation and gene expression analyses of T and B cells extracted from tumors or from blood showed that all 11 and 7 of these 11 genes were associated with T cells and B cells, respectively. This indicates that T cells are the predominant lymphocyte population that infiltrates breast tumors. Finally, a subtype-specific survival analysis showed that some of the 11 genes had a prognostic value in the different intrinsic subtypes. Ten out of the 11 genes were prognostic in luminal B tumors, 5 in basal-like and HER2-overexpressing tumors and none in luminal A tumors. In summary, this work showed a prognostic value of lymphocytes, mainly T cells, in basal-like, HER2-overexpressing and luminal B breast tumor subtypes.

Finak *et al.* focused on the tumor stroma, with gene expression analyses on laser capture microdissected stromal regions of 53 invasive primary breast carcinomas[42]. They identified 3 groups of tumors with different gene expression profiles. These 3 groups of tumors had different clinical outcomes. The signature of the group with a good prognosis (18 out of 53 samples) was enriched in genes involved in Th1 function, cytotoxic activity (*GZMA*, *GZMB*) and antigen processing. IHC indicated high infiltration of $CD8\alpha^+$ and $CD3z^+$ cells in the stroma of tumors of this group and low infiltration in that of tumors with a poor prognosis. Like in Curtis *et al.*, the good prognosis immune-related group was not enriched with TN tumors. On the contrary, all 6 TN tumors were in the poor-outcome group, whereas the good-outcome group contained ER^+HER2^- (13 out of 18) and $HER2^+$ tumors (5 out of 18).

These studies showed by different methods that T cells have a prognostic value in primary breast tumors. Noteworthly, immune gene signatures show signs of T cell

activation and cytotoxic activity in tumors with high T cell infiltration. Surprisingly, tumors with immune gene signatures were not necessarily TN or $HER2^+$ tumors.

A fourth study focused on TN tumors and identified a 'basal-like immune-activated' gene expression profile[43]. This subtype had the best prognosis and showed upregulation of genes related to B cells, T cells and NK cells. This result illustrates the heterogeneity that is still present within a breast tumor subtype.

1.2.2.4 Tertiary lymphoid structures

TILs are associated with tertiary lymphoid structures (TLS) in breast carcinoma as well as in other types of tumors[44,45]. TLS are organized immune cell clusters, which are observed in non-lymphoid tissues with chronic inflammation (infection, autoimmune disease, chronic graft rejection disease and tumors). TLS have been observed in breast cancer, colo-rectal cancer, metastatic melanoma and non-small cell lung cancer (NSCLC)[44,46]. The architecture of TLS resembles lymphoid follicles of lymph nodes. B cells, follicular DCs and T follicular helper cells constitute follicles with surrounding T cells, mature DC and high endothelial venules (HEV). TLS are thought to host immune responses to persistent antigens. However, no tumor-specific T cell responses have been demonstrated in tumor-associated TLS.

No study had analysed directly the prognostic or predictive values of IHC-characterized TLS in breast cancer. Gu-Trantien *et al.* focused on T follicular helper cells within the follicles and found a T follicular helper signature to be of prognostic value in previously untreated primary breast cancer[24]. Martinet *et al.* analysed the presence of HEV by IHC (stained with the MECA-79 mAb)[45]. Ninety-four out of 127 (74%) primary breast tumors contained MECA-79^+ vessels at very different densities: from less than 0.01 to more than 1 HEV per mm^2 of tumor tissue. Tumors within the highest tercile of HEV density were defined as high HEV density tumors. They contained high numbers of infiltrating CD4 T, CD8 T and B cells, as assessed by IHC and flow cytometry. In their retrospective analysis of nearly 150 primary breast tumors stained with MECA-79, they observed a prognostic value of high HEV density in the tumor.

These data suggest that an organized peritumoral adaptive immune response is associated with a favorable clinical outcome in breast cancer.

1.2.2.5 PD-L1 expression

PD-L1 expression in tumors is another interesting marker of immune response. PD-L1 is expressed on a wide range of hematopoietic and non-hematopoietic cells and this expression can also be stimulated by various proinflammatory cytokines, such as IFNγ[47,48]. Tumor cells can also express PD-L1 constitutively. Amplification of its gene, *CD274*, has been observed in Hodgkin lymphomas, diffuse large B-cell lymmphome (DLBCL) and in gastric adenocarcinomas, mostly in the EBV^+ subtype[49-51]. Chromosomic alterations at 9p24.1 lead to amplification of genes *CD274*, *PDCD1LG2* (encoding PD-L2) and *JAK2,* with associated increased mRNA expression[49,51]. *CD274* overexpression can also result from alterations in the 3'UTR of the gene, which leads to truncated 3'UTR and stabilization of the *CD274* transcripts[52].

PD-L1 binds to the inhibitory receptor PD-1 expressed on activated T cells, reducing T cell functions. The PD-1/PD-L1 axis modulates T cell responses and prevents excessive and deleterious T cell activity. In a tumor, $PD\text{-}L1^+$ cells could therefore decrease antitumor T cell responses. This is the hypothesis that led to the blocking anti-PD-1 or anti-PD-L1 antibodies in cancer immunotherapy.

The analysis of PD-L1 expression is interesting for two reasons. First, it has been associated with clinical reponse to these blocking antibodies and could help to predict patients who benefit most from these drugs[53]. Second, PD-L1 expression can be the sign of an ongoing antitumor immune response. Activated antitumor T cells can secrete IFNγ in the tumor microenvironment, leading to the expression of PD-L1 on tumor and stromal cells[12]. This is probably the explanation for the positive prognostic value of PD-L1 expression in tumor samples of NSCLC, metastatic melanoma and Merkel cell carcinoma patients[13].

PD-L1 expression is positively associated with a favorable clinical outcome in breast cancer. In one study, patients with PD-L1-expressing tumors had a longer recurrence-free survival[54]. In a second study, Denkert *et al.* observed that *CD274* expression in the pre-treatment tumor biopsies of $HER2^+$ and TN primary tumors predicted complete pathological response following neodjuvant chemotherapy[36]. In both studies, *CD274* expression was correlated with T and B cell markers. The expression of PD-L1 in the second study ($HER2^+$ and TN tumors) could be due to IFNγ-secreting T cells as gene *CD274* was co-expressed with two other IFNγ-

regulated genes (*IDO1* and *CXCL9*). Thus, PD-L1 gene expression could be a consequence of the presence of recently activated tumor-infiltrating T cells.

At the protein level, PD-L1$^+$ cells were mostly observed in TN tumors[55]. In addition, PD-L1$^+$ cells were associated with CD8$^+$ cells[55,56]. However, an IHC analysis of nearly 4,000 primary breast tumors did not confirm yet supported the prognostic value of PD-L1 expression[55].

An amplification of *CD274* is a rare event in primary breast cancer (5 tumors out of 1980)[55]. It occurs almost exclusively in a subset (<2%) of basal-like tumors. Compared to the high copy number gain resulting from gene amplification, small copy number gains of *CD274* are more frequent, mostly in basal-like tumors (~16% of basal-like tumors, ~3% of all breast tumors). The level of expression of gene *CD274* is expectedly correlated with its copy number status[55]. In breast cancer the consequences of *CD274* copy number gains and upregulated *CD274* expression by 3'UTR disruption are not documented.

Another mechanism can modify PD-L1 gene expression in breast tumors. Mittendorf *et al.* showed that the PI3K/AKT/mTOR pathway upregulated PD-L1 expression in TN primary tumors. *PTEN* knockdown by shRNA led to higher PD-L1 cell surface expression. Inhibition of the pathway by an AKT inhibitor or the mTOR inhibitor rapamycin decreased PD-L1 expression[56]. Interestingly, around half of the PD-L1$^+$ TN tumors were not stained for PTEN in IHC, suggesting that PTEN loss could be responsible for PD-L1 expression in some breast tumors (early-stage tumors without previous treatment, PD-L1 positivity: >5% of positive cells). The authors also observed a higher PD-L1 mRNA expression in TN tumors of the TCGA data set. This is interesting because the TN subtype displayed the highest PI3K pathway activity in the TCGA data set and 30% of TN tumors had homozygous or hemizygous PTEN deletions[57].

Thus constitutive PD-L1 expression is rare in primary breast carcinomas (~3%) and present mostly in TN/basal-like tumors. PD-L1 expression is associated with T cells at mRNA level and with CD8$^+$ cells at protein level. The positive associations of PD-L1 expression with T cells and clinical outcome suggest antitumor T cell responses. In TN/basal-like tumors, it is not clear whether PD-L1 expression is constitutive, induced by IFNγ-secreting T cells or by an increased activity of the PI3K/AKT/mTOR pathway.

1.2.3 Tumor antigens recognized by T cells on breast carcinomas

As mentioned above, five distinct genetic mechanisms can lead to the presence on the surface of tumor cells of HLA-peptide complexes that can be recognized by T cells. Three mechanisms lead to the expression of antigens of high tumoral specificity (tumor-specific antigens) while the two others lead to the expression of antigens of low tumoral specificity (tumor-associated antigens). Most of the experimental results that support this classification have been obtained with melanomas. However the analysis of antigens on other types of tumors and the analysis of human antitumor T cell responses have not revealed other mechanisms of tumor-specific antigenicity.

1.2.3.1 Antigens encoded by mutations

In 1995, tumor-specific T cells recognizing an antigen encoded by a gene that was mutated in the tumor compared to the autologous normal cells (mutant antigen) were discovered in the blood of a patient with metastatic melanoma[58]. Since then, mutant antigen-specific CD4 or CD8 T cells have been found in the blood or in metastases of many melanoma patients[59-66] or in patients with other cancers such as metastatic gastro-intestinal carcinoma[11], chronic lymphocytic leukemia[67], head and neck carcinoma[68] or ovarian carcinoma[69]. Even though most immunogenic mutations are passenger mutations, some are driver mutations. For example, Tran *et al.* identified recently HLA-C*08:02-restricted anti-$KRAS^{G12D}$ CD8 TILs in a metastatic colon carcinoma[11]. $KRAS^{G12D}$ is the most frequent KRAS mutation in human cancer (35%) and drives tumor cell proliferation[70]. Beside this rare exception of an immunogenic hot-spot mutation, most immunogenic mutations are unique mutations resulting from single nucleotide variants (SNVs). Out of 48 reported immunogenic mutations, 37 are SNVs (reported in the peptide database of Cancer Immunity[71], October 2015 update). Within the 37 SNVs, 34 are missense mutations, 1 is a splice site modifier, 1 is a start gain mutation and 1 is a nonsense mutation. Small insertions or deletions (indels) with a frame shift, and chromosomal aberrations are less frequent (4 frame shift mutations, 6 fusion gene and 1 tandem duplication).

Like other tumors, breast carcinomas exhibit somatic mutations. Compared with other solid tumor types, the median number of nonsynonymous mutations is low and similar to that found in prostate, hepatocellular and serous endometrial tumors (Figure 1-3).

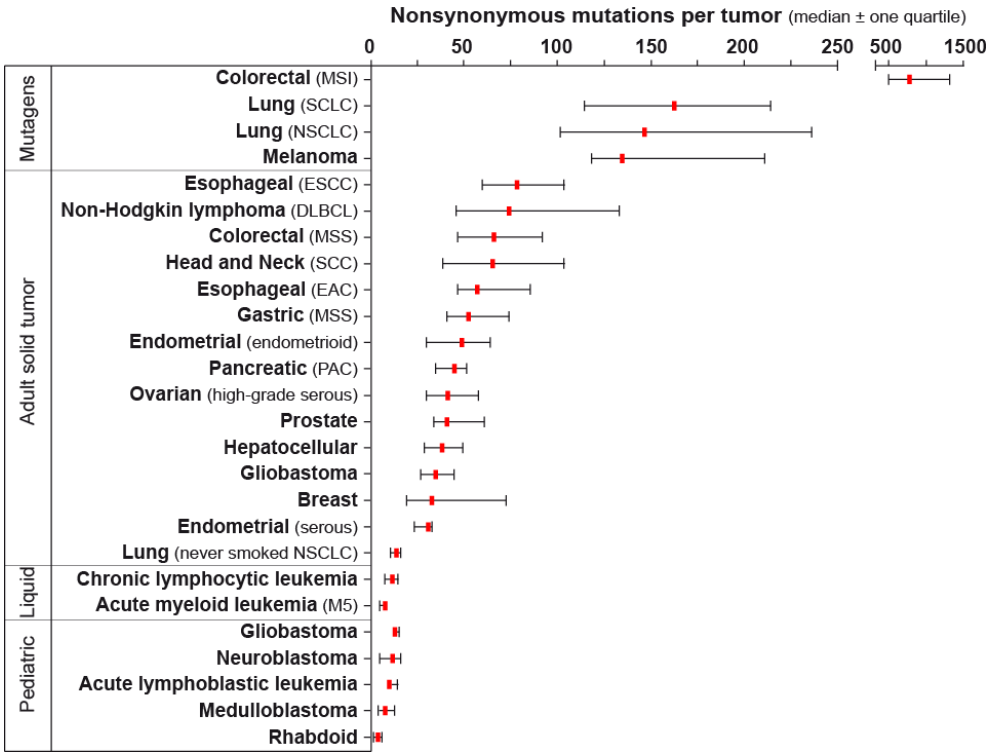

Figure 1-3. Number of nonsynonymous somatic mutations for several cancer types.

The median numbers of nonsynonymous mutations are shown for different cancer types (red dot). Horizontal bars indicate the 1rst and 3rd quartile. MSI, microsatellite instability; SCLC, small cell lung cancer; NSCLC, non-small cell lung cancer; ESCC, esophageal squamous cell carcinoma; DLBCL, diffuse large B cell lymphoma; MSS, microsatellite stable; EAC, esophageal adenocarcinoma; PAC, pancreatic adenocarcinoma; M5, M5 subtype. Figure adapted from Vogelstein *et al.*[72]

The TCGA network published in 2012 an extensive analysis of primary breast tumors with whole-exome sequencing and gene expression profiles[57]. In total, 28,316 SNVs and 2,302 indels were identified by whole-exome sequencing of 510 tumors. Most SNVs were missense mutations (67%) and each tumor carried on average 37 missense mutations. The average non-silent mutation rate per megabase (Mb, size of an exome is ~30Mb[73]) varies between the intrinsic subtypes: 2.05 mutations/Mb in HER2-overexpressing tumors, 1.68 mutations/Mb in basal-like tumors, 1.38 mutations/Mb in luminal B tumors and 0.84 mutations/Mb in luminal A tumors (Figure 1-4). The authors identified potential driver mutations with a statistical method. For each gene, the observed mutation rate was compared to the background mutation rate and 35 genes were found to be significantly more mutated. Nearly all known driver genes that have been implicated in breast cancer were in this list (*TP53*, *PIK3CA*, *PTEN*, *GATA3*, *RB1*, ...). New candidate genes were identified. Genes *TP53* and *PIK3CA* were the most mutated and 73% of the tumors carried mutations in either of these two genes. Significantly mutated genes were enriched in some intrinsic subtypes. The number and diversity of mutated genes were the highest in the luminal A and B subtypes. Eighty percent of basal-like tumors had a mutation in *TP53* while other significantly mutated genes were rarely mutated (e.g. *PIK3CA*). HER2-overexpressing tumors were often mutated in *TP53* and *PIK3CA* and other significantly mutated genes were rarely mutated (Figure 1-4). A recent analysis of 560 breast cancers extended the list of genes with probable driver mutations (*MED23*, ...) to 93 protein-coding genes[74]. In 95% of the tumors, at least one of these 93 genes was mutated.

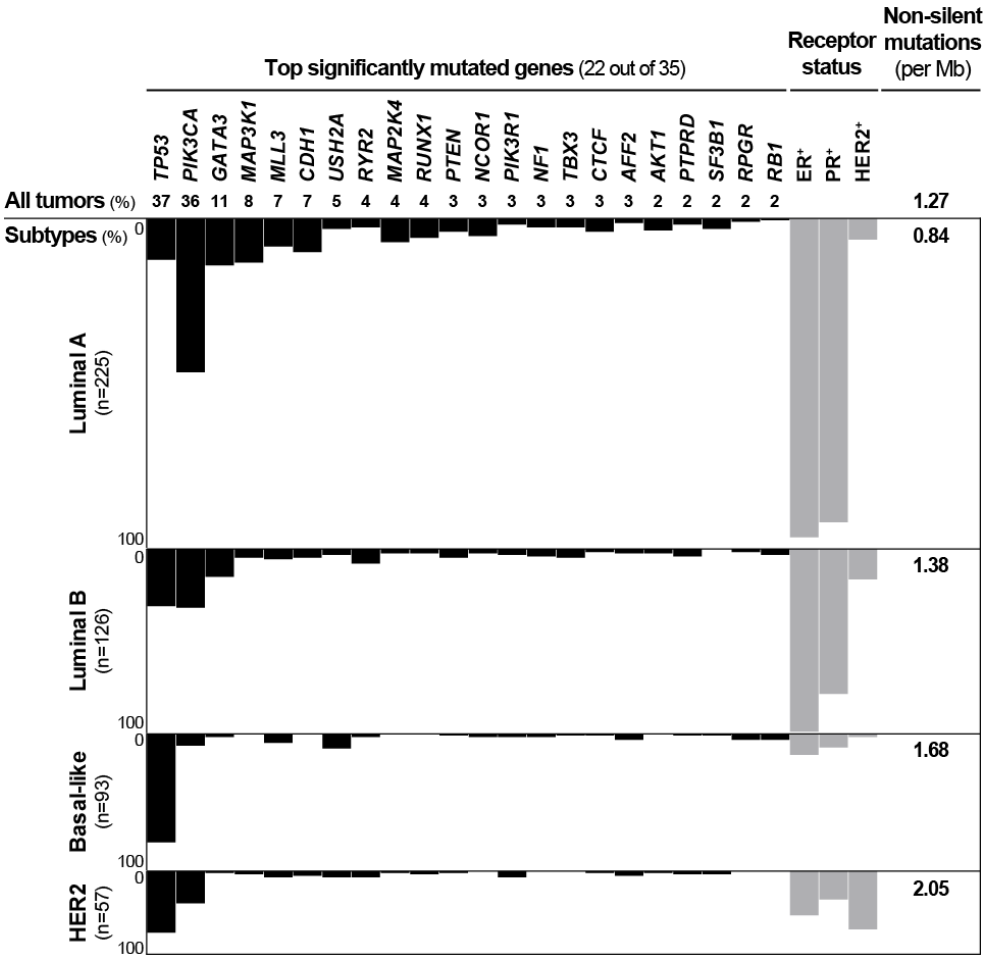

Figure 1-4. Somatic mutation profile of 510 primary breast carcinomas.

The top 22 out of 35 significantly mutated genes in breast cancer are shown. The rate of mutations for each gene is indicated below the name of each gene and drawn as columns for each intrinsic tumor subtype (proportions from 0 to 100 % in a linear range). For each subtype, the proportion of tumors with ER^+, PR^+ and $HER2^+$ status are shown with grey columns. According to the size of each subtype group, the dimensions of columns are adapted. On the outer right side, the mean number of non-silent mutations for all tumors and for the 4 intrinsic subtypes are highlighted (adapted from reference [57]).

The mutational processes that generate somatic mutations in breast cancer have remained poorly understood for a long time. In 2013, Alexandrov *et al.* analysed nearly 5,000,000 SNVs and indels of more than 7,000 primary cancers of 30 different types[75]. From all tumors, 20 different signatures of mutational processes were identified based on a 96-trinucleotide classification. This classification comprises the 6 possible base substitutions (only the pyrimidine (C or T) of the mutated base pair is used: C>A, C>G, C>T, T>A, T>G and T>C) and their flanking nucleotides (16 possibilities/substitution): 5'-NpNpN-3' (the base substitution is underlined)[76].

Five out of the 20 signatures were found in breast tumors (signatures 1, 2, 3, 8 and 13). All of them were shared with at least one other cancer type and several coexisted within a tumor. In 2016, the group updated their analyses for breast cancer with the wole-genome sequencing of 560 tumors[74]. They confirmed the 5 previous mutational signatures and discovered 7 new ones (signatures 5, 6, 17, 18, 20, 26 and 30) (Figure 1-5). Nine out of 12 signatures were related to an etiology.

- Signature 1 is common in many cancer types (>70% of all tumors) and is associated with age at the time of cancer diagnosis. The etiology is probably a spontaneous deamination of 5-methyl-cytosine in CpG dinucleotides (NpCpG context). Signature 5 is also associated with age at the time of cancer diagnosis but the cause is unknown.

- Signatures 2 and 13 are probably generated by cytidine deamination by some members of the APOBEC (apolipoprotein B mRNA editing enzyme, catalytic polypeptide) family. The members APOBEC1, APOBEC3A, APOBEC3B and APOBEC3C show *in vitro* a preference for the sequence context of signatures 2 and 13 (TpCpN)[76]. APOBECs are part of the innate immune response to retroviruses, but their role in cancer is not understood.

- Signatures 3 and 8 are associated with homologous-recombination deficiency and loss-of-function of *BRCA1* and *BRCA2*. These proteins are involved in homologous recombination-based repair of DNA double-strand breaks. Germline mutations in *BRCA1* or *BRCA2* are responsible for many hereditary breast cancers[77].

- Signatures 6, 20 and 26 are rare in breast tumors (<2%) and contain numerous small indels in regions of microsatellites. This is characteristic for DNA mismatch repair-deficient tumors[74,75].

None of the signatures with a related etiology is specific for breast tumors. Interestingly, APOBEC activity and DNA mismatch repair deficiency are present in rare tumors with a very high number of mutations (Figure 1-5).

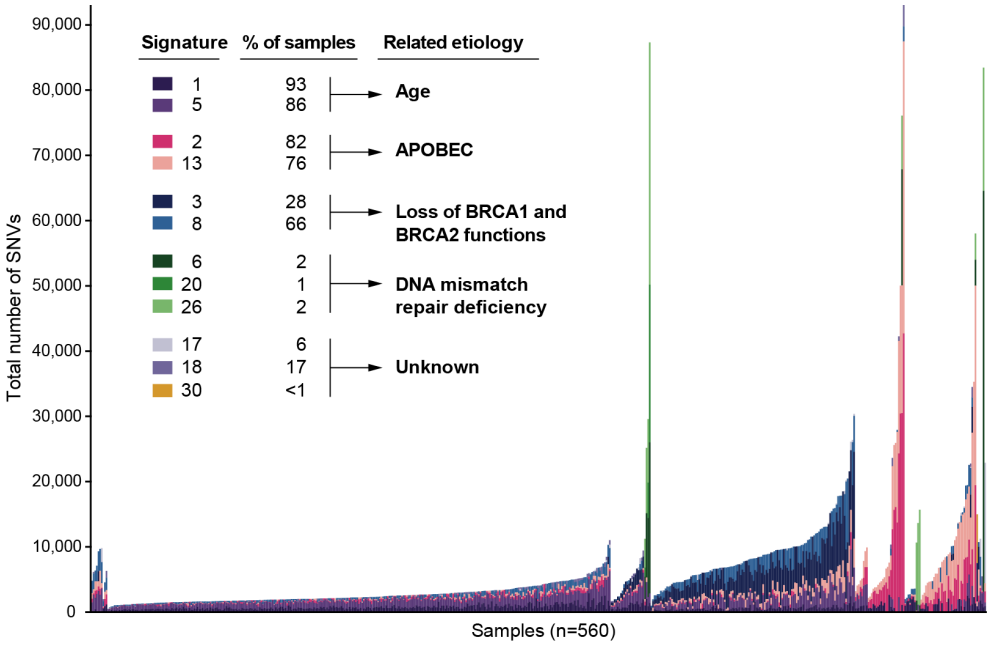

Figure 1-5. SNV-based signatures of mutational processes in breast cancer.

The bar plot displays for each sample the number of SNVs associated with one out of the 12 signatures. Samples are clustered according to their profile of mutational signatures and sorted in ascending order of SNVs. Signatures are grouped according to related etiology. For each signature, the proportion of breast tumors with ≥1 SNV of the specific signature is shown. The y-axis is the total number of SNVs, not that of nonsynonymous or non-silent mutations. Figure adapted from Nik-Zainal *et al.*[74]

With these sequencing data of breast tumors, the number of mutant peptides that can bind to autologous HLA class I molecules can be predicted by using MHC-binding prediction algorithms. Rajasagi *et al*. analysed a public dataset of more than 700 breast carcinomas with associated whole-exome sequences[67]. For each tumor, they identified the HLA class I molecules (HLA-A, -B and -C) and the missense and frame-shift mutations. Then, HLA-binding peptides of 9 or 10 amino acids with a high binding affinity (Kd ≤500 nM) were predicted for each of these nonsynonymous mutations. This *in silico* approach predicted a mean number of 50 HLA class I-binding mutant antigens per tumor, with a large variation between tumors (first quartile at 0, third quartile at 1000). The actual number of different mutant antigenic peptides that can be recognized by T cells on the surface of the tumor cells will depend, additionally, on the level of expression of the mutated genes and of the capacity of the antigen processing machinery of the tumor cells to produce a sufficient amount of each peptide. Assuming the expresssion of one third of the mutated genes[78], around 15 mutant antigens may be presented by tumor cells of a given tumor. The actual proportion of these antigenic peptides that is effectively processed is unknown.

1.2.3.2 Antigens encoded by cancer-germline genes

Some breast carcinomas express cancer-germline genes. The expression frequency is in the middle range compared with other tumors. Metastatic melanomas, lung carcinomas and infiltrating bladder carcinomas express more often cancer-germline genes. Colorectal and renal carcinomas express them less often (Table 1-2).

Genes	Breast Carc.	Melanoma (metastatic)	Lung Carc.	Bladder Carc.	Colorectal Carc.	Renal Carc.
MAGEA1	19	46	46	32	0	5
MAGEA3	13	74	47	57	17	0
MAGEA4	6	25	51	45	11	2
MAGEA6	15	72	51	57	22	0
MAGEA10	4	47	44	38	0	0
MAGEA12	13	62	30	34	11	5
NYESO1	23	35	27	47	0	0
CTAG2	23	33	41	47	0	0

Table 1-2. Expression profiles of cancer-germline genes in selected cancer types.

Proportions (%) of tumors with cancer-germline gene expression. Expression was measured by RT-PCR. Lung carcinomas (carc.) include adenocarcinomas and squamous-cell carcinomas with similar cancer-germline gene expression profiles. Bladder carcinomas are only T2 tumors (infiltrating). NYESO1 is also known as CTAG1 or LAGE-2. CTAG2 is also known as LAGE-1. Data from Coulie *et al.* and van der Bruggen *et al.*[6,79].

Cancer-germline genes are expressed due to a demethylation of their promoters[79]. In more advanced tumors, the global demethylation is increased with a higher proportion of tumors that express cancer-germline genes. This pattern has also been observed in primary breast carcinomas: the expression of MAGEA3/A6 is associated with tumor grade using semiquantitative RT-PCR[80]. In the same study, MAGEA3/A6 expression was also associated with ER^- tumors, which can be explained by the very high proportion of high grade tumors (>90%) among ER^- tumors[81].

As cancer-germline genes are expressed in some breast tumors, it is very likely that MAGE-type antigens are presented at the surface of the corresponding tumor cells. Indeed, Wang *et al.* showed in 1998 that NYESO1-derived antigens were presented on breast tumor cells[82]. They isolated an HLA-A31-restricted anti-NYESO1 CTL clone from a melanoma metastasis. This anti-NYESO1.A31 clone recognized allogeneic HLA-A31^{+} fresh-frozen breast tumor digests from two different tumors (1295, 1315), as well as a cell line derived from tumor 1315. Both breast tumor digests expressed *NYESO1* by RT-PCR and a fibroblast culture (no expression of *NYESO1*) derived from the tumor 1295 was not recognized.

There is no report of T cell responses to MAGE-type antigens in breast cancer patients.

1.2.3.3 HER2 antigens

HER2 is a transmembrane receptor tyrosine kinase that is overexpressed, mostly by gene amplification, in 15-20% of primary breast tumors[21]. HER2 overexpression or the amplification of its gene, *ERBB2*, is associated with poor prognosis and HER2 overexpression predicts reponse to HER2-targeted drugs such as anti-HER2 monoclonal antibodies (trastuzumab, pertuzumab, trastuzumab-emtansine) or small molecule tyrosine kinase inhibitors (*e.g.* lapatinib)[17]. Thus, HER2 is an important molecule in breast oncology and several groups have investigated the presence of HER2-specific T cells in the blood or in the tumor of patients with breast cancer.

Several HER2 peptides have been reported to be recognized by CD8 T cells[71]. The first anti-HER2 CD8 T cell clones were derived from the malignant ascites of an ovarian cancer patient[83]. Two clones recognized the predicted HLA-A2-binding peptide E75 ($HER2_{369-377}$ KIFGSLAFL) and the antigenic processing of the peptide was indicated by the lysis of an HLA-A2-transfected HER2-overexpressing tumor cell line (SK-OV-3) by one E75-specific T cell clone. However, Zaks *et al.* could not confirm antigenic processing of peptide E75. Their E75-specific CTL lines or clones did not recognize several HLA-A2^{+} HER2-overexpressing (tumor) cell lines (including SK-OV-3/HLA-A2), unless they were pulsed with the E75 peptide[84]. Thus, whether or not peptide E75 is naturally processed remains unclear. Nevertheless, this peptide has been used in multiple small vaccine trials[85]. For example, in a phase I/II trial, patients with primary breast cancer received in the adjuvant setting an intradermal vaccine of peptide E75 combined with GM-CSF[86].

According to their HLA type, 187 patients were stratified into a vaccination and control arm. Vaccinated patients had a better clinical outcome (5-year disease-free-survival: 89,7%) than non-vaccinated patients (80,2%; p=0.08). Recently, a phase III vaccination trial started with the same vaccine based on the results of this phase I/II. Surprisingly, only patients with low expression of HER2 in their tumors will be vaccinated. The decision is based on an increased immune reaction towards E75 in patients with tumors without HER2 overexpression in the phase I/II trial[87].

The questioned antigenic processing of peptide E75, the limited clinical efficacy of HER2-based vaccines as well as the counterintuitive use of a E75-based vaccine in tumors without HER2 overexpression cast doubts on the antigenicity and the immunogenicity of this peptide. Moreover, while the higher expression ('overexpression') of HER2 in some tumors as compared with normal tissues suffices for a differential antitumor activity by antibodies such as trastuzumab, the expression difference may be insufficient to confer tumor-specificity to anti-HER2 lytic CD8 T cells. Along this line, adoptive transfer of HER2-specific chimeric antigen receptor (CAR)-transduced autologous T cells has led to deadly toxicity[88].

1.2.3.4 Other possible antigens

NY-BR-1 is a breast differentiation antigen. The encoding gene, *ANKRD30A*, is expressed in about 70% of breast tumors and in two normal tissues: breast and testis[89]. Therefore, NY-BR-1 antigens could be breast-tissue specific assuming that gene expression in testis is limited to germline cells, which are devoid of HLA class I molecules. Wang *et al.* isolated from the blood of a patient with breast cancer a CD8 T cell clone which was specific for a HLA-A2-restricted NY-BR-1 antigenic peptide[90]. The clone recognized an allogenic NY-BR-1^{+} HLA-A2^{+} breast tumor cell line, but not an NY-BR-1^{-} HLA-A2^{+} breast tumor cell line. It is however doubtful that such an antigen could be used in immunotherapy, except against metastatic disease after bilateral mastectomy.

The MUC1 glycoprotein and hTERT may also be antigenic in breast cancer. Both are reported to be overexpressed in human tumors and their antigenicity for T cells has been documented with tumor cell lines, though not with breast tumor cell lines[91,92]. However, MUC1 and hTERT are also present on some normal cells and the notion of overexpression must be taken with caution.

1.2.4 Reports of *in vitro* antitumor reactivity of breast TILs

In the 1990s, two groups published results on the recognition of breast tumor cells by autologous TILs.

The group of S. Rosenberg tested the cytolytic activity and cytokine secretion of TILs cocultured with autologous tumor cells. Tumor cell suspensions were obtained from minced and enzymatically digested primary breast tumors or tumor-infiltrated lymph nodes. From these suspensions of tumor and stromal cells, TIL cultures were started in the presence of IL-2 and a part of each suspension was frozen for further recognition assays by TILs. In their first two publications, none of the 7 and 21 TIL cultures showed a cytolytic activity that was specific for the autologous tumor cell suspension[93,94]. Cytokine secretion assays showed that TIL populations from 3 out of 11 patients secreted GM-CSF, IFNγ and TNFα in the presence of autologous but not allogenic tumors. Two of these 3 TIL populations were highly enriched in CD4 T cells (96-98%) and one of them was tested for HLA class II restriction. Cytokine secretion was significantly reduced when the autologous tumor cells were preincubated with an anti-HLA class II antibody. In their third paper, the group confirmed their previous results. None of the 35 tested TIL cultures displayed a cytolytic activity that was specific for the autologous tumor cells. Additionally, CD4 and CD8 TIL populations were tested for cytokine secretion in the presence of tumor cells[95]. Three out of 21 tested CD4 TIL cultures displayed HLA class II-restricted tumor-specific cytokine secretion. No significant cytokine secretion was observed for the 21 tested CD8 TIL populations, although 3 of them showed small autologous tumor-specific secretion of GM-CSF.

Baxevanis *et al.* assessed the cytolytic activity of *in vitro* expanded TILs against breast tumor cells[96]. Cells were extracted from primary tumors or metastatic pleural effusions. From the tumor cell suspensions, mononuclear cells and tumor cells were separated by two-phase density gradients. TILs were expanded *in vitro* in the presence of IL-2 and autologous tumor cells. The tumor cells were frozen for further TIL testing. Out of 12 TIL cultures, the 5 CD8-predominant TIL cultures (from 3 tumors and 2 pleural effusions) displayed cytolytic activity directed preferentially against autologous tumor cells (28-92% of lysis). CD8 TIL clones were derived from one primary tumor and lysed autologous tumor cell suspensions (15-29% of lysis) better than allogenic tumor cell suspensions (3-7% of lysis).

These reports suggested the presence of tumor-specific CD4 TILs in human breast tumors. For CD8 TILs, the results were contradictory.

1.2.5 Preliminary results of immunostimulatory antibodies in breast cancer

At this moment, no T cell-mediated immunotherapy is used routinely for breast cancer. The anti-CTLA-4 monoclonal antibody tremelimumab was tested in combination with the aromatase inhibitor exemestane (hormone therapy) in patients with metastatic hormone receptor-positive breast tumors. The best overall response was stable disease in this small phase 1 study (n=26)[97].

Anti-PD-1 and anti-PD-L1 monoclonal antibodies were tested in patients with advanced or metastatic breast carcinoma and the first preliminary results of 4 phase I clinical trials are available. In the JAVELIN trial, the anti-PD-L1 antibody avelumab was tested in patients with advanced or metastatic breast cancer. Intermediate data were presented at the San Antonio Breast Cancer Symposium (SABCS) 2015. Out of 168 patients, 8 had a radiologically documented response (1 complete response and 7 partial responses). Despite the low overall response rate of 4.8%, the tumor subtype analysis was interesting. Five out of the 8 responding patients had a TN tumor (n=58, 8.6% of response), 2 had an $ER^{+}HER2^{-}$ tumor (n=72, 2.7%) and 1 had an $HER2^{+}$ tumor (n=26, 3.8%). Then the authors combined tumor subtypes with PD-L1 expression by IHC. Nine TN tumors were PD-L1-positive (≥10% $PD\text{-}L1^{+}$ immune cells) and 4/5 responding patients with TN tumors had $PD\text{-}L1^{+}$ tumors[98,99]. Importantly, the response to these drugs can be long-lasting (Figure 1-6).

This observation is in line with two other studies that observed overall response rates of 18.5 and 19% in $PD\text{-}L1^{+}$ advanced or metastatic TN tumors (Table 1-3)[100-102].

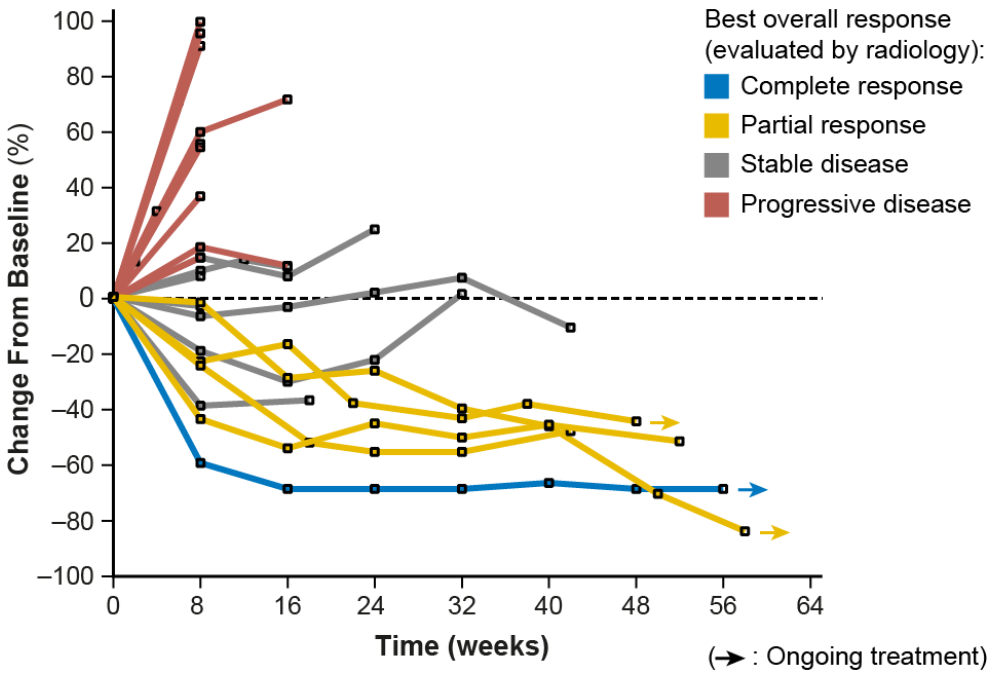

Figure 1-6. Response to the anti-PD-1 antibody pembrolizumab in the KEYNOTE-012 trial.

Change from baseline tumor size in function of time. Tumor size is measured as the sum of the diameters of target lesions (criteria RECIST v1.1). The patient with complete response had a nodal disease. Therefore, the change from baseline does not reach 100% because according to RECIST v1.1, metastatic lymph nodes that regress to <1 cm short axis are evaluated as normal[103]. Patients with ongoing treatment are marked by an arrow. The other patients stopped treatment after detection of new lesions, growth in target or in non-target lesions. Figure adapted from Nanda *et al.*[101]

Target	Drug	Definition of PD-L1 positivity (IHC)	Response rate	Ref.
PD-L1	Atezolizumab	≥5% of immune cells	4 out of 21 (19%) (2 CR, 2 PR)	100,102
PD-1	Pembrolizumab	Any stromal cells OR ≥1% of tumor cells	5 out of 27 (18.5%) (1 CR, 4 PR)	101

Table 1-3. Results of 2 clinical trials with PD-1 pathway inhibitors in PD-L1$^+$ advanced or metastatic triple-negative tumors.

CR, complete response; PR, partial response

TN tumors are not the only ones that respond to PD-1 pathway inhibitors. An overall response rate of 12% (3 responding patients out of 25 treated patients) with pembrolizumab has been reported for patients with PD-L1-positive ER^+HER2^- advanced breast cancer in the KEYNOTE-028 trial (PD-L1 positivity: Any stromal cells, or ≥1% of tumor cells)[104,105]. Whether breast tumors need to be PD-L1-positive for a response to anti-PD-1 or anti-PD-L1 antibodies is not clear. The JAVELIN trial with atezolizumab is still ongoing and results of patients with TN PD-L1-negative tumors have not been published yet. There is probably a correlation between PD-L1-positive tumors and clinical efficacy of PD-1 pathway inhibitors like in advanced NSCLC and melanomas, even if some PD-L1-negative tumors have responded to these drugs[3].

Noteworthily, the response rate of TN $PD\text{-}L1^+$ metastatic breast cancer to PD-1 pathway inhibitors is lower than that of $PD\text{-}L1^+$ advanced melanoma, NSCLC or bladder cancer[3] (Table 1-4). A low proportion of immunogenic breast tumors could explain this difference, but different IHC protocols and different definitions of PD-L1 positivity prevent reliable comparisons.

Advanced $PD\text{-}L1^+$ tumors	**Drug**	**Response rate (%)**
Melanoma	Anti-PD-1 (nivolumab)	44-53
NSCLC	Anti-PD-1 (nivolumab, pembrolizumab)	37-45
Bladder cancer	Anti-PD-L1 (atezolizumab)	43
TN breast cancer	Anti-PD-1 (pembrolizumab), Anti-PD-L1 (atezolizumab)	18.5-19
ER^+HER2^- breast cancer	Anti-PD-1 (pembrolizumab)	12

Table 1-4. Response rate of advanced $PD\text{-}L1^+$ tumors to PD-1 pathway inhibitors.

Data from Callahan *et al.*[3]

There are several ongoing clinical trials with PD-1 pathway inhibitors in breast cancer. Most studies focus on TN tumors, some on $HER2^+$ tumors, but there is few interest in ER^+HER2^- tumors (Clinicaltrials.gov, Feb 2016 : 10/17 studies in TN tumors, 3/17 studies in $HER2^+$ tumors).

To conclude, the first clinical results of PD-1 pathway inhibitors show promising tumor regressions in some PD-L1-positive breast tumors. Whether these responses involve lytic tumor-specific CD4 or CD8 T cells is unknown. No analyses of T cell infiltration or of T cell effector functions have been reported.

1.3 Objective of the work

Spontaneous antitumor T cell responses are thought to be present in breast cancer patients as suggested by analyses of TILs and of gene expression profiles, by the presence of tertiary lymphoid structures inside tumors and by the first clinical results of PD-1 pathway inhibitors. Our objective was to analyse a few primary breast carcinomas in order to prove or disprove the hypothesis that these tumors are immunogenic for autologous CD8 T cells.

To probe the immunogenicity of those tumors, from which the establishment of cell lines is currently not possible, we have resorted to testing the reactivity of a set of about 100 CD8 TIL clones towards the most likely tumor-specific antigens expressed by the tumor, based on gene sequencing and expression.

We used autologous EBV-transformed B cells (EBV-B cells) to present candidate antigenic peptides, thus screening all the HLA class I molecules of the patients for the presentation of tumor-specific antigens. Furthermore we did not restrict the candidate antigenic peptides to those that are predicted to bind to HLA class I molecules, also to have an immunogenicity analysis as comprehensive as technically possible.

2 Results

We established sets of CD8 TIL clones from breast tumors with representatives of the 3 subtypes. Six tumors (2 $ER^{+}HER2^{-}$, 2 $HER2^{+}$ and 2 triple-negative) with a TIL clone set of about 100 clones for each tumor were selected for assays of recognition of candidate tumor-specific antigens by the TIL clones (Figure 2-1). Exome and RNA sequencing identified missense single nucleotide variants (SNVs) and indels in expressed genes, expressed cancer-germline genes, and *ERBB2* overexpression. After identification and selection of candidate antigenic peptides, all TIL clones were tested for recognition of autologous EBV-B cells loaded with peptides or transduced with cancer-germline genes or *ERBB2*.

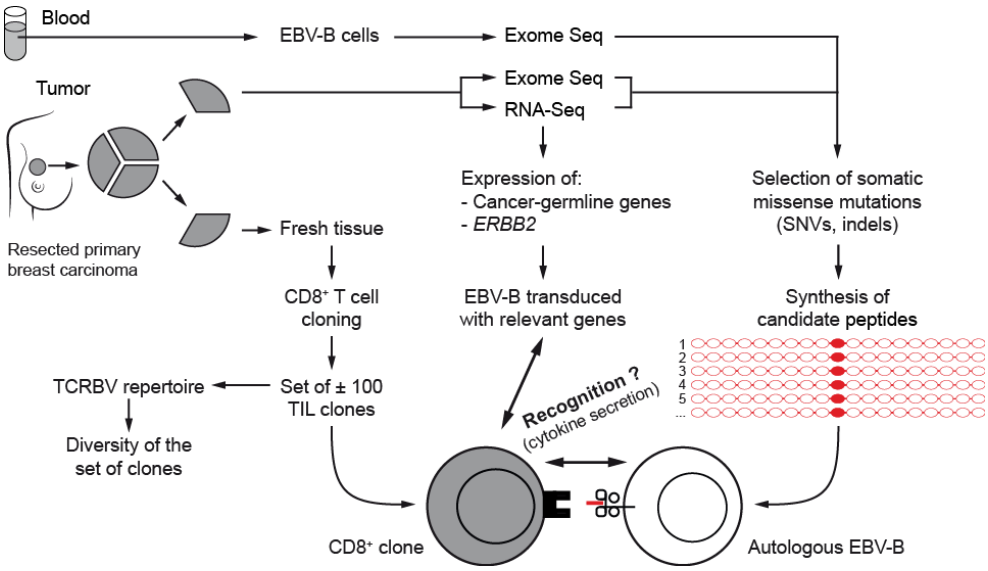

Figure 2-1. Work plan to test CD8 TILs for candidate tumor antigens.

SNVs, single nucleotide variants; TCRBV repertoire, repertoire of the variable part of the TCR beta chain.

We identified several tumor-specific CD8 TIL clones in one of the 6 patients. Four antigenic peptides and presenting HLA molecules were identified. The frequencies of these tumor-specific T cells were measured in the tumor and in the blood of the patient. Then we tried to unders tand why the other tumors did not stimulate detectable CD8 T cell responses.

2.1 Cloning of CD8 TILs

Fresh tumor samples were obtained from untreated patients undergoing tumor resection for invasive non-metastatic breast carcinoma (tumor size ≥2 cm). A part of the sample was frozen for later RNA/DNA extraction and the remaining fresh part was used for T cell extraction. The fresh sample was weighed and cells were dissociated mechanically and enzymatically. Living $CD3^+CD8^+CD4^-$ T cells were sorted out and cloned from the tumor cell suspension by flow cytometry (Figure 2-2). $CD3^+CD8^+CD4^-$ T cell clones were expanded during 20 to 30 days by stimulation with soluble anti-CD3 antibody, cytokines (IL-2, IL-7) and irradiated feeder cells (allogenic EBV-B cells and a mix of allogenic peripheral blood mononuclear cells) in order to obtain stable CD8 TIL clones. The proportion of proliferating clones among the sorted cells varied from 0.7% to 9.0% (median: 4.3%, n=10). We increased the cloning efficiency by a factor of 3 by increasing the number of feeder cells (6x more EBV-B cells and 15x more PBMCs per well) (median cloning efficiency with the improved protocol: 12.0%, n=4).

For further analysis, we selected for each breast tumor subtype the two tumors with the highest number of CD8 TIL clones. Out of 14 sets of clones, 6 sets were selected (71 to 203 clones per set). These 6 sets were derived from 2 ER^+HER2^- tumors (patient P142 and P143), 2 $HER2^+$ tumors (patient P154 and P195) and 2 triple-negative tumors (patient P223 and LB5784) (Table 2-1).

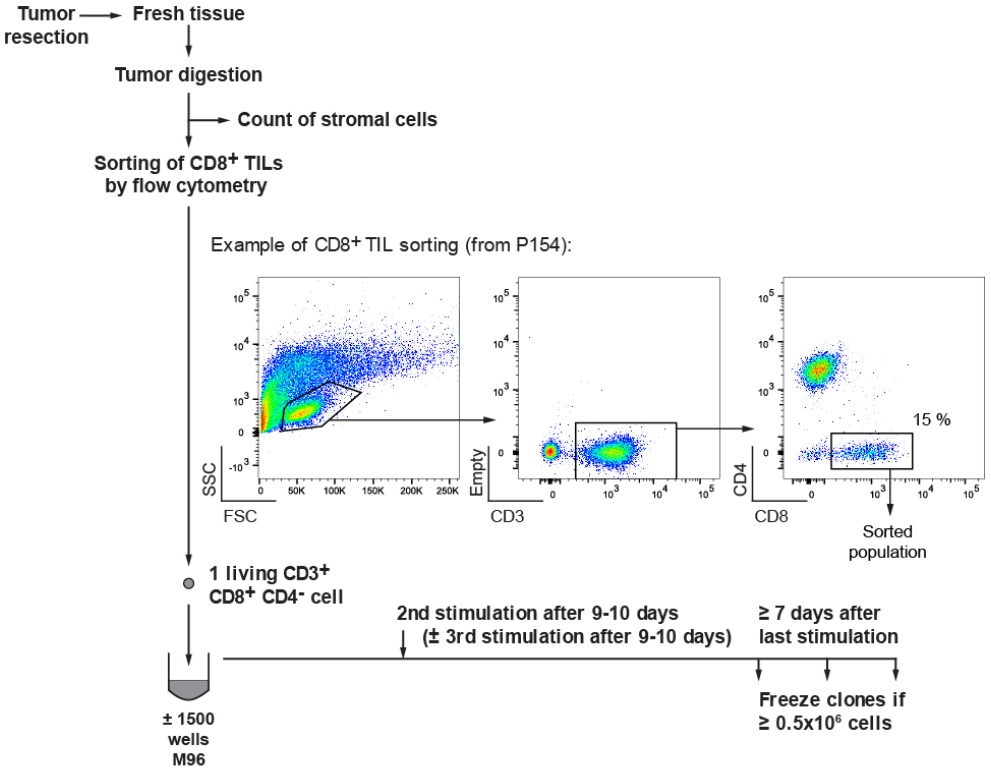

Non-specific T cell amplification	Old protocol	New protocol
> Anti-CD3 mAb	1 µg/mL	40 ng/mL
> Irradiated feeder cells		
Allogenic PBMC	20,000	300,000
Allogenic EBV-B cells	10,000	60,000
> IL-2	50 U/mL	50 U/mL
> IL-7	10 ng/mL	10 ng/mL

Figure 2-2. Cloning of CD8 TILs.

Mononuclear cells of a size similar to that of red blood cells were called stromal cells (excluding the large tumor cells and red blood cells). mAb, monoclonal antibody; PBMC, peripheral blood mononuclear cells; M96, 96-well microtiter plate.

Patient	P142	P143	P154	P195	P223	LB5784
Age	70	51	65	43	79	82
Tumor histopathology						
Histology	Ductal	Ductal	Ductal	Ductal	Meta-plastic	Ductal
Grade	High	Interm.	High	High	High	High
ER	+	+	+	+	-	-
PR	+	+	-	+	-	-
HER2	-	-	+	+	-	-
Ki67 (%)	40	80	40	40	75	40
Stage	IIIA	IIA	IIA	IIB	IIB	IIB
Tumor-infiltrating T cells						
Stromal cells / g of tissue (x10^6)	0.4	11.3	1.3	0.3	2.2	2.1
Proportion of CD8 TILs (%)	22	59	15	54	31	39
Number of cloned CD8 TILs	1,472	1,472	1,428	1,536	1,536	1,536
Amplification method	Old	Old	Old	New	New	New
Number of stable clones	132	71	75	166	100	203
Cloning efficiency (%)	9.0	4.8	5.3	10.8	6.5	13.2

Table 2-1. Characteristics of the 6 tested breast carcinomas.

Tumor grade, ER status, PR status, HER2 status and tumor cell proliferation were determined by the pathology department of the hospital. Tumor grade was established according to Nottingham grading system (Interm. = intermediate). ER and PR positivity was defined as >1% tumor cells stained in IHC. HER2 positivity was defined by overexpression in IHC (3+ score) or gene amplification if equivocal result in IHC (2+ score) (Chromogenic/fluorescent *in situ* hybridization, *ERBB2*/chr17 ratio ≥2.0). Tumor cell proliferation is estimated by the proportion of tumor cells stained with anti-Ki67 nuclear antigen in IHC. Tumor stage was established according to the UICC TNM classification (7th edition). Stromal cells are non-red cells and non-tumor cells. Proportions of $CD8^+$ T cells within the $CD3^+$ TIL populations were measured by flow cytometry.

2.2 TCRBV repertoire of the sets of CD8 T cell clones

2.2.1 Presence of repeated clones in all TIL clone sets

We probed the TCR diversity of the TIL clone sets. An ongoing antitumor T cell response in the tumor should be accompanied by clonal amplifications of the antitumor T cells, and the corresponding TCR sequences should appear repeatedly in the repertoire. Note that these repeated clones can be detected in our experiments only if their frequency is higher than 1% of the CD8 T cells.

We sequenced the complementarity determining region 3 (CDR3) of the TCRß chain for each clone, and established a TCRBV repertoire. Each clonotype has a unique TCR which is a heterodimer of the α and ß chain. Each chain contains a hypervariable CDR3 region that interacts with the antigenic peptide presented on the HLA molecule. The CDR3 of the TCRß chain is the product of somatic recombinations of Vß, Dß and Jß gene segments with random insertions or deletions of nucleotides at the recombination junctions. These genetic processes create the diversity of the TCRß CDR3 sequence, estimated at 10^6 in the blood[106].

In the TIL clone set of P142, the 132 clones expressed 100 different TCRß sequences, thus corresponded to 100 clonotypes. Eighteen clonotypes were represented by at least two clones (clonotypes of repeated clones). They represented 50 clones, or 38 % of all clones. We observed a similar presence of repeated clones in all of the 6 sets of CD8 TIL clones (Figure 2-3). Between 22 and 38 % of all clones were repeated clones.

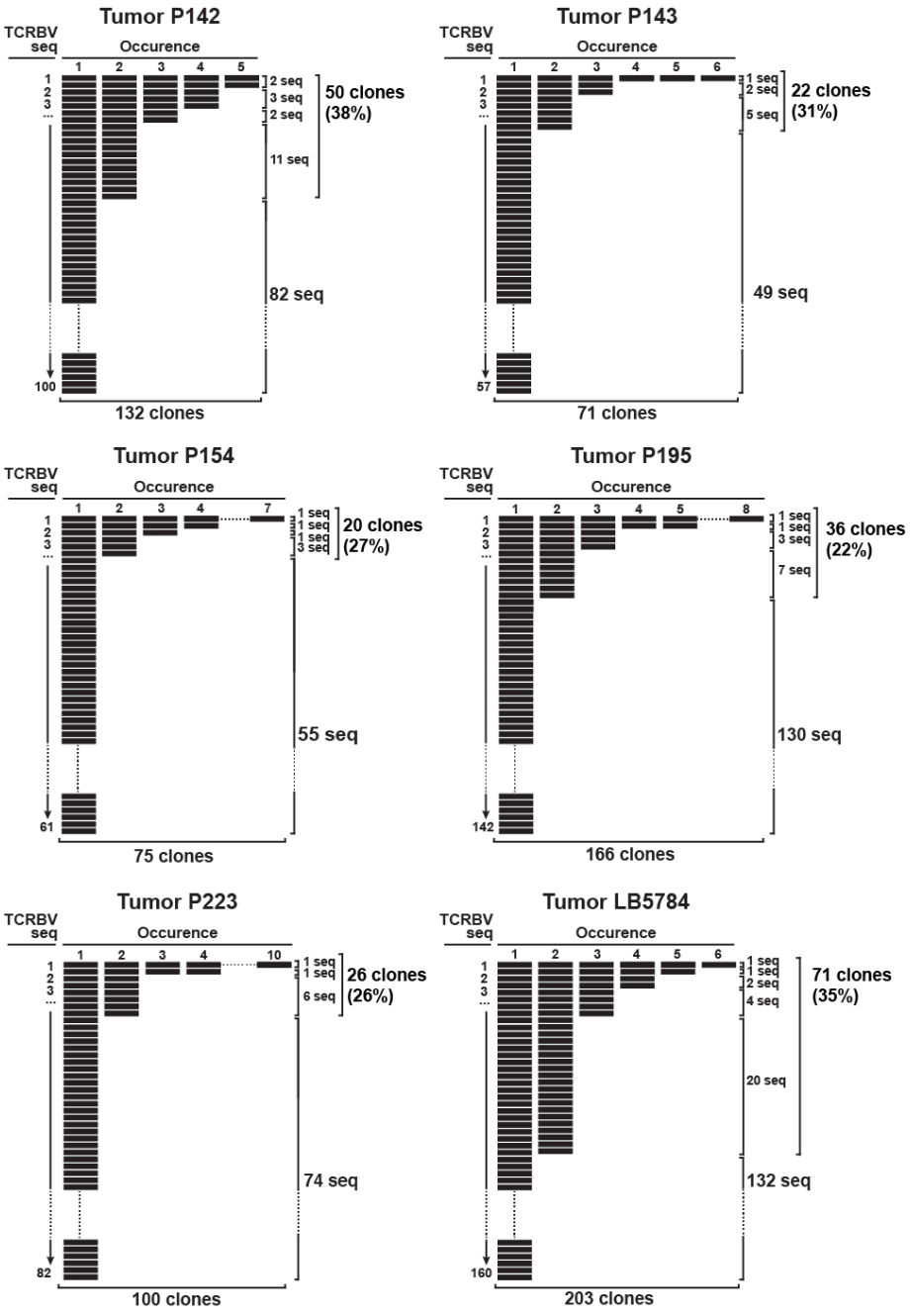

Figure 2-3. TCRBV repertoire of the 6 set of CD8 TIL clones.

Each black rectangle represents one clone. Each line of rectangles represents one clonotype (unique CDR3ß sequence). Seq, sequence.

2.2.2 Presence of repeated clones in normal breast tissue

We then asked whether this oligoclonality was associated with the presence of a tumor, and therefore possibly with antitumor T cell responses. To this end we analysed the TCRBV repertoire of similar numbers of CD8 T cell clones derived from 3 normal breast tissues. Clones from patient LB3410 were derived from normal breast tissue adjacent to a fibroadenoma (benign breast tumor) and those from patients LB3466 and LB5673 were derived from normal breast tissue collected during surgical breast reduction. We observed repeated clones also in these three sets. For patient LB3466, more than half of the clones were repeated (58%). We concluded that the presence of repeated CD8 T cell clones was not necessarily linked to antitumor T cell responses.

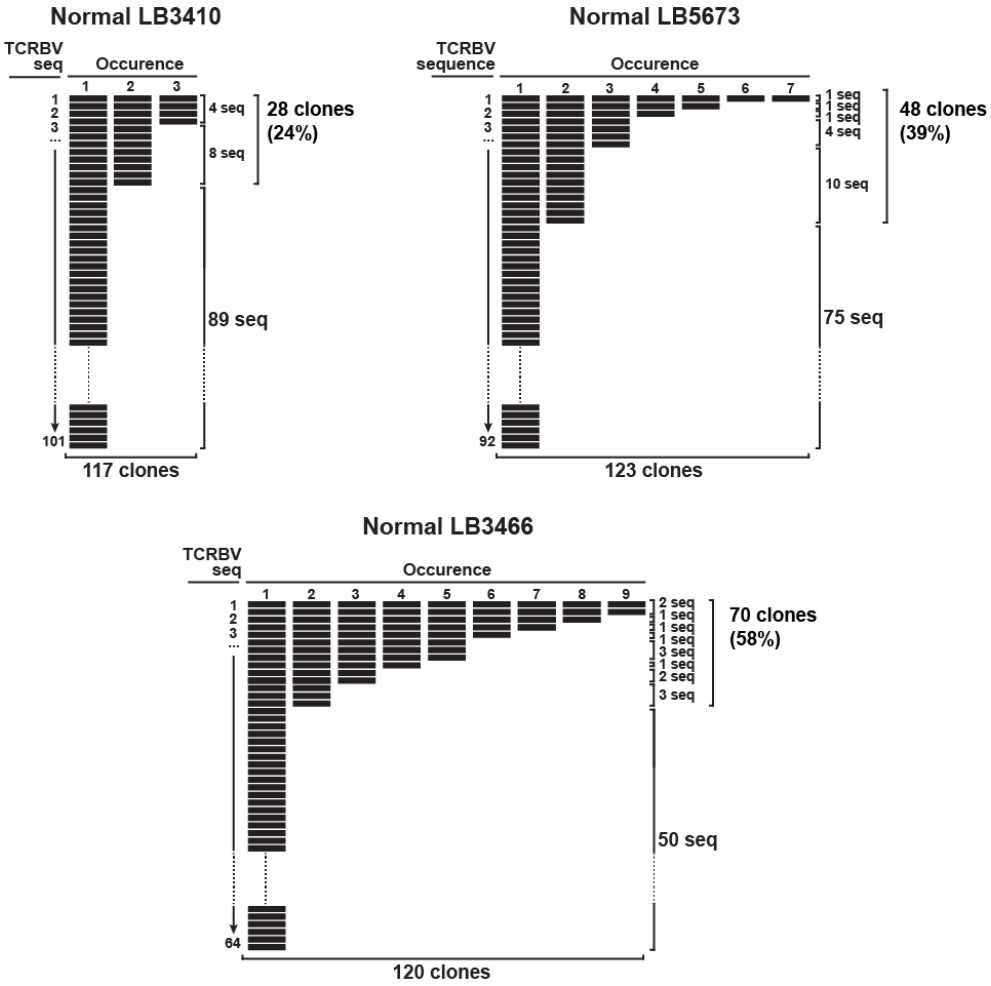

Figure 2-4. TCRBV repertoire of CD8 T cell clones derived from normal breast tissue.

2.3 Identification and selection of candidate tumor antigens

For each analysed tumor we identified candidate tumor antigens that could be recognized by the TIL clones, encoded by mutations, by cancer-germline genes and by *ERBB2*.

2.3.1 Selection of candidate mutant antigens

Paired-end whole-exome sequencing of matched tumoral and normal tissues was performed for the 6 patients (Figure 2-5). Somatic SNVs (single nucleotide variants) and indels were identified using Mutect[107] and VarScan2[108], respectively. Each variant was annotated by SnpEff[109] to select missense SNVs and STOP loss or frameshift indels (Figure 2-6). O. Bricard performed this analysis by adapting the best practice guidelines for variant discovery analysis of the Broad Institute (https://www.broadinstitute.org/gatk/guide/best-practices.php).

Our objective was to select the variants that were in expressed genes and to filter out uncertain variants, which could be due to sequencing errors that occur in exome sequencing. A first selection step used variant calling criteria to filter out uncertain variants. In the second step, only variants in expressed genes were selected. The last selection step was also used to filter out uncertain variants by invalidating them visually with the integrative genomics viewer (IGV)[110,111].

Our variant selection approach changed slightly during the study. After the analyses of tumors of patients P142 and P143, we modified the variant calling criteria and gene expression criteria.

For tumors of P142 and P143, our criteria were:

- Select variants with >10 variant reads in the exome of the tumor sample (varT >10),
- And: The proportion of variant reads in the exome of the normal sample is lower than 5% of variant reads in the tumor sample (varN <0.05 x varT).

(A read is the output sequence of a massive parallel sequencing, see Figure 2-5)

For the 4 other tumors, we simplified the criteria:

- Select variants with no variant read in the exome of the normal sample (varN = 0).

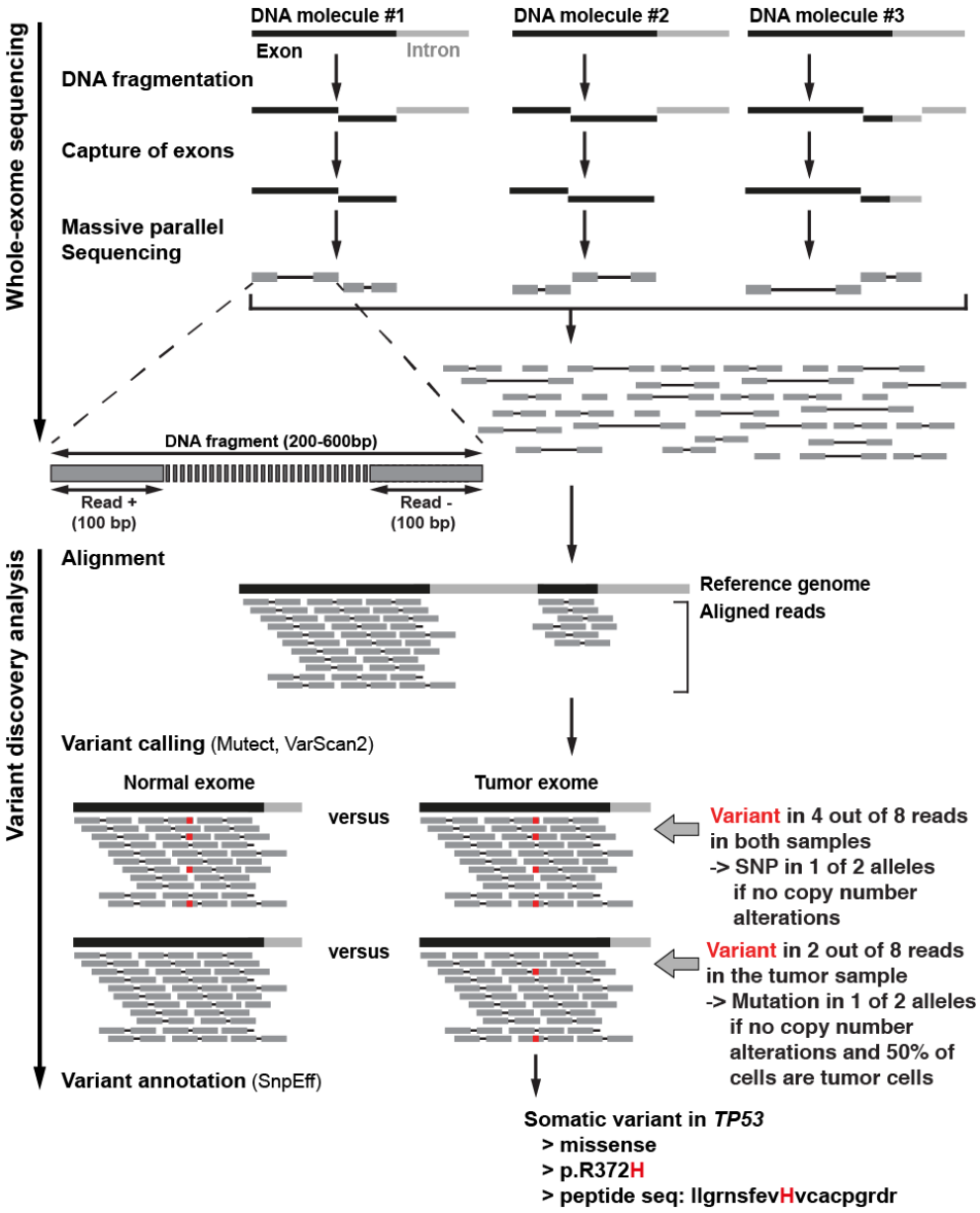

Figure 2-5. Overview of whole-exome sequencing and variant discovery analysis.

Major steps of whole-exome sequencing and variant discovery analysis. The sequenced part of a DNA fragment is called a read. A *TP53* missense mutation from the tumor of P143 is used as an example of variant annotation. SNP, single nucleotide polymorphism.

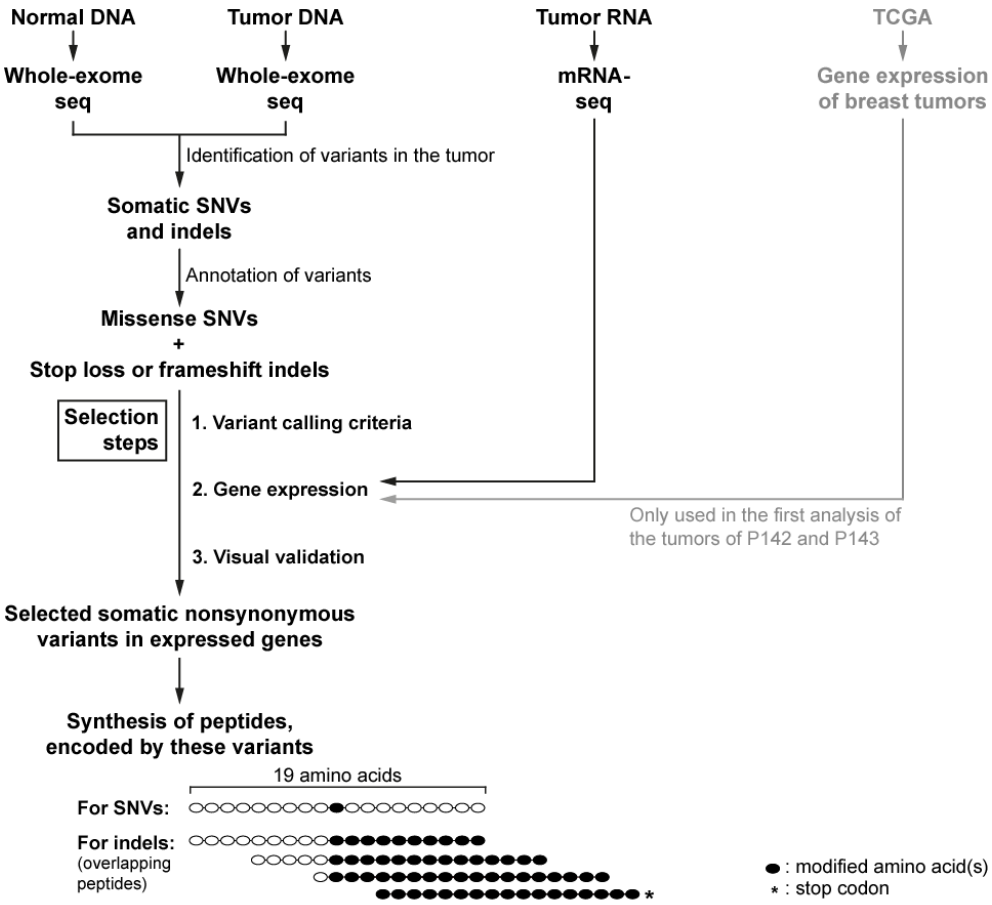

Figure 2-6. Identification and selection of potential mutant antigens

For P142 and P143 we had no RNA-Seq data and used instead a public gene expression data set of breast tumors (data generated by the TCGA Research Network: http://cancergenome.nih.gov/; data downloaded by N. van Baren). For each gene with a tumor variant, the percentile 5 of gene expression was calculated for the >1,000 samples of the public database and compared to the percentile 5 of *ACTB*. Variants were selected if the gene/*ACTB* ratio was ≥0.3% (P142) or ≥1% (P143). The threshold of 0.3% was selected arbitrarily for P142. We raised it to 1% for P143 because more missense variants were found and we restricted the selection to the most expressed genes. In addition, 9 and 10 variants were selected that passed only two of our three selection steps for

tumors P142 and P143 (the patient identity is used hereinafter to identify each tumor), respectively. This was an exploratory approach to probe with a small number of variants our selection criteria.

For the 4 other tumors, mRNA sequencing was performed, analysed by O. Bricard and the variants were selected if the expression of the gene was equal or higher than the median expression of all protein-coding genes.

Later on, to standardize the identification and selection of somatic non-synonymous mutations for all 6 tumors, whole-exome sequencing (WES) data of P142 and P143 were reanalyzed entirely, mRNA-Seq performed and analysed with the selection criteria of the 4 latter tumors. Most previously selected variants were identified (28 out of 35 mutations for P142, 106 out of 117 mutations for P143). As the variant calling criteria and gene expression selection were less stringent, additional variants were identified, but we did not test them for recognition by TIL clones. Figure 2-7 and Figure 2-8 highlight the similarity of the first and second analyses for the missense variants of P142 and P143.

In summary, 22 to 106 missense SNVs and 1 to 4 indels were selected for each of the 6 tumors by our standardized approach (Table 2-2). For each SNV, a precursor peptide of 19 amino acids (19mer) with the mutated amino acid at position 10 was synthesized (Figure 2-6). Five mutations (2 for P143, 1 for P154 and 3 for LB5784) were close to a splice site with 2 alternative mRNA transcripts, and the precursor peptide for each of the 2 mRNA transcripts was synthezised. For frameshift mutations (*i.e.* indels), we selected overlapping 19mer precursor peptides to cover the new protein sequence resulting from the frameshifts, until the first stop codon.

	P142	P143	P154	P195	P223	LB5784
SNVs :						
Missense	113	450	71	58	122	67
+ varN = 0	102	405	65	46	109	58
+ Gene expr >median	48	267	39	24	49	34
+ Accepted in IGV	47	251	31	22	45	34
Selected	28	106	31	22	45	34
% of select./missense	25	24	44	38	37	51
Peptides	28	108*	32*	22	45	37*
Indels :						
Frameshift	36	105	16	30	38	43
+ varN = 0	13	31	8	9	21	24
+ Gene expr >median	3	21	3	7	11	17
+ Accepted in IGV	1	3	0	1	4	2
Selected	1‡	0†	0	1	4	2
Peptides	3	0	0	1	16	13

Table 2-2. Selection of candidate mutant antigens.

First selection step: varN = 0 (no read supporting the variant in normal sample).
Second selection step: Gene expression higher than the median expression of all protein-coding genes.
* Variants with 2 tested peptides (2x for P143, 1x for P154 and 3x for LB5784).
‡ 2 indels were selected in the old analysis and only 1 re-identified.
† Any indel was selected in the old analysis and 3 new were found in the new selection.

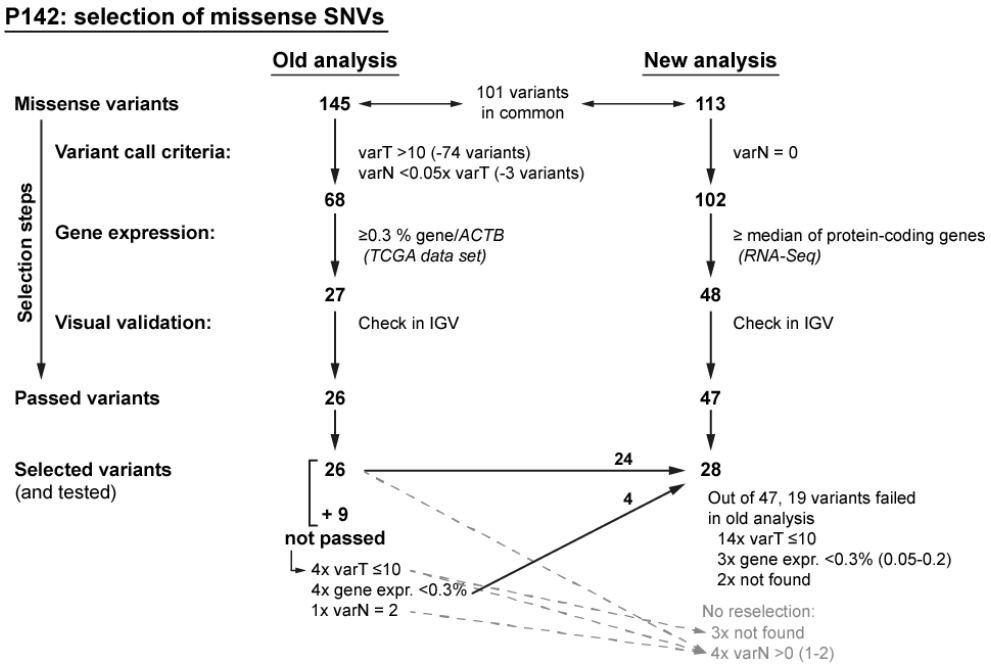

Figure 2-7. Details of missense mutation selection for the tumor of P142.

Missense SNVs are not completely identical for the old and new variant discovery analysis due to version changes of the used algorithms (from read alignment to variant annotation). Hundred and one missense variants were shared. The others are mostly variants with low number of reads supporting the variant (varT <10 in more than 80% of variants). Small changes of read numbers impact likely the variant call of Mutect when varT is low. Much more variants were eliminated in the first selection step with the old variant calling criteria (77 versus 11 variants). Around half of variants were eliminated by the gene expression selection (41 versus 54 variants). In the old selection, 9 unselected variants were selected for further testing in an exploratory approach. Four out of these 9 passed the selection in the new analysis. varT= number of variant reads in the tumor sample, varN = number of variant reads in the normal sample.

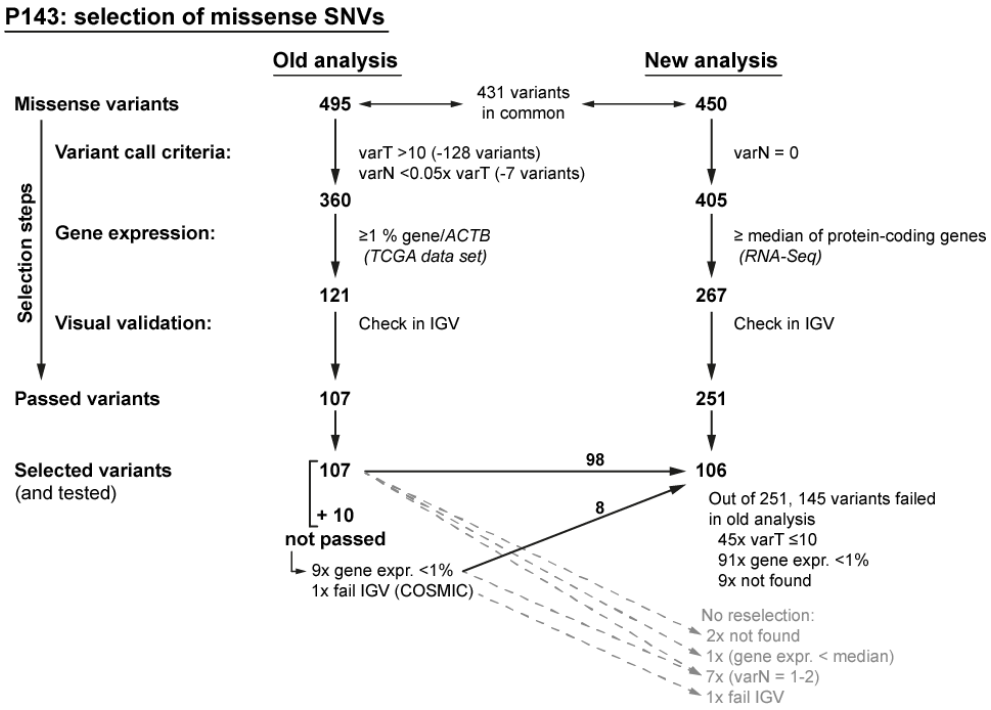

Figure 2-8. Details of missense mutation selection for the tumor of P143.

Missense SNVs are not completely identical for the old and new variant discovery analysis. 431 missense variants are shared. The others result mostly from the same cause as for P142. Additional difference is caused by variant annotation errors of SnpEff (±25% of reads). Many more variants were eliminated in the old analysis by the variant calling criteria (135 versus 45 variants). More variants were also eliminated by gene expression selection in the old analysis (64%) than in the new (34%) because of the used thresholds. In the old selection, 10 unselected variants were selected for further testing in an exploratory approach. Eight out of these 10 passed the selection in the new analysis. varT= number of variant reads in the tumor sample, varN = number of variant reads in the normal sample.

2.3.2 Selection of candidate MAGE-type antigens

Autologous EBV-B cells were retrovirally transduced with cancer-germline genes selected for their expression in the tumor (Table 2-3). In preliminary experiments we verified gene expression and antigen processing of *MAGEA3*-transduced EBV-B cells from HLA-A1^{+} patients (P142 and P223) and activation of T cell clone WEIS3E5, which is specific for a MAGEA3 antigenic peptide presented by HLA-A1 (Figure 2-9).

Gene expression (FPKM)	**P142**	**P143**	**P154**	**P195**	**P223**	**LB5784**
MAGEA1	0	0	0	0	0	0
MAGEA3	117	0	33	0	25	12
MAGEA4	0	0	0	0	2	48
MAGEA6	58	0	22	0	24	9
MAGEA9	0	0	0	0	0	55
MAGEA10	0	0	11	0	0	33
MAGEA12	49	0	6	0	0	3
NYESO1	0	0	4	0	0	51
CTAG2	0	0	2	3	0	6
ERBB2	46	61	1,924	2,178	47	30
ACTB	1,414	1,767	2,516	2,953	1,891	1,688

Table 2-3. Expression of some cancer-germline genes, *ERBB2 and ACTB*.

Gene expression analysed by mRNA-seq and indicated in fragments per kilobase of transcript per million fragments mapped (FPKM). Highly expressed cancer-germline genes and overexpressed *ERBB2* were selected (in bold). We did not succeed to transduce EBV-B cells from LB5784 with a *MAGEA9* construct. Expression profiles of 8 cancer-germline genes were confirmed by RT-PCR for P142, P143, P154, P195 and P223 (data not shown). Expression of *ACTB* is given as a reference point.

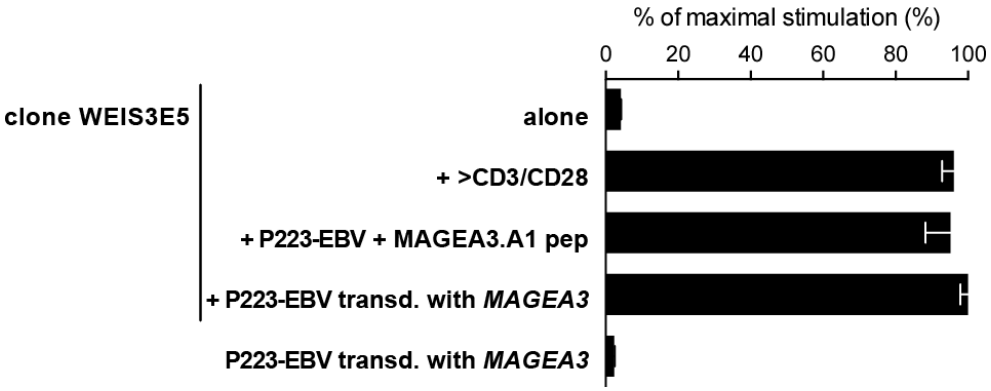

Figure 2-9. Recognition of *MAGEA3*-transduced P223-EBV by an anti-MAGE3.A1 CTL clone.

MAGEA3-transduced EBV-B cells were tested for antigen presentation. An example is shown with *MAGEA3*-transduced EBV-B cells from P223 (P223-EBV). CTL clone WEIS3E5 is specific for peptide $MAGEA3_{168-176}$ presented by HLA-A1 (MAGEA3.A1). WEIS3E5 was stimulated with anti-CD3/CD28 beads to test its cytokine secretion. Peptide MAGEA3.A1 was pulsed at 2 µM on non-transduced P223-EBV cells as a control. T cell activation was assessed with the M-07e assay (detection of IL-3 and GM-CSF). Test performed in triplicates (Mean value, ±SD).

2.3.3 HER2

The EBV-B cells of patients with HER2^{+} tumors (P154 and P195) were transduced with an *ERBB2* cDNA. HER2 expression was confirmed by flow cytometry (Figure 2-10). About half of the transduced EBV-B cells expressed HER2 stably. This proportion suffices to stimulate anti-HER2 TIL clones.

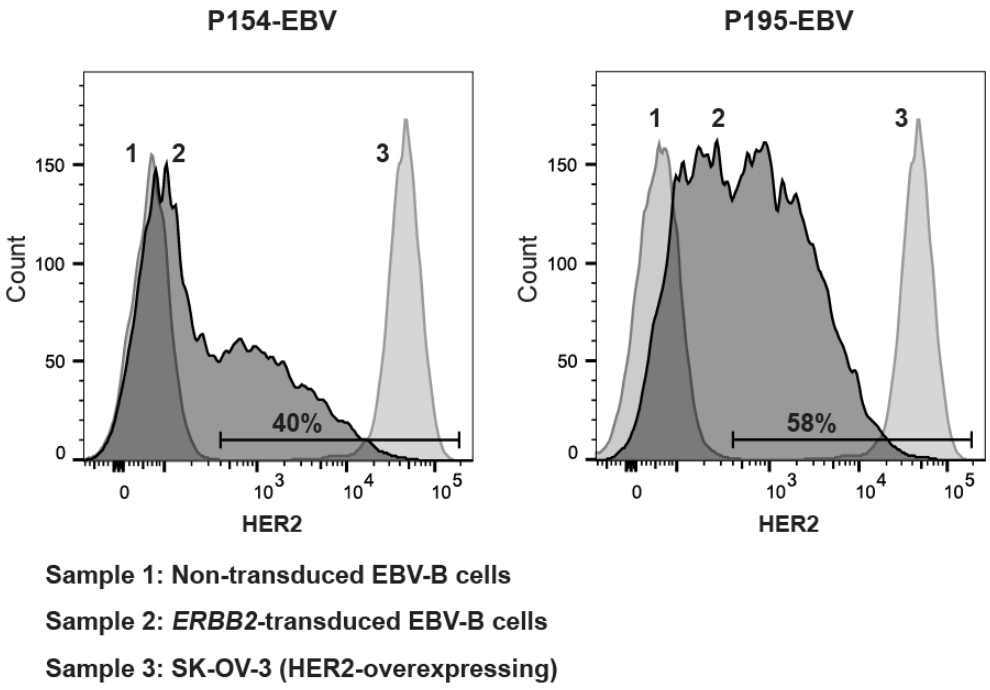

Figure 2-10. HER2 expression by *ERBB2*-transduced EBV-B cells.

Analysis of HER2 expression by flow cytometry. Cells were first selected in FSC-SSC gate. SK-OV-3 is a HER2-overexpressing human ovarian tumor cell line.

2.4 Screening of CD8 TIL clones for recognition of the candidate tumor antigens

Each CD8 TIL clone was tested individually for its recognition of the mutant precursor peptides, selected cancer-germline genes or *ERBB2*. Peptides were tested at 20 µM either individually (poorly soluble peptides) or in pools of 2-4 peptides (only clones of P142 were tested at 10 µM and in pools of 5-7 peptides). Autologous EBV-B cells were first incubated 2 hours with the peptides, before addition of the TIL clones for an overnight co-culture. The cytokine secretion upon T cell activation determined the activation of clones. Cytokine secretion was measured with the M-O7e cell assay (Figure 2-11). The proliferation of the human megakaryoblastic leukemia cell line M-07e depends mostly on either IL-3 or GM-CSF, with lower growth factor activities for IL-2, IL-4, IL-6 and IL-9[112,113].

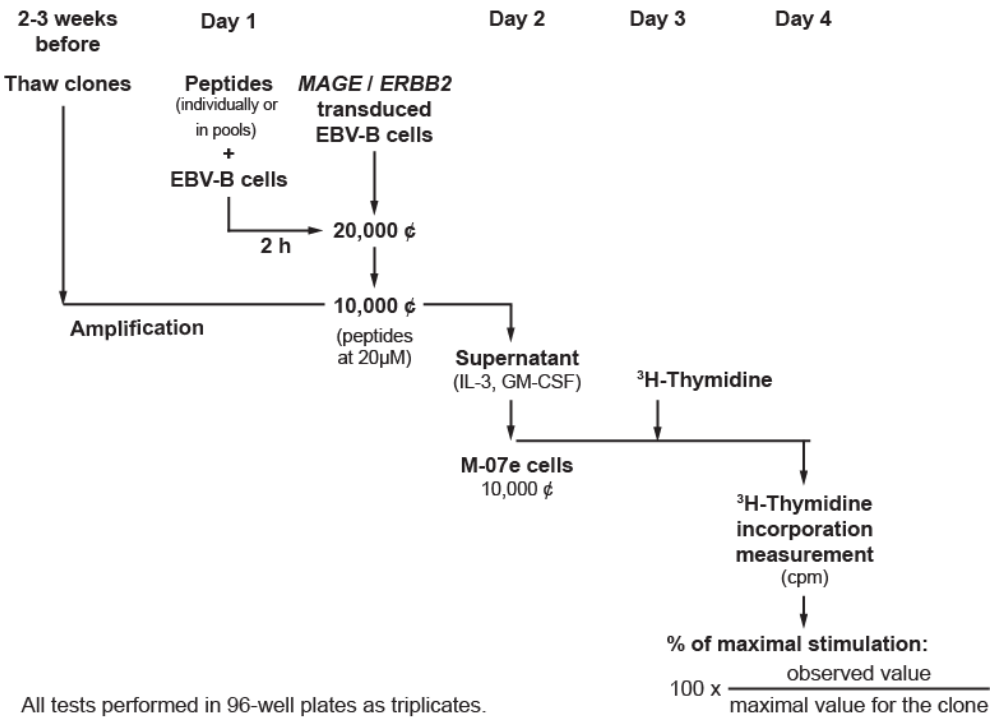

Figure 2-11. Screening of CD8 TIL clones for recognition of tumor antigens.

2.4.1 Recognition of mutant peptides by clones of patient P143

As shown on Table 2-4, most results of our screening were negative. None of the clones of 5 out of the 6 patients recognized any of the candidate mutant peptides. A total of 485 CD8 TIL clones failed to recognize candidate mutant peptides encoded by 23 to 49 mutations per patient. Moreover, 343 TIL clones from 4 patients were screened against MAGE-type antigens encoded by 2 or 3 cancer-germline genes, also with negative results. Finally, 203 TIL clones from two patients were tested for recognition of *ERBB2*-encoded antigens, with negative results. We tentatively conclude that in the majority of primary breast carcinomas, even of the triple-negative subtype, tumor-specific TIL clones are not present at frequencies around or higher than 10^{-2} of the CD8 TILs.

	P142	**P143**	**P154**	**P195**	**P223**	**LB5784**
Tumor	ER^+HER2^-	ER^+HER2^-	$HER2^+$	$HER2^+$	TN	TN
Candidate tumor antigens, encoded by:						
Mutations	29	106	29	23	49	36
Cancer-germline genes	MAGEA3 MAGEA6 MAGEA12		MAGEA3 MAGEA6		MAGEA3 MAGE*A6*	MAGEA4 MAGEA10 NYESO1
ERBB2			ERBB2	ERBB2		
Tested clonotypes	100	57	61	142	82	100
Results	0	6	0	0	0	0

Table 2-4. Results of CD8 TIL clone screening.

For P154, 2 out of 31 mutations (SNVs) could not be tested and are not reported in this table. The 2 resulting peptides were tested together in a mix that was toxic to the EBV-B cells (data not shown). One hundred out of 203 TIL clones from the patient LB5784 were tested for recognition of candidate tumor antigens.

However the conclusion was different for patient P143. We found 7 clones of 6 clonotypes that recognized 4 different mutant peptides (Figure 2-12, Table 2-5). Clones 23/29 (same clonotype) and 99 recognized the same precursor peptide within a mix of 2 peptides (data not shown). Clones 26 and 44 recognized another precursor peptide in a mix of 2 peptides (data not shown). Clones 52 recognized 3 different peptides and clone 57 recognized 2 other different peptides. However after purification of the synthesized peptides, single precursor peptides were recognized by clones 52 and 57 (data not shown).

Clone (918/...)	**Mutated gene**	**Precursor peptide sequence**
23/29 and 99	PRR12	HDELYLPPMWKIDGLLNEH
26 and 44	ATP2A2	AKTASEMVLVDDNFSTIVA
52	NOC2L	AYQHAFLYIHQLAIHLRNA
57	TKT	MAVLFFHTMCYKSQDPRNP

Table 2-5. Recognition of mutant peptides by the 6 different TIL clonotypes of P143.

The mutant amino acid is underlined.

Based on these results, we pursued our work along two lines. First, we analyzed in detail the antitumor T cell response of P143. Which are the exact antigenic peptides recognized by the 6 clones? Which HLA class I molecules present these peptides? Are these peptides naturally processed in cells? Are these TIL clones cytolytic T lymphocytes? Are they present in the blood?

Then we investigated differences between the tumor P143 and the other 5, trying to find explanations for the immunogenicty of the former but not of the latter.

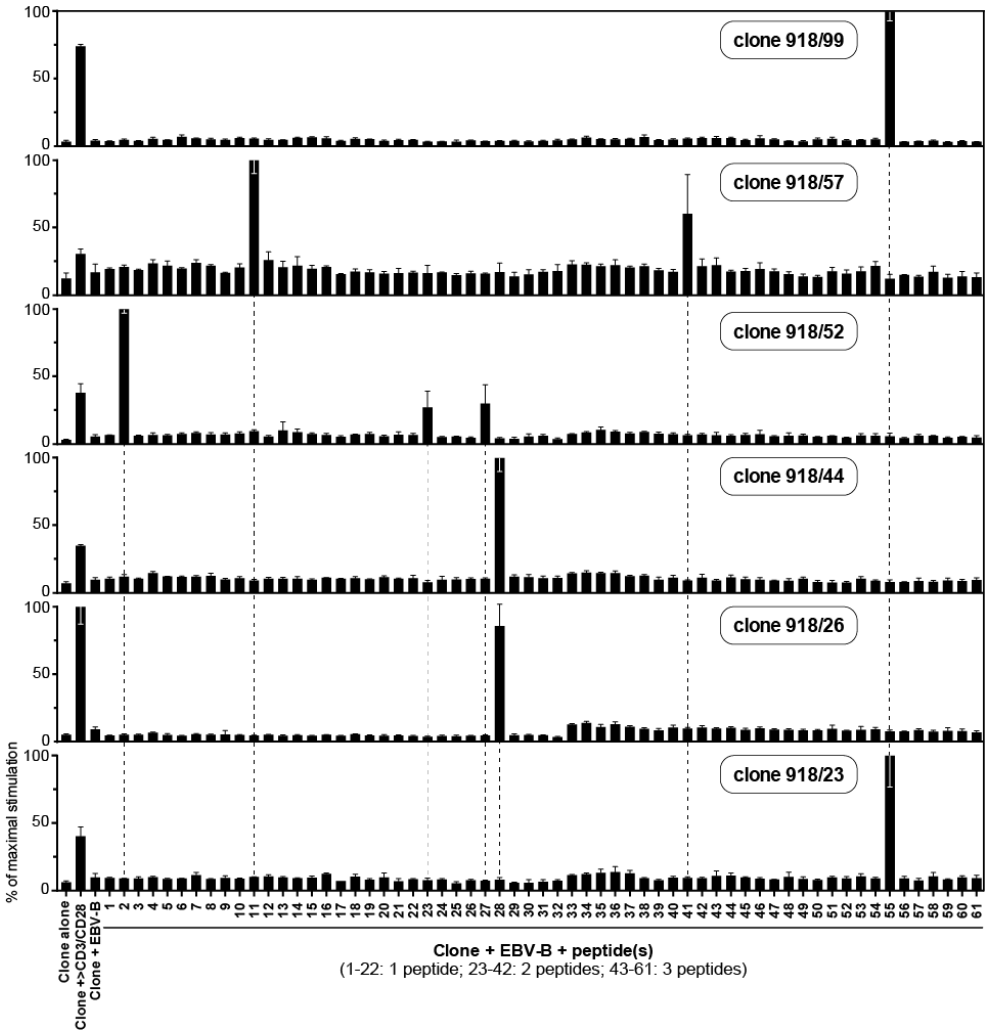

Figure 2-12. Presence of CD8 TIL clones of P143 that recognized mutant peptides.

Tests performed in triplicates (Mean value, ±SD).

2.5 Detailed specificities of P143 TIL clones

2.5.1 Identification of the antigenic peptide recognized by TIL clones

Clones 23 and 99 recognized the precursor peptide HDELYLPPMWKIDGLLNEH encoded by gene *PRR12*. We synthesized peptides shortened at the N-terminus or the C-terminus. The loss of aspartic acid at position 2 abrogated T cell activation (Figure 2-13). Peptides of 8 to 11 amino acids with the aspartic acid at the N-terminus were tested and maximal activation of clones 23 and 99 was observed with the $PRR12_{1875\text{-}1883}$ peptide DELYLPPMW of 9 amino acids.

We used the same approach for the precursor peptide AKTASEMVLVDDNFSTIVA encoded by gene *ATP2A2*, recognized by clones 26 and 44. Trimming of serine at P5 or phenylalanine at P14 abrogated T cell recognition. The $ATP2A2_{730\text{-}739}$ peptide SEMVLVDDNF of 10 amino acids stimulated optimally the 2 clones.

We carried out similar experiments to identify the optimal antigenic peptides encoded by genes *NOC2L* and *TKT* and recognized by TIL clones 52 and 57, respectively. The optimal antigenic peptides are shown in Table 2-6.

Clone (P143 918/...)	Mutated gene	Optimal antigenic peptide	
23 and 99	PRR12	DELYLPPMW	($PRR12_{1875\text{-}1883}$)
26 and 44	ATP2A2	SEMVLVDDNF	($ATP2A2_{730\text{-}739}$)
52	NOC2L	FLYIHQLAI	($NOC2L_{378\text{-}386}$)
57	TKT	VLFFHTMCY	($TKT_{50\text{-}58}$)

Table 2-6. Optimal antigenic peptides recognized by the 6 TIL clones of P143.

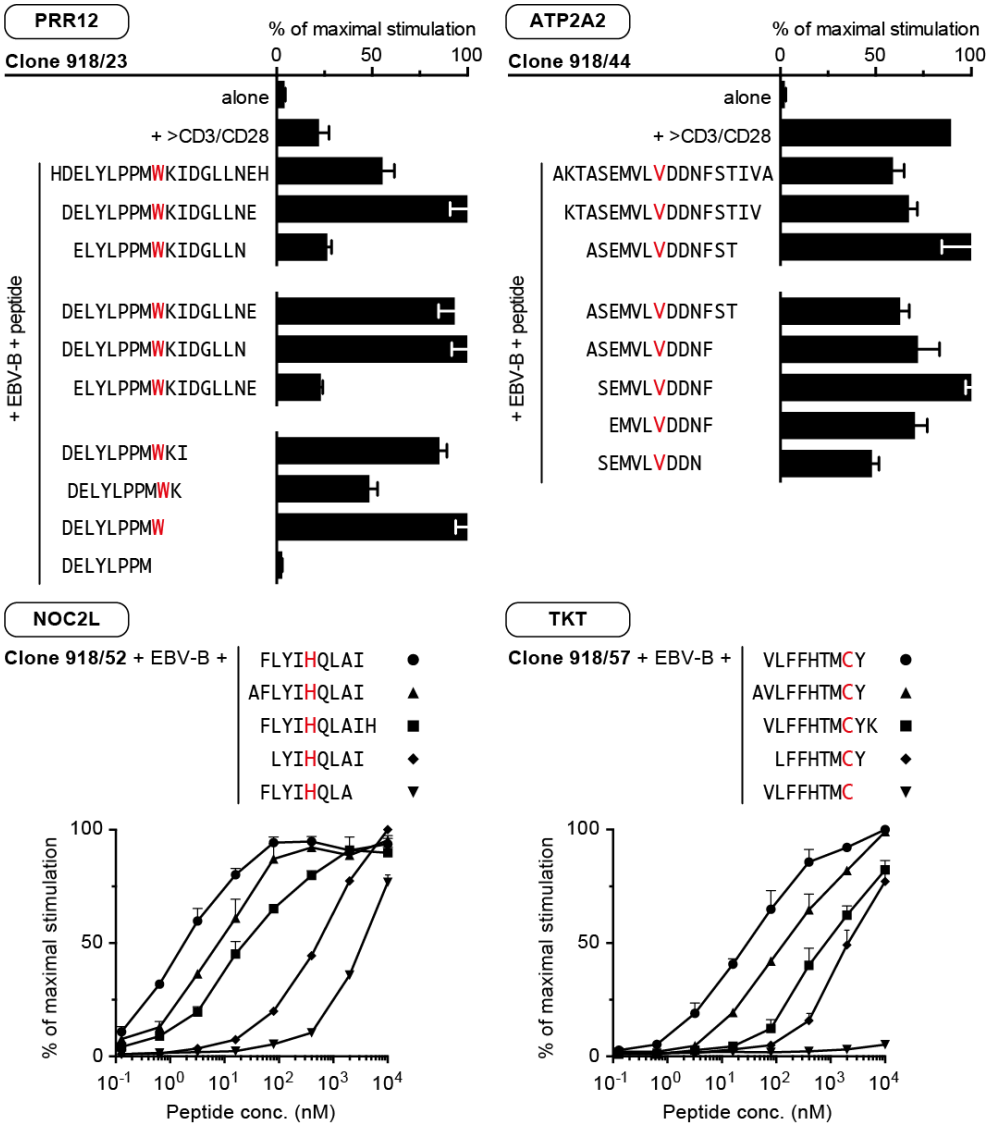

Figure 2-13. Determination of the optimal antigenic peptides.

Trimming of the precursor peptides of 19 amino acids was performed in different experiments for each precursor peptide. The mutant amino acid is highlighted in red. The experiments with the PRR12 peptide used TIL clone 23: the 1rst and 2nd experiments were performed with 20 µM of peptides and the 3rd experiment was performed with 0.5 µM. The experiments with the ATP2A2 peptide used clone 44: all experiments with 10 µM of peptides. For the NOC2L and TKT peptides, only the results with the peptides of 8 to 10 amino acids are shown. T cell activation was tested with the M-07e assay (mean, ±SD).

2.5.2 Specificity of the TIL clones for the mutant vs wild-type peptides

For each TIL clone, we tested their specificity for the mutant antigenic peptide by titrating both mutant and wild-type peptides. The clones were not or 1,000-fold less activated by the wild-type peptides, demonstrating their tumor-specificity (Figure 2-14).

The concentrations of mutant peptides required for half-maximal activation ranged from 1-30 nM for clones 26, 52 and 57 to 100-400 nM for clones 23 and 99, and more for clone 44 (plateau not reached). Except for clone 44, these results are similar to those observed for several tumor-specific CD8 T cell clones from a patient with metastatic melanoma[60], even though half-maximal activations at 1 nM have been observed for other tumor-specific CD8 T cells[58,59,62].

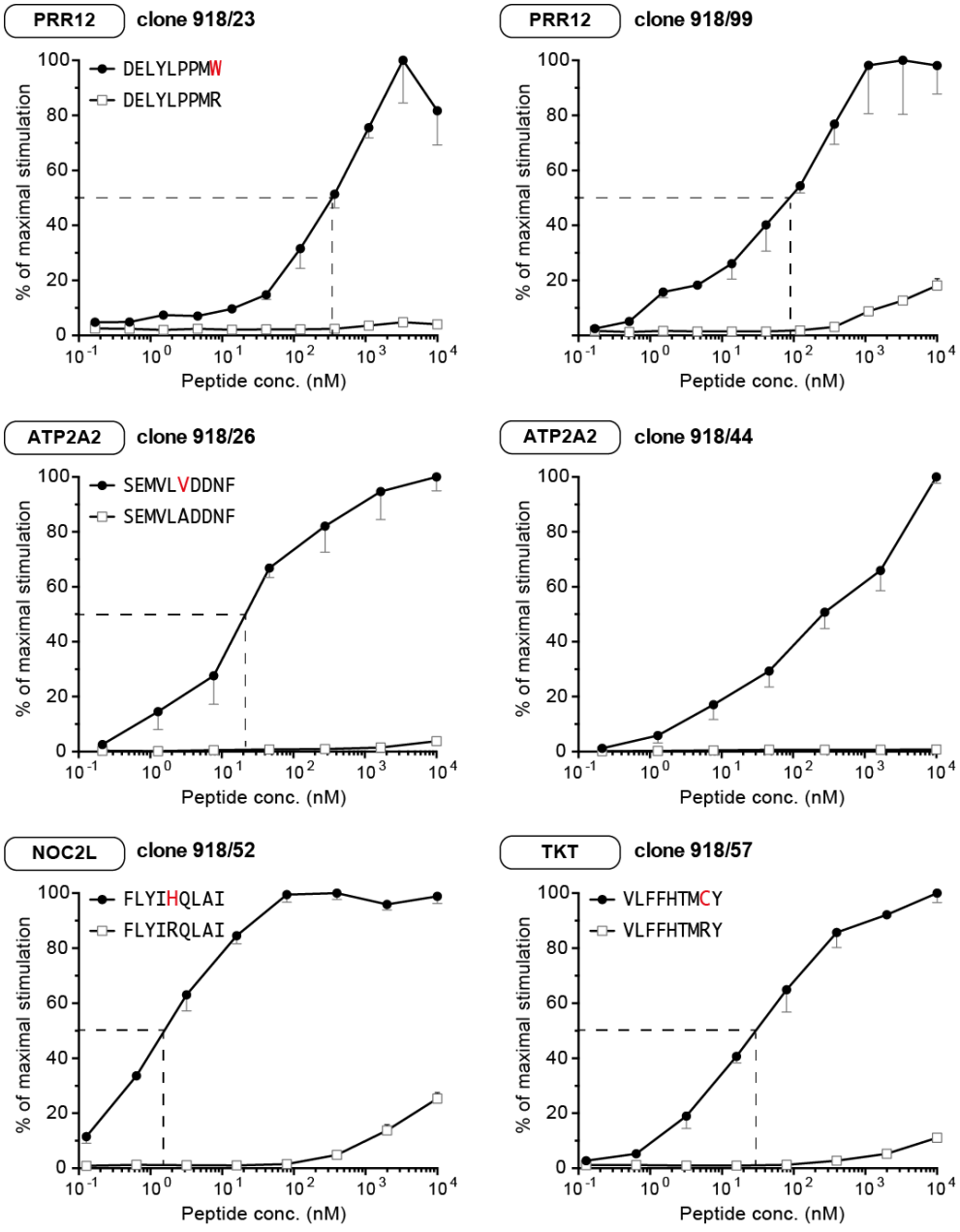

Figure 2-14. Titration of mutant and wild-type peptides.

Mutant peptides and wild-type peptides were pulsed on autologous EBV-B cells. Mutant and wild-type PRR12 peptides were purified. T cell activation was measured with the M-07e assay (mean, -/+SD).

2.5.3 Identification of the presenting HLA molecules

Having defined the 4 optimally recognized mutant antigenic peptides, we used the NetMHC algorithm (v3.4[114-116]) to predict the presenting HLA molecules. These were HLA-B*44:03 for both the PRR12 and ATPA2 peptides, A*02:01 for the NOC2L peptide and A*80:01 for the TKT peptide.

We confirmed these predictions with allogenic EBV-B cell lines that shared HLA class I molecules with the patient. The specific HLA for each antigenic peptide can be identified by testing the T cell recognition of peptide-pulsed EBV-B cells that match only for one HLA allele with P143. The $PRR12_{1875-1883}$-specific clones 23 and 99 recognized an HLA-B*44:03-matched peptide-pulsed EBV-B cell line (LB-17, Figure 2-15-A). The $ATP2A2_{730-739}$-specific clones 26 and 44 recognized the same HLA-B*44:03-matched peptide-pulsed EBV-B cell line (Figure 2-15-B). For the $NOC2L_{378-386}$-specific clone 52, the antigenic peptide was presented by HLA-A*02:01 (Figure 2-15-C). NetMHC predicted the binding of the TKT peptide to HLA-A*80:01. This HLA is very rare in the Caucasian population (0.01-0.02% of allele frequency[117]) and was not present in our EBV-B collection. With an allogenic EBV-B cell line that matched all HLA class I molecules except HLA-80:01 (LB2369), we tested the loss of recognition with LB2369-EBV cells compared with P143-EBV cells. Indeed, we observed that clone 57 could not recognize the TKT_{50-58}-pulsed LB2369-EBV cells (Figure 2-15-D).

Missense mutations can create an epitope (*i.e.* part of the peptide that interacts with the TCR) or an agretope (*i.e.* part of the peptide that interacts with the HLA molecule) in an antigenic peptide. The last situation applies to PRR12 peptide DELYLPPMW. Changing wild-type arginine into tryptophan at P9 creates a binding motif for HLA-B*44:03 molecules. Hydrophobic aromatic amino acids (phenylalanine, tryptophan or tyrosine) are preferred at the C-terminal anchor for HLA-B44:03, but not the charged arginine (IEDB[118]: www.iedb.org). As a consequence, the wild-type peptide has a low predicted binding affinity (Kd of 8,559 nM, NetMHC) when compared to the mutant peptide (Kd of 47 nM).

The 3 other mutations resulted in new epitopes recognized by the TCR. Both wild-type and mutant peptides were predicted to have similar HLA-binding affinity (Kd <50 nM, Table 2-7).

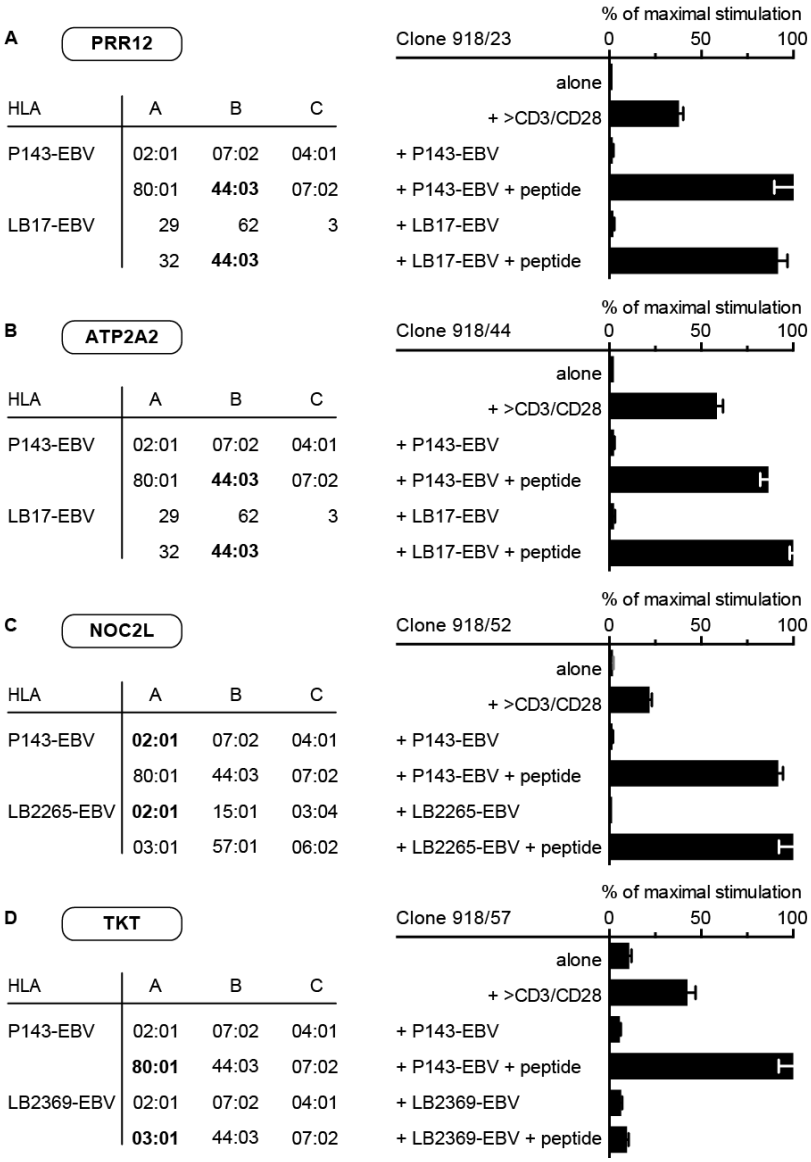

Figure 2-15. Determination of the presenting HLA class I molecules.

The HLA class I molecules shared between P143-EBV and allogenic EBV-B cell lines are in bold for the experiments with the PRR12, ATP2A2 and NOC2L peptides (A-C). For the TKT peptide, the HLA class I molecules that differ between P143-EBV and the allogenic EBV-B cells are in bold (D). For PRR12 and ATP2A2, representative results for TIL clones 23 (A) and 44 (B) are shown (peptides tested at 50 nM). Peptides at 80 nM for the anti-NOC2L TIL clone 52 (C), and at 1 µM and washed for the anti-TKT TIL clone 57 (D). T cell activation was measured with the M-07e assay (mean ±SD).

2.5.4 Cytolytic activity and cytokine secretion by T cells

We tested the cytolytic activity and the cytokine secretion profile of the 6 tumor-specific TIL clones. All of them lysed autologous EBV-B cells pulsed mutant peptides, while no lysis was observed after pulsing with the wild-type peptides (Figure 2-16-A). NK target cells K562 were not lysed either. Thus all these CD8 TIL clones are tumor-specific CTLs.

Regarding the cytokine secretion profiles, all clones secreted TNFα and IL-13. IFNγ and IL-5 were secreted at low levels, whereas GM-CSF, G-CSF, IL-6 and IL-17 were secreted at very low levels or not at all (Figure 2-16-B, maximal concentration of G-CSF, IL-6 and IL-17 was 60 pg/mL). IL-2 was not tested as it was present (7.5 U/mL) in the culture medium. IL-8 and IL-10 were significantly secreted by clone 26 (530 pg/mL and 130 pg/mL, respectively) and less by clone 44 (~5x and ~1.5x less). Clone 57 also secreted IL-8 (130 pg/mL). IL-1β, IL-4, Il-7, IL-12 and MCP-1 were not secreted. The EBV-B cells themselves secreted CCL4.

As often observed with human T cell clones, the cytokine profiles are neither clearly Th1 (IFNγ, TNFα, GM-CSF) nor clearly Th2 (IL-4, IL-5, IL-13). The trend is nevertheless a Th2-like profile (IL-5 and IL-13 with low IFNγ) for clones 44, 99 and 52, while clone 26 is Th1-like (IFNγ, TNFα with low IL-5).

We observed little GM-CSF (a maximum of 45 pg/mL by clone 918/26). As M-07e cells depend mostly on GM-CSF or IL-3 for growth, we surmised but did not check that our clones produced IL-3. TNFα could have been an alternative to IL-3 and GM-CSF for the analysis of T cell activation. However, EBV-B cells can also secrete TNFα, which would have hampered the interpretation of the results.

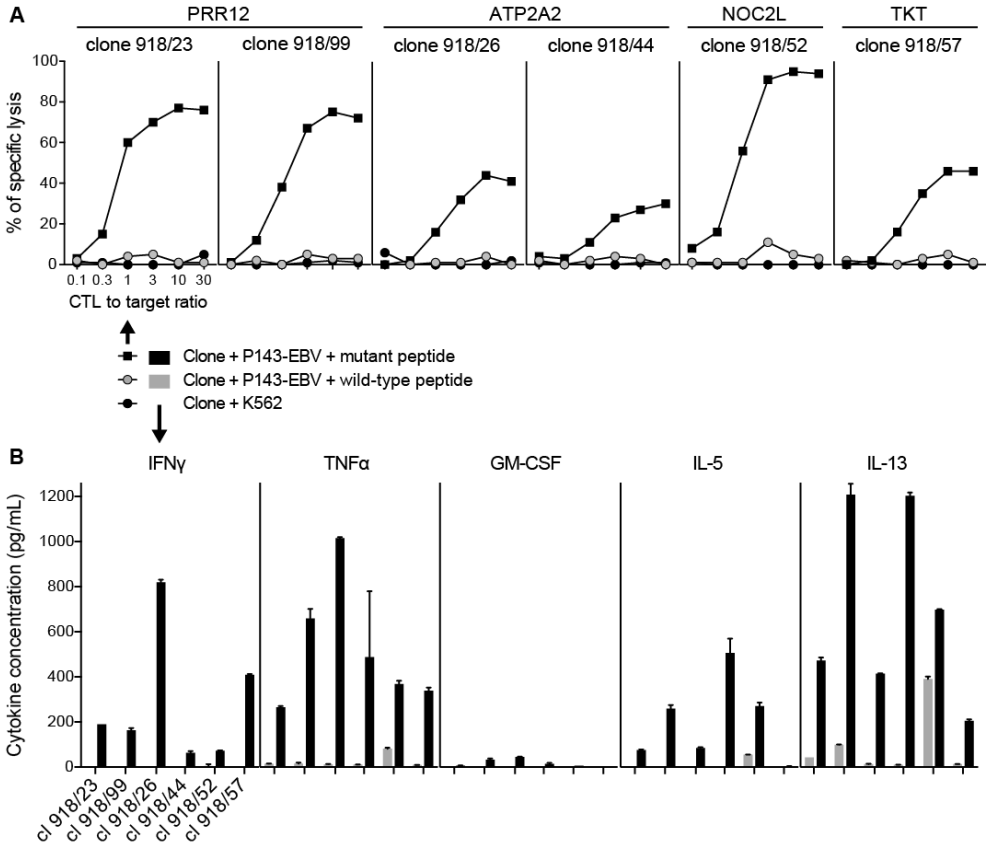

Figure 2-16. Cytolytic activity and cytokine secretion profile of the tumor-specific TIL clones.

A. Cytolytic activity was tested in a standard 4-hour ^{51}Cr-release assay. Target cells included P143-EBV cells pulsed with wild-type and mutant peptides at 10 µM, and K562 cells. The means of triplicates are shown.

B. Cytokine secretion (array of 17 cytokines). The most secreted cytokines are shown, except for GM-CSF. Test performed in duplicates (mean ±SD).

2.5.5 Antigenicity of tumor P143

We used HLA-matched allogenic tumor cell lines or HLA-A*80:01 transfected 293T cells to verify that the identified mutant antigenic peptides could indeed be naturally processed by these cells. Cells were transfected with mutated or wild-type (WT) minigene constructs coding for proteins of 100 amino acids with the mutant or wild-type amino acid in their middle (Figure 2-17-A). The tumor-specific CTL clones recognized transfectants expressing the mutated but not the wild-type constructs (Figure 2-17-C). We conclude that the mutant antigenic peptides can be processed, most probably through the classical proteasome/TAP/ER pathway, from the mutated gene products.

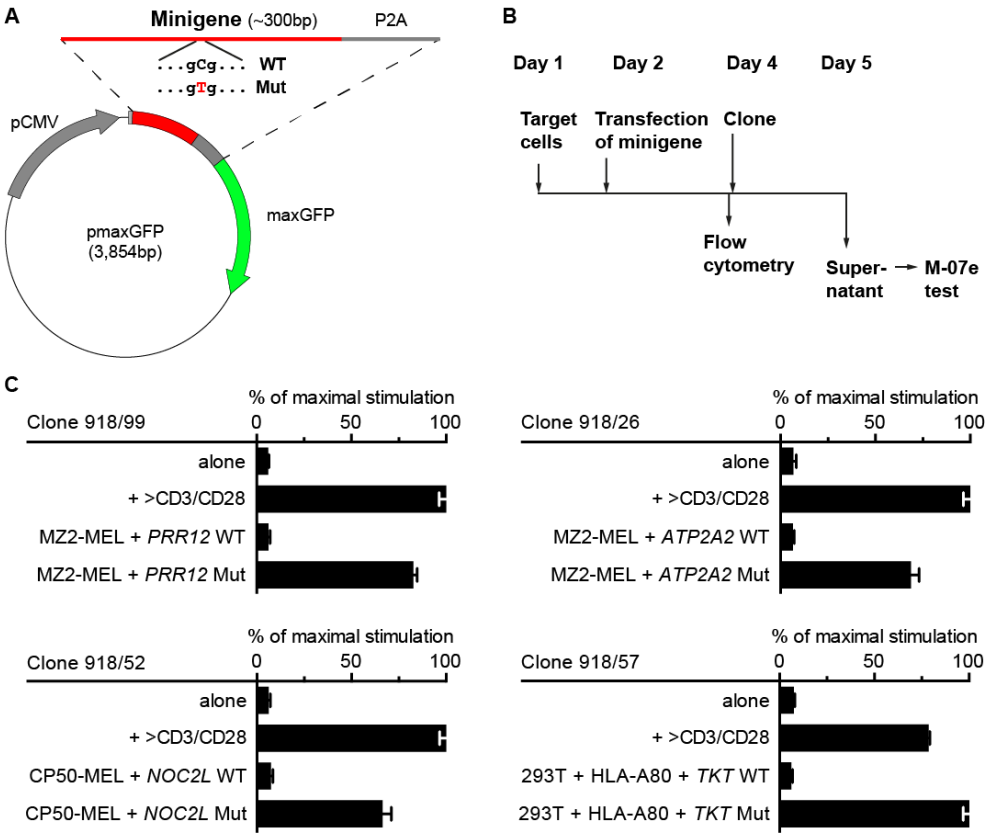

Figure 2-17. Antigen processing.

A. The wild-type (WT) and mutated (Mut) minigenes were cloned into the pmaxGFP vector in frame with the P2A sequence ('self-cleaving' peptide) and maxGFP.

B. Two days after transfection, maxGFP expression was checked by flow cytometry. The proportions of GFP^+ target cells were similar for the WT and Mut transfectants: 8% for *PRR12*-transfected tumor cells (MZ2-MEL), 5-6% for *ATP2A2*-transfected tumor cells (MZ2-MEL), 13% for *NOC2L*-transfected tumor cells CP50-MEL and 58-60% for [*TKT* + HLA-A*80:01]-cotransfected 293T cells. Experiments were performed twice with one TIL clone per antigen. T cell activation was measured with the M-07e assay (mean ±SD).

2.5.6 Mutated genes encoding the four antigenic peptides

Table 2-7 summarizes our results. CD8 TIL clones of 6 distinct clonotypes recognized four different mutant antigenic peptides presented by three different HLA class I molecules. Each antigen was encoded by a missense SNV in a distinct gene.

The Proline-rich protein 12 (*PRR12*) gene is an ubiquitously expressed protein-coding gene[119] of unknown function (gene expression profile provided by the Human Protein Atlas[120]: www.proteinatlas.org).

Gene *ATP2A2* codes for one member of the sarcoplasmic/endoplasmic reticulum Ca^{2+}-ATPase (SERCA2) family, which translocates Ca^{2+} from the cytosol into the sarcoplasmic or endoplasmic reticula in muscle cells[121]. The protein is involved in the regulation of the contraction/relaxation cycles by changing the cytosolic Ca^{2+}-concentration. The gene is expressed ubiquitously at low levels and in heart and skeletal muscle at high levels[120]. Germline mutations cause the autosomal dominant Darier-White skin disease. The somatic mutation in tumor P143 is not reported as causative in Darier-White patients. Decreased or increased expression of *ATP2A2* has been reported in oral squamous cell carcinomas, colon and lung carcinomas[121]. A change of gene expression has also been associated with cell proliferation of the human tumor cell lines MCF-7[122] (breast carcinoma) and SW872[123] (liposarcoma).

The ubiquitously expressed gene *NOC2L* (NOC2-like nucleolar associated transcriptional repressor) encodes an inhibitor of the histone acetyltransferase p300/CBP and prevents histone acetylation[124]. NOC2L is a transcriptional corepressor that binds to p53-regulated promoters and inhibits p53-mediated gene expression[125]. There is no reported role for NOC2L in cancer.

Gene *TKT* encodes the enzyme transketolase, active in the pentose phosphate pathway[126]. Its expression is ubiquitous[120]. *TKT* expression is increased in hepatocellular carcinomas with aggressive clinico-pathological features[126].

Table 2-7. Tumor-specific CTL clones and their target antigens.

Clones (918/)	Gene	Mutation	Entries in COSMIC (v76)	Mutated allele frequency in the exome	Gene expr. (FPKM)	Mutant residue	Antigenic peptide	HLA	HLA-binding prediction (Kd, nM)	
									Mut. pept.	WT pept.
23/29 + 99	*PRR12*	C > T	0	0.11	9	R1883W	DELYLPPMW	B*44:03	47	8559
26 + 44	*ATP2A2*	C > T	1‡	0.14	75	A735V	SEMVLVDDNF	B*44:03	40	37
52	*NOC2L*	C > T	1†	0.17	44	R382H	FLYIHQLAI	A*02:01	16	31
57	*TKT*	C > T	0	0.17	155	R57C	VLFFHTMCY	A*80:01	10	12
	TP53	C > T	704 / 79*	0.17	33	R273H			276	313

TIL clones 23 and 29 are of the same clonotype. The missense mutation in *TP53* is given as an example. COSMIC (catalogue of somatic mutations in cancer): ‡ found in one kidney cancer; † found in one endometrial cancer; * found in 704 cancers and 79 breast cancers. Expression levels of genes *ACTB* and *GAPDH* were 1,767 and 1,161 FPKM, respectively. HLA class I binding affinity predicted with NetMHC v3.4.

While we cannot exclude that these mutations have an oncogenic effect in tumor P143, it is more likely that they are passenger mutations. They are absent, or present in a single tumor, in more than 25,000 tumors (≤ 0.004%) of the COSMIC[127] database (Catalogue of somatic mutations in cancer, v.77: cancer.sanger.ac.uk/cosmic). By contrast, the *TP53* missense mutation R273H, which is present in tumor P143, is reported in 0.6% of the COSMIC tumors and 11% of these *TP53*-mutated tumors are of breast origin. Moreover, the 4 mutated genes in tumor P143 are not significantly mutated in any cancer type of the TumorPortal database (http://www.tumorportal.org/[128]). Altogether these observations suggest that the 4 mutations are passenger mutations. We did not test the biological effects of the mutations.

All 4 mutations are C to T transitions. C>T transitions are the most frequent base substitutions (72% of all missense SNVs) in tumor P143 but are less frequent in the other 5 tumors analysed in this study (32-48%).

We verified that the mutated genes were indeed expressed in the P143 tumor sample. In the RNA-Seq data, the mutated alleles represent at least 29% of all reads of the gene (Table 2-8). These mutated allele frequencies (MAF) in the transcriptome are higher than those observed in the exome sequencing results, suggesting preferential or monoallelic expression of the mutated alleles by tumor cells.

Mutated gene	**Mutated allele frequency**	
	in the RNA-Seq	**in the Exome-Seq**
PRR12	0.31	0.11
ATP2A2	0.29	0.14
NOC2L	0.47	0.17
TKT	0.43	0.17

Table 2-8. Expression of the mutated genes that encode tumor antigens.

The number of reads mapped to each mutation site was counted in the genomic viewer IGV. The resulting mutated allele frequency (MAF) is the ratio of mapped reads with the mutation to all mapped reads at a mutation site. The mutated allele frequencies of the exome sequencing were calculated by Mutect.

The levels of expression of the 4 mutated genes varied from 9 to 155 FPKM, within the 38% of the most expressed protein-coding genes in tumor P143. Noteworthy, the level of expression of gene *PRR12* (9 FPKM) is only 0.5% of that of gene *ACTB* (1,767 FPKM), but sufficient to drive the surface expression of a CTL-targeted tumor-specific antigen. These observations are relevant to establish a gene expression threshold when using sequencing data to predict (mutant) tumor antigens for cancer immunotherapy.

Another issue is the possibility that functional tumor-specific CTL should decrease the proportion of antigen-positive cells and therefore the proportion of mutated reads in the exome sequencing data. Therefore the clinically most relevant tumor antigens might have escaped detection. Is there evidence for immunoselection against the 4 mutant antigens in tumor P143 ? The frequencies of the mutated reads range from 11% for PRR12 to 14% for ATP2A2 and 17% for NOC2L and TKT. The frequency of mutated reads for TP53 is also 17%. Assuming that the TP53 mutation is heterozygous, without any copy number alterations and is present in all tumor cells, about 34% of the sample is composed of tumor cells, a proportion slightly lower than that estimated by the pathologist on a frozen section (40-50%). If the 4 mutant antigens of tumor P143 are also encoded by heterozygous mutations, the proportions of antigenic tumor cells range from 65% for the PRR12-encoded antigen to 100% for the NOC2L- and TKT-encoded ones. Thus our results suggest that the six different tumor-specific CTLs detected in tumor P143 have not significantly 'immunoedited' the tumor.

2.5.7 Presence of tumor-specific CD8 T cells in the blood of P143

To further characterize the antitumor CD8 T cell response in patient P143, we looked for tumor-specific CD8 T cells in the blood. We expected, at best, a low frequency of these cells among blood CD8 T cells ($\leq 10^{-4}$), as observed previously for other tumor-specific CTL responses[10]. Thus we used a sensitive approach, mixed lymphocyte-peptide cultures (MLPC) in limiting dilution conditions, followed by multimer detection, to detect the tumor-specific T cells. Blood CD8 T cells were first stimulated with peptide during two weeks in microcultures under limiting dilution conditions. Then the cells of all microcultures were labeled with fluorescent HLA-peptide multimers and analysed by flow cytometry. The frequency of antigen-specific CD8 T cells in the blood was calculated with the

proportion of negative microcultures and the number of CD8 cells at the onset of the stimulation.

We used multimers corresponding to 3 out of the 4 tumor antigens:

- PRR12.B44 dextramers (antigen-HLA complexes bound to a dextran polymer backbone labeled with a fluorochrome),
- ATP2A2.B44 dextramers and
- NOC2L.A02 tetramers (antigen-HLA complexes bound to a fluorochrome, courtesy of D. Colau).

We produced TKT.A80 tetramers but they generated a very high non antigen-specific staining for which we have no explanation. Therefore we did not monitor the anti-TKT response.

Before the MLPC experiments we used multimers to stain directly PBMC collected 2 weeks before and one month after tumor resection. Frozen PBMC were thawed and half of them were labeled with PE-coupled NOC2L.A02 tetramers and control APC-coupled BMLF1.A02 tetramers (HLA-A*02:01-restricted EBV antigen). The other cells were labeled with the PE-coupled PRR12.B44 dextramers and APC-coupled ATP2A2.B44 dextramers. We observed a small cluster (11 cells) of ATP2A2.B44-stained cells, with a frequency at 3.3×10^{-4} of the CD8 T cells at 2 weeks before surgery (Figure 2-18). No multimer-stained cells were detected for the two other antigens.

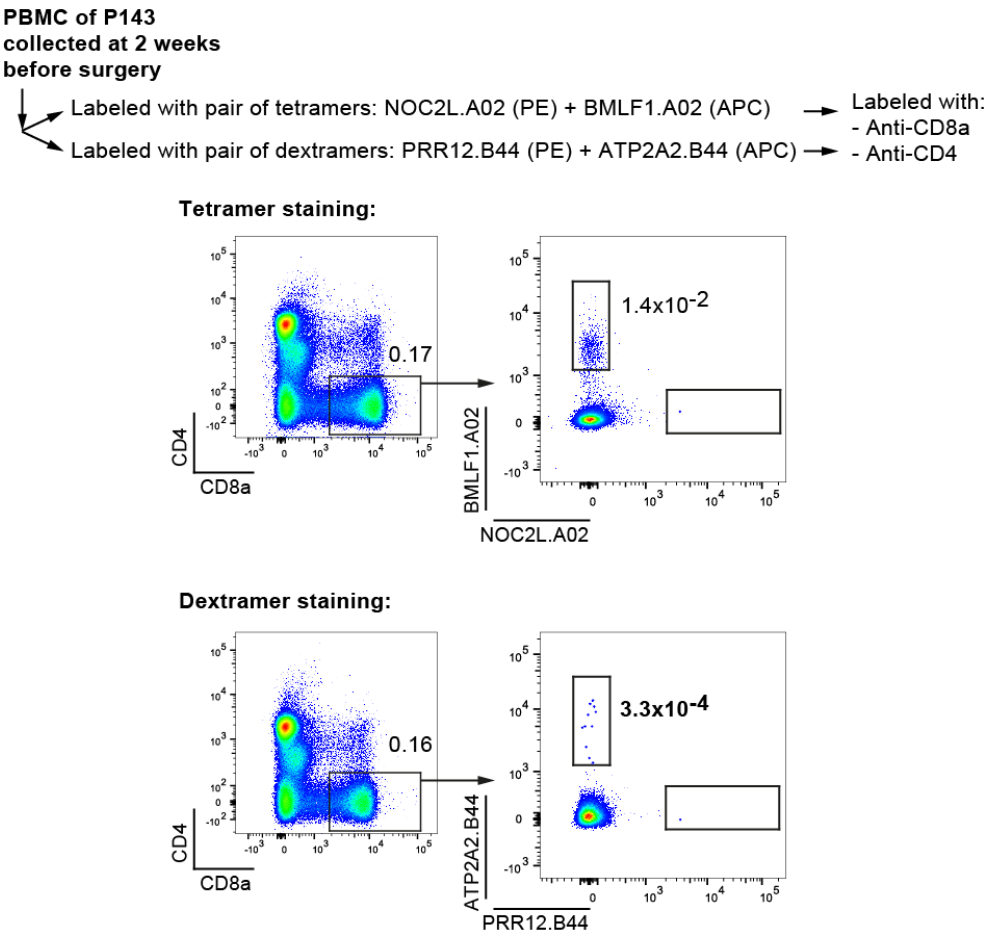

Figure 2-18. *Ex-vivo* multimer staining of PBMC of P143.

Ex-vivo analysis of PBMCs collected 2 weeks before tumor resection is shown. Labeled cells were gated first in FSC-SSC and autofluorescent cells were eliminated in an empty PercP gate. Note the presence of anti-BMLF1.A02 CD8 T cells. Positive control consisted in 3 tumor-specific TIL clones diluted among allogenic PBMCs (not shown).

We performed MLPC experiments with PBMCs collected 2 weeks before, 1 month after and 13 months after tumor resection. Frozen PBMCs were thawed, counted and the proportion of CD8 T cells determined by flow cytometry. The cells were pulsed with 10 µM of each of the 3 antigenic peptides, washed and distributed at 100,000 living cells/well (microcultures) in 100 µL of culture medium containing IL-2 and IL-7. The cells were restimulated by addition of the antigenic peptides at day 8. The presence of antigen-specific CD8 T cells was evaluated at day 15 by flow cytometry. Half of the cells of each microculture were labelled with the NOC2L.A02 and control BMLF1.A02 tetramers, the others with the PRR12.B44 and ATP2A2.B44 dextramers. Examples of positive microcultures (≥1% multimer-stained CD8 T cells) are shown in Figure 2-19.

For each of the 3 tested antigenic peptides we found at least 1 positive microculture in each PBMC collection (Table 2-9). For PBMCs collected 2 weeks before surgery, 3 out of 82 microcultures were positive for NOC2L.B44. The low proportion of positive microcultures indicates that one precursor cell was present in each microculture of 14,867 CD8 T cells. Thus, the frequency of NOC2L.A02-specific CD8 T cells is 3/(82x14,867), or 2.5×10^{-6} among all CD8 T cells. For the ATP2A2.B44 antigen, 51 out of the 82 microcultures were positive, suggesting that more than one precursor cell was present in some positive microcultures. Thus the calculated frequency of 51/(82x14,867) underestimates the precursor frequency of antigen-specific T cells among all CD8 T cells. The Poisson distribution allows to calculate a precise frequency with the probability that more than one precursor cell was distributed in some microcultures.

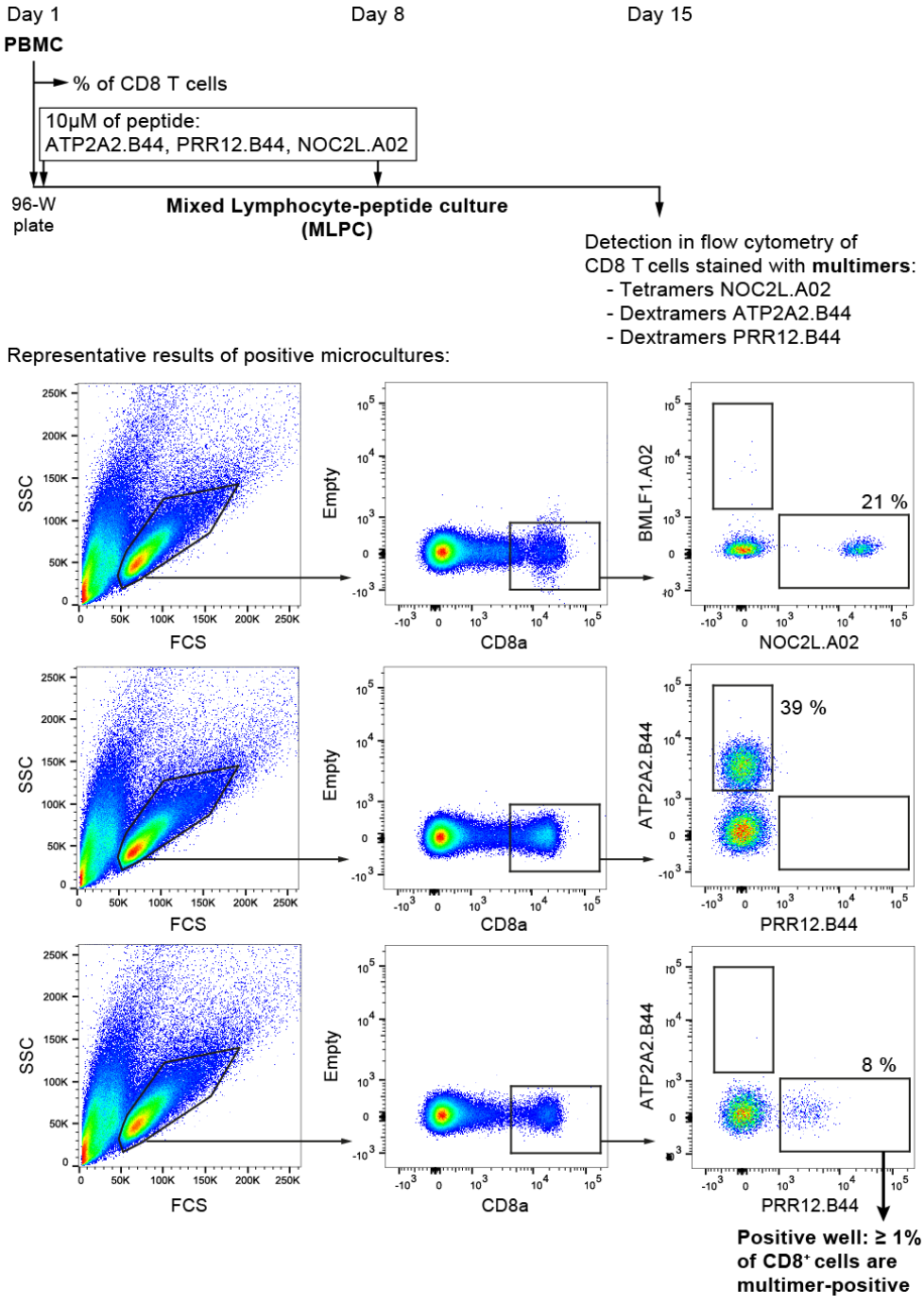

Figure 2-19. MLPC-multimer approach for PBMCs of patient P143.

The number of microcultures with one, two and more precursor cells is unknown, but the proportion of negative microcultures is known (31 out of 82 for ATP2A2.B44). For the probability of no precursor cell within a microculture, the Poisson equation is simplified to:

$$P(0) = e^{-\mu} \Rightarrow \mu = -\ln(P(0))$$

P(0) : probability of 0 precursor cell (negative microcultures)
μ : average number of precursor cells per microculture

The frequency of antigen-specific cells per microculture is the ratio of μ to the total number of cells per microculture.

$$Frequency = \frac{-\ln(P(0))}{total\ number\ of\ cells\ per\ microculture}$$

The frequency of ATP2A2.B44-specific CD8 T cells among all CD8 T cells is 6.5 x10^{-5} (equals to: -[ln(31/82)]/14,827). Table 2-9 indicates the numbers of positive microcultures and the frequencies of antigen-specific CD8 T cells in the 3 blood samples from P143.

Time from surgery (month)	**Number of stimulated CD8 T cells**	**Number of positive microcultures**			**Frequency among all CD8 T cells (x 10^{-6})**		
		NOC2L	**PRR12**	**ATP2A2**	**NOC2L**	**PRR12**	**ATP2A2**
- 0.5	82 x 14,867	3	12	51	2.5	10.6	65.4
+ 1	96 x 12,067	2	4	25	1.7	3.5	25.0
+ 13	96‡ x 14,391	1	1	7	0.7	0.8	5.5

Table 2-9. Frequencies of tumor-specific CD8 T cells in the blood of P143.

‡ 4 out of the 96 microcultures from the third time point were eliminated for PRR12.B44 and ATP2A2.B44 due to a technical problem during the flow cytometry analysis.

In all 3 blood samples, ATP2A2.B44-specific CD8 T cells were the most frequent. They were 160 times more frequent in blood collected 2 weeks before surgery than the naive CD8 T cells againt a given HLA class I-peptide complex (estimated at 4 x 10^{-7} among all CD8 T cells[7]). The frequency estimated with the MLPC-multimer approach (6.5 x 10^{-5} of the CD8 cells) was 5 times lower than that obtained with the *ex vivo* analysis (33 x 10^{-5} of the CD8 cells), suggesting that 20% of the antigen-specific CD8 T cells had proliferated sufficiently to be detected by the MLPC-multimer approach. For the same time point, anti-PRR12.B44 and anti-NOC2L.A02 CD8 T cells were 27 and 6 times more frequent than the naive cells, respectively. For all 3 antigens, the frequency of specific T cells decreased after tumor resection, reaching 0.7-5.5 x 10^{-6} of the CD8 T cells after one year (4 to 13 times less than before resection). Figure 2-20 shows the decreasing frequency of these tumor-specific blood CD8 T cells following tumor resection.

Noteworthily, the frequencies of BMLF1.A02-specific CD8 T cells were similar before and 1-month after surgery: 1.46 and 1.48 x 10^{-2} of the CD8 cells, respectively. Thus chemotherapy (fluorouracil-epirubicin-cyclophosphamide combination followed by docetaxel) did not appear to decrease the blood frequencies of antigen-experienced CD8 T cells.

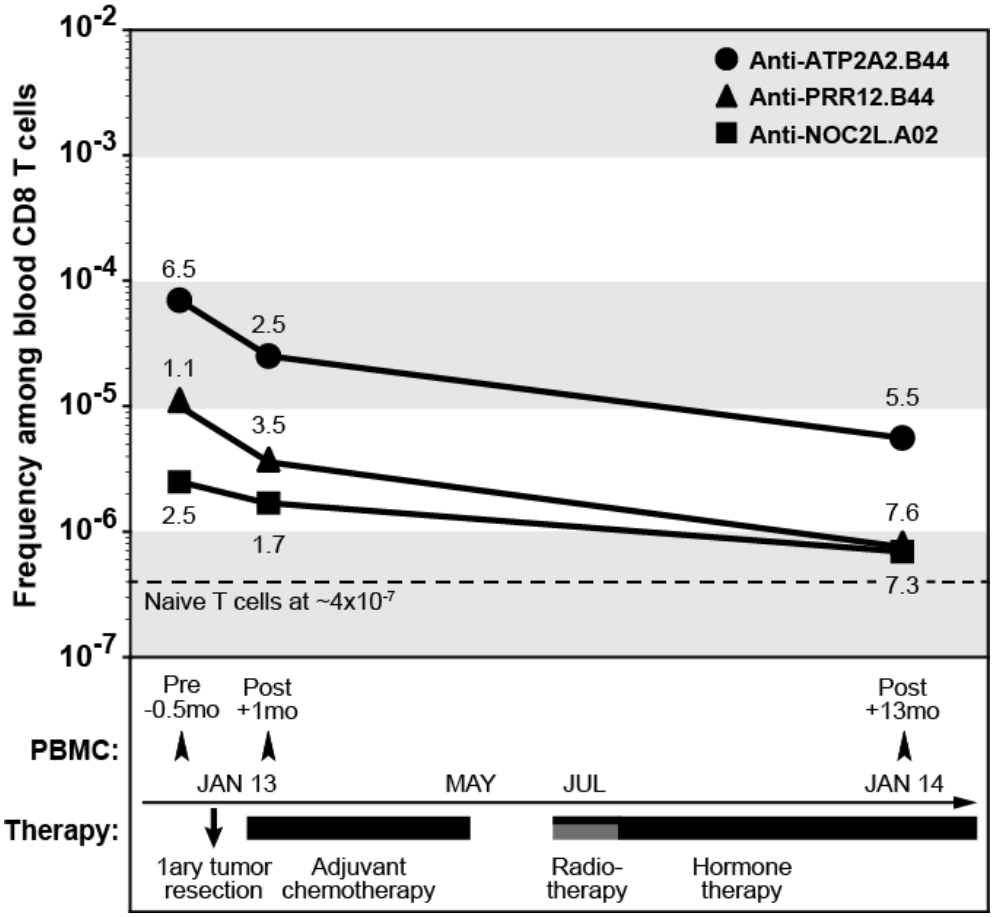

Figure 2-20. Frequency of antigen-specific CD8 T cells in the blood of P143.

mo, month. 1ary, primary.

We next identified the clonotypes of some multimer-stained cells present in blood in order to compare them with those of the TIL clones. For the blood sample 1-month after tumor resection, multimer-positive cells from 17 out of 31 positive microcultures were sorted by FACS at 1 cell per well in 60 wells and at 3, 30 or 1,000 cells per well in 24, 6 and 1 well, respectively. Sorted cells were stimulated with anti-CD3 antibodies as for the TIL cloning. After 3 stimulation cycles of 9-10 days, cells proliferated in 8 microcultures. They were labeled with multimers and their TCR CDR3ß was sequenced. Multimer staining was confirmed for all cells. NOC2L.A02-specific T cells were of the same clonotype as TIL clone 918/52 (Table

2-10). For the anti-PRR12.B44 cells (939-22/1), we found a new clonotype. Four out of the 6 ATP2A2.B44-positive populations were of the same clonotype as TIL clone 918/26. One population contained two clones with distinct intensities of ATP2A2.B44-dextramer staining: one clone belonged to clonotype 918/26, the other one (939-25/2) corresponded to a new clonotype. The last population (939-27/1) corresponded also to a new clonotype.

Antigen	Nbr of sorted among all positive microcultures	Nbr of micro-cultures with proliferating cells	Nbr of sorted cells / well	Identified clonotype(s) in the well
NOC2L.A02	2 out of 2	1	1,000	TIL clone 52
PRR12.B44	4 out of 4	1	1	New (939-22/1)
ATP2A2.B44	11 out of 25	6	1	TIL clone 26
			1	TIL clone 26
			3	TIL clone 26
			3	TIL clone 26
			1,000	TIL clone 26 + New (939-25/2)
			3	New (939-27/1)

Table 2-10. Clonotypes of multimer-positive blood CD8 T cells in P143.

Nbr, numbers.

Thus, we confirmed for NOC2L and ATP2A2 the presence of antigen-specific T cells in the blood at 1-month post-surgery. This blood sample contained predominantly the anti-ATP2A2.B44 clone 26. Moreover new antigen-specific clonotypes were identified in the blood, broadening the TCR diversity of the spontaneous tumor-specific response of patient P143.

2.5.8 Significant antitumor CTL responses exist in P143

Approximately 11% (6/57) of the analyzed TIL clonotypes of P143 were tumor-specific (Figure 2-21). In addition, a complete TCRBV repertoire analysis of the TILs of tumor P143 was carried out by J. Carrasco in order to estimate the frequencies of the tumor-specific T cells independently from the biases introduced by the *in vitro* stimulation and culture conditions.

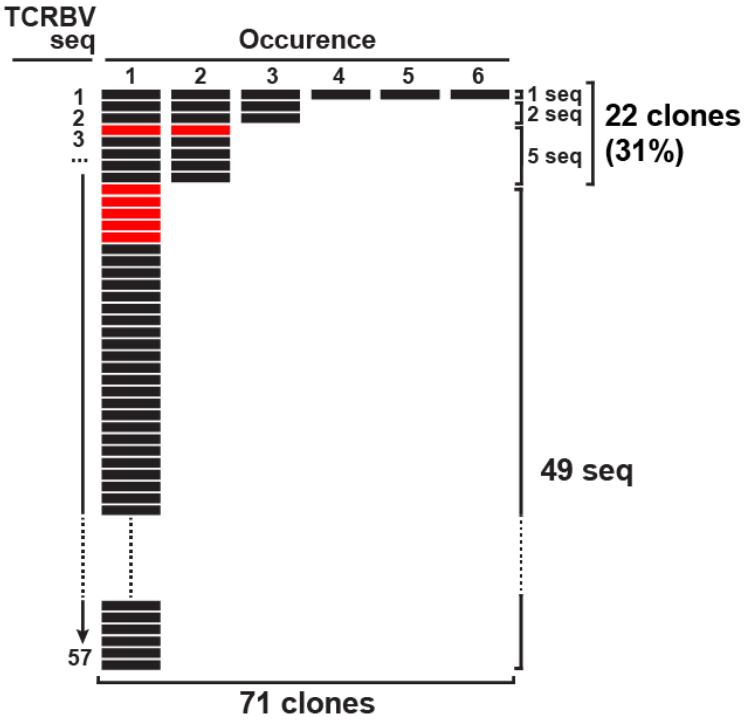

Figure 2-21. TCRBV repertoire of the TIL clone set from P143.

The tumor-specific clones are indicated in red. One PRR12.B44-specific T cell clonotype was found in 2 clones (918/23 and 918/29). The 5 other tumor-specific clonotypes were found each in one clone. Seven out of 71 clones are tumor-specific, which is very similar to the proportion of tumor-specific clonotypes (11%).

RNA extracted from the tumor P143 was used to generate a cDNA library of TCRß molecules (thus from CD4 and CD8 T cells). This library was then sequenced by massive parallel sequencing to obtain the TCRBV repertoire of the tumor P143. 37,058 TCRß cDNA molecules were sequenced and corresponded to 4,134

different clonotypes of CD4 or CD8 T cells. Fifteen out of these clonotypes were identified in our set of CD8 TIL clones and included all six tumor-specific clonotypes. The corresponding tumor-specific CD8 TIL clones were found at various frequencies (2×10^{-4} to 5×10^{-2} of all T cells, see Figure 2-22). Out of the 10 most frequent clones of the tumor TCRBV repertoire, 3 corresponded to tumor-specific clones (clones 918/26, 23 and 52), 4 corresponded to tested clones that did not recognize the candidate tumor antigens and 3 did not match with any clone of our set of CD8 TIL clones (Figure 2-22). These 3 clones could correspond to CD4 T cells. The most frequent clone of the tumor TCRBV repertoire corresponded to TIL clone 918/26 (5×10^{-2} of all T cells). This clone was also the most frequent anti-ATP2A2.B44 T cell clone in the blood at one month after tumor resection (see Table 2-10). The two other anti-ATP2A2.B44 clones that we found in the blood (939-25/2 and 939-27/1) were found also in the tumor TCRBV repertoire, at frequencies of 7-9 $\times 10^{-4}$ of all T cells. The anti-PRR12.B44 clone present in in the blood (939-22/1) was not present in the tumor TCRBV repertoire.

In summary, the total frequency of tumor-specific T cells in the TCRBV repertoire of tumor P143 was 9% of all T cells and the frequency of different tumor-specific CTLs varies 100-fold from 10^{-4} to 10^{-2} among all T cells. We conclude that tumor-specific CTLs are a significant part of the tumor-infiltrating T cells in this patient and that some ATP2A2-, PRR12- and NOCL2-specific CTLs were the predominant tumor-specific CTLs.

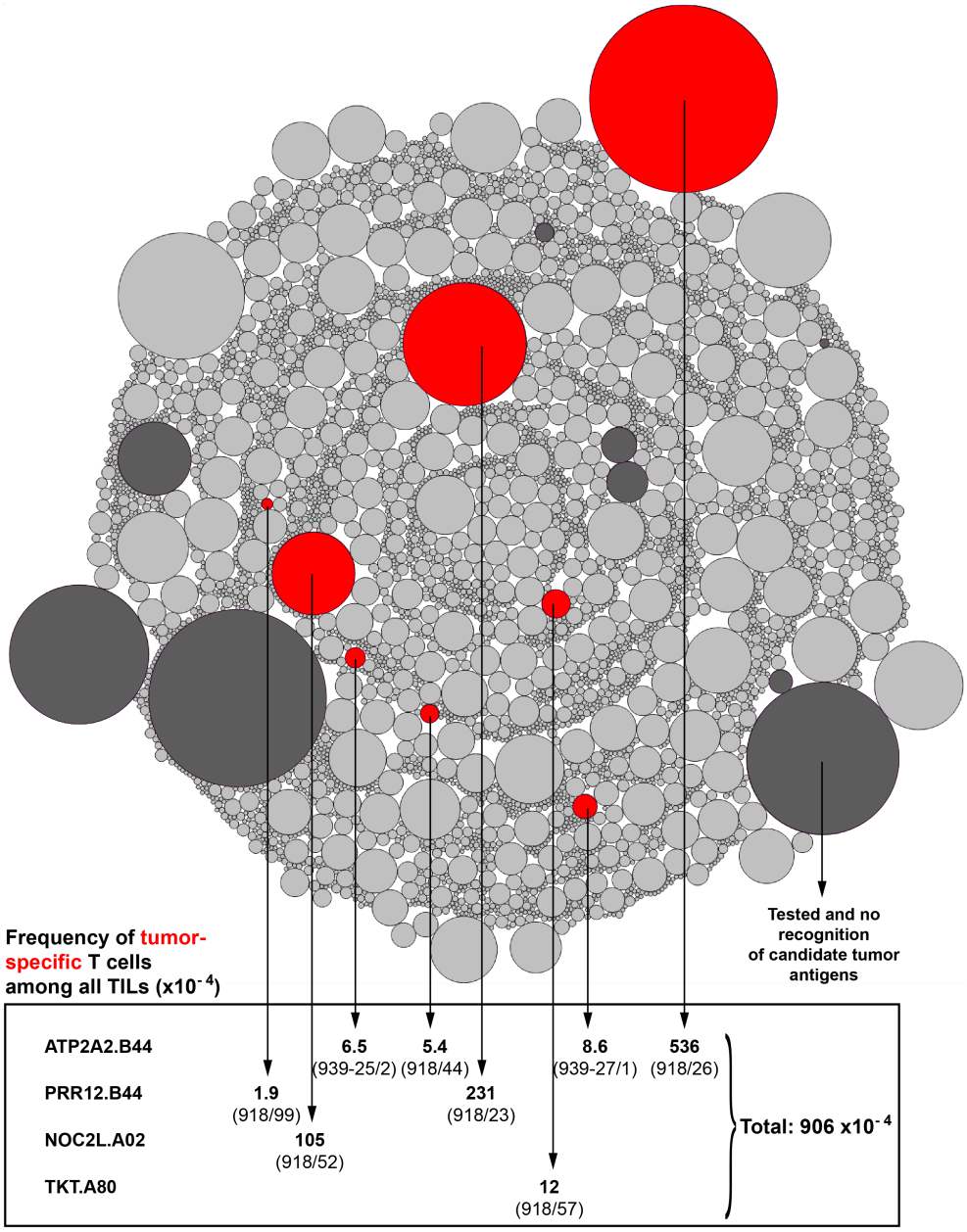

Figure 2-22. TCRBV repertoire of tumor P143.

Each circle represents a unique TCRBV cDNA and its surface is proportional to the number of these cDNAs among all TCRBV cDNAs present in the sample. Tumor-specific clonotypes are in red. Clonotypes of the CD8 TIL clone set that did not recognize candidate tumor antigens are in dark grey. Adapted from figures provided by J. Carrasco.

2.6 Looking for unique characteristics of tumor P143

We next tried to explain why tumor P143 but none of the other 5 tumors that we had analysed were immunogenic (Table 2-11). Most tumor characteristics (hormone receptors status, HER2 status, histology, Ki67 or tumor stage) did not distinguish tumor P143 from the others. However the number of stromal cells extracted from tumor P143 was at least 5 times higher than for the other tumors and the proportion of CD8 TILs obtained from tumor P143 was also higher, indicating high infiltration by CD8 TILs.

What could explain the difference in immunogenicity were the numbers of missense SNVs: 4 to 7 times higher in tumor P143 than in the other tumors. This difference should lead to a higher number of antigenic mutant peptides in tumor P143, with a higher probability of priming a CD8 T cell response recognizing a tumor-specific mutant peptide. To further explore this hypothesis, we first tried to explain the higher mutation rate of tumor P143.

Patient	P142	P143	P154	P195	P223	LB5784
Age	70	51	65	43	79	82
Tumor characteristics						
ER, PR and HER2 status	ER^+ PR^+ $HER2^-$	ER^+ PR^+ $HER2^-$	ER^+ PR^- $HER2^+$	ER^+ PR^+ $HER2^+$	TN	TN
Histology	Ductal	Ductal	Ductal	Ductal	Metapl.	Ductal
Grade	High	Interm.	High	High	High	High
Ki67 (%)	40	80	40	40	75	40
Stage	IIIA	IIA	IIA	IIB	IIB	IIB
Missense SNVs	113	450	71	58	122	67
Tumor-infiltrating T cells						
Stromal cells / g of tissue ($x10^6$)	0.4	11.3	1.3	0.3	2.2	2.1
% of CD8 TILs	22	59	15	54	31	39
Nbr of clonotypes	100	57	61	142	82	100
Tested candidate tumor antigens						
Mutations	29	106	29	23	49	36
Cancer-germline genes (MAGE-)	A3 A6 A12		A3 A6		A3 A6	A4 A10 NYESO1
ERBB2			ERBB2	ERBB2		
Results	0	6	0	0	0	0

Table 2-11. Summary of the 6 breast carcinomas with tested CD8 TIL clones.

Metapl., metaplastic; interm., intermediate

2.6.1 Mismatch repair deficiency in the tumor of P143

Somatic nonsynonymous SNVs or indels were not present in genes encoding proteins involved in DNA repair or DNA replication such as *BRCA1* and *POLE*, respectively. With the help of F. Duhoux, R. Helaërs and C. van Marcke de Lummen, we reanalyzed our WES data with the Highlander analysis pipeline[129] to identify potential deleterious germline variants, without success (data not shown). When we looked at somatic variants we found a previously unknown frameshift deletion in gene *MSH2* (V598fs). The MSH2 protein is part of the DNA mismatch repair system and a truncated MSH2 protein fits with the DNA mismatch repair deficiency suggested by the mutation profile. Indeed, an IHC of the 4 main proteins of the DNA mismatch repair system showed a loss of MSH2 expression in the tumor cells (Figure 2-23). On the contrary, MHS2 was expressed in stromal cells. The loss of MSH6 expression in tumor cells was due to its instability without its heterodimer partner MSH2[130].

The DNA mismatch repair (MMR) system identifies and corrects errors of DNA polymerases (Pol δ an Pol ε) during DNA replication. The heterodimers MutSα (MSH2-MSH6) and MutSβ (MSH2-MSH3) preferentially recognize mononucleotide or oligonucleotide DNA mismatches, respectively[131]. After mismatch recognition each heterodimer binds to another heterodimer, MutL. MutSα binds to MutLα (MLH1-PMS2) and MutSβ binds to three different MutL complexes (γ, β or α). The MutS-MutL complex moves along the newly synthesized DNA strand until it reaches the DNA polymerase. They form a new complex with exonuclease-1 and the proliferating cell nuclear antigen (PCNA). This complex degrades the newly synthesized DNA strand back to the mismatch site where a new DNA synthesis is initiated by the DNA polymerase after the other partners have fell off[132] (Figure 2-24).

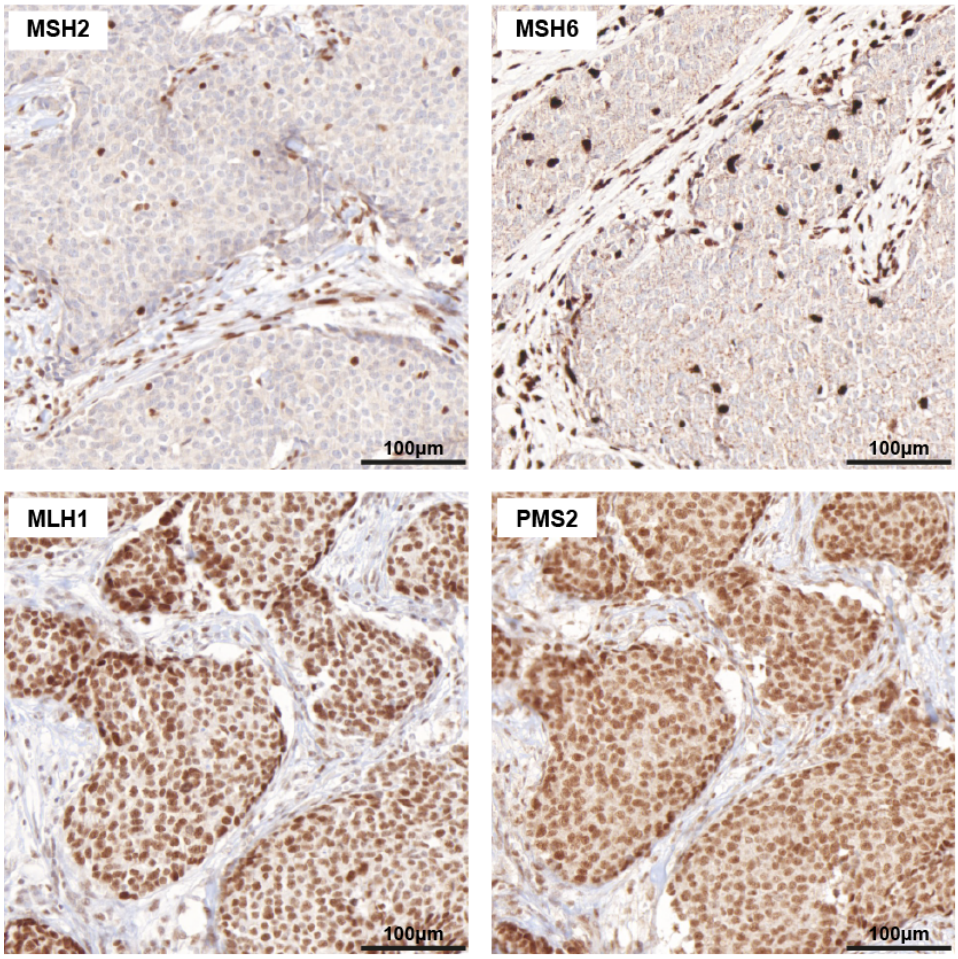

Figure 2-23. IHC of the 4 main proteins of the DNA mismatch repair system.

Labeling of MSH2, MSH6, MLH1 and PMS2 was performed twice with concordant results. All 4 proteins were expressed in stromal cells. MSH2 and MSH6 are undetectable in the tumor cells. Courtesy of Pr A. Mourin, Pathology department, Cliniques universitaires St Luc.

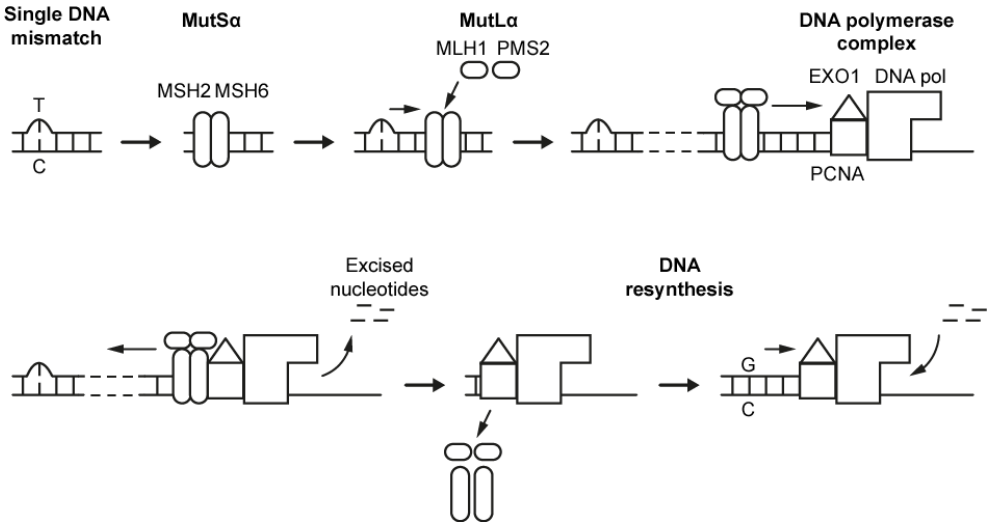

Figure 2-24. Single DNA mismatch repair system.

EXO1, exonuclease-1; DNA pol, DNA polymerase; PCNA, proliferating cell nuclear antigen
Figure adapted from [132].

The polymerase-induced errors occur in 1 out of 10^7 new synthesized nucleotides and the MMR system reduces the rate of mutations by 100-fold, down to 1 in 10^9 nucleotides. A defect in the MMR system gives rise to an increased number of mutations and MMR-deficient tumors are characterized by a high number of SNVs and indels as well as by a DNA microsatellite instability (MSI)[76,130]. DNA microsatellites are 1-6bp sequences repeated 10 to 60 times (*e.g.* stretch of 20 adenosine)[130]. Their lengths are very heterogeneous between individuals but conserved within a person. Microsatellites are prone to induce DNA polymerase errors by their sequence nature and a MMR deficiency results in variations of those repeated sequences, called microsatellite instability. We observed indeed a microsatellite instability in the tumor P143 and not in the other 5 tumors (Figure 2-25).

We conclude that the high number of missense SNVs in tumor P143 is due to a MMR deficiency as indicated by the loss of MSH2 expression and by the DNA microsatellite instability. This DNA mismatch repair deficiency was a surprise, as it is rare in breast tumors (<2% or 10/560 analyzed by Nik-Zainal *et al.*[74]).

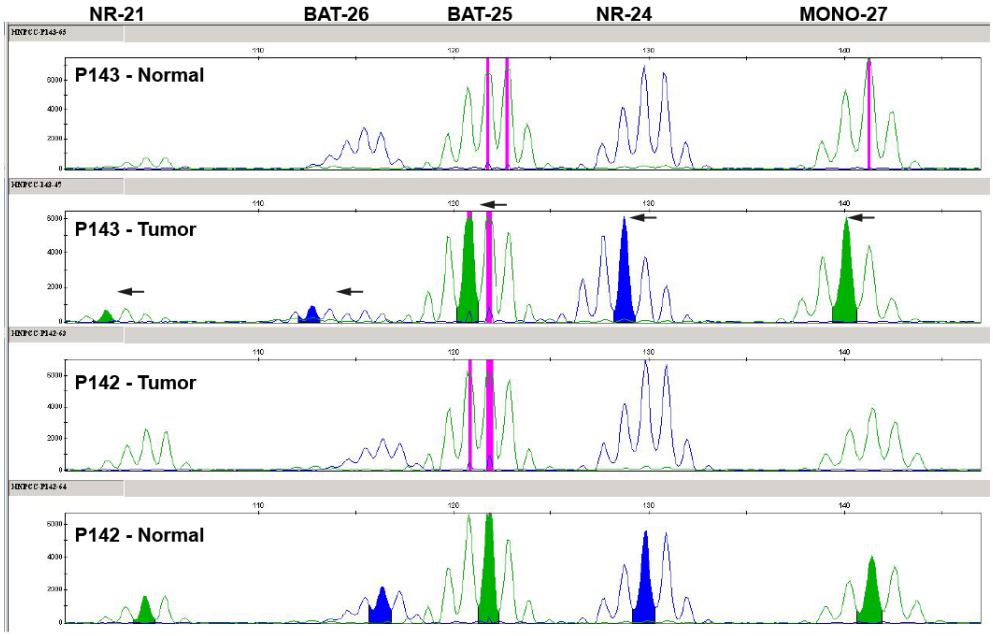

Figure 2-25. Microsatellite instability in tumor P143.

MSI Analysis System performed on matched tumoral and normal tissues of all 6 tumors. Representative results of P143 and P142 are shown. PCR products of 5 mononucleotide repeats (NR-21, BAT-26, BAT-25, NR-24, MONO-27) migrate on gel. All 5 markers had a distinct electrophoretic mobility in tumor P143 compared with matched normal sample indicating different size of these mononucleotide repeats in tumor P143, thus a microsatellite instability. Courtesy of P. Vannuffel, Institut de Pathologie et de Génétique.

2.6.2 Estimation of tumor antigenicity

The sum of tested mutations in expressed genes of the 5 non-P143 tumors outnumbered those of tumor P143 (166 vs 106). If the probability of priming a tumor-specific CD8 T cell response is approximately the same for every mutation, we should have found some tumor-specific TIL clones among the 485 clones derived from the 5 non-P143 tumors. We tried to be more precise in the estimation of the numbers of antigenic mutant peptides present in our tumors, by taking into account the HLA class I presentation and the processing of the antigenic peptides.

We used NetMHC to predict the binding of mutant peptides to the HLA class I molecules of each patient. We first carried out this analysis for the 4

'immunogenic' mutations in tumor P143. The 4 mutant precursor peptides of 19 amino acids were submitted to the NetMHC algorithm to predict HLA class I-binding for peptides of 9 or 10 amino acids (Figure 2-26). The antigenic peptides that we found to be recognized by tumor-specific TIL clones were all predicted by NetMHC to bind to HLA molecules with a high affinity (Kd <50 nM). Interestingly, each of these 4 peptides was ranked with the highest HLA-binding affinity within the set of all the peptides of 9 or 10 amino acids derived from the same precursor. Thus if we had used NetMHC with each precursor peptide and selected the best (9 or 10 mer) binder to any class I molecule with a Kd lower than 50 nM, we would have identified immediately the correct antigenic peptides.

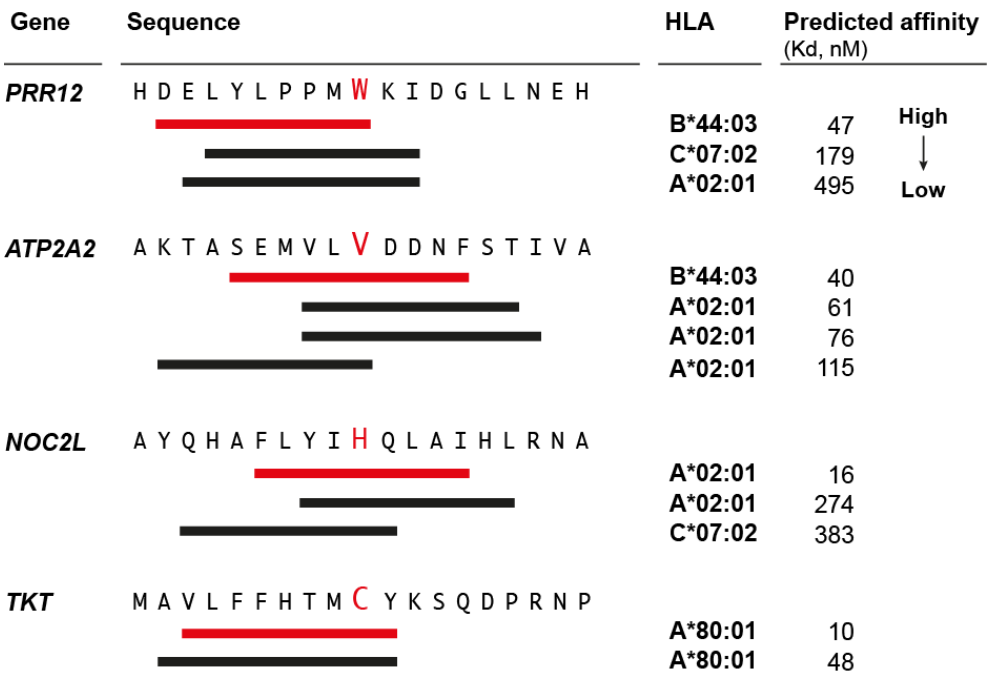

Figure 2-26. HLA class I-binding prediction for mutant antigens of tumor P143.

For each mutant precursor peptide we indicate the peptides of 9 or 10 amino acids predicted by NetMHC to bind to any HLA class I molecule of the patient with a Kd ≤500 nM. They are listed by decreasing binding affinity. The peptides recognized by the antitumor CTLs are indicated in red. All 6 HLA class I alleles of patient P143 were used in the analysis.

We applied this selection to 8 other mutant peptides known to be recognized by tumor-specific CTLs from 2 patients with metastatic melanoma (LB33[58-60] and MZ7[62], Figure 2-27). Five out of 5 and 4 out of six HLA class I alleles could be used for the analysis. The criteria mentioned above allowed to find 5 of the 8 antigenic peptides. As the NetMHC predictions for HLA-B*38:01 missed completely the correct peptide we surmise that an algorithmic correction is needed there. Altogether we consider that 9 out of 11 antigenic peptides can be identified directly with NetMHC, which is a very good performance (82%).

On Figure 2-28 we show how many mutant antigenic peptides with the above-used criteria (best binder of 9 or 10 amino acids with a Kd ≤50 nM) are predicted with NetMHC for the missense SNVs in expressed genes of all the 6 tumors that we have analysed. We show them separately for each presenting HLA class I molecule. As expected, tumor P143 stands out with 72 predicted peptides. Most of them (41/72 or 57%) are presented by HLA-A2. Only one is predicted to bind to HLA-C molecules. The four mutant peptides identified in this work are indicated in red. However we screened our CTL clones against 106 of the 293 expressed missense SNVs, selecting the best expressed mutated genes and those with high confidence to be real mutations. Therefore it is possible that 3-5 other mutant peptides are also recognized by CD8 TIL clones in this tumor. Assuming a total number of 8 immunogenic mutant peptides, only 11% (8/72) of the mutant peptides that are predicted to bind best to HLA class I molecules have stimulated a CTL response.

Does this proportion correspond to the fraction of predicted antigenic peptides that are actually processed in the tumor cells, or does it reflect an incomplete antitumor CTL response, i.e. that only some of the tumor-specific antigens have stimulated a CTL response? To try to answer this question we need to interrogate the HLA ligandome because only a fraction of peptides predicted to bind to HLA class I molecules will actually be processed in sufficient amounts for presentation to CD8 T cells by surface HLA class I molecules.

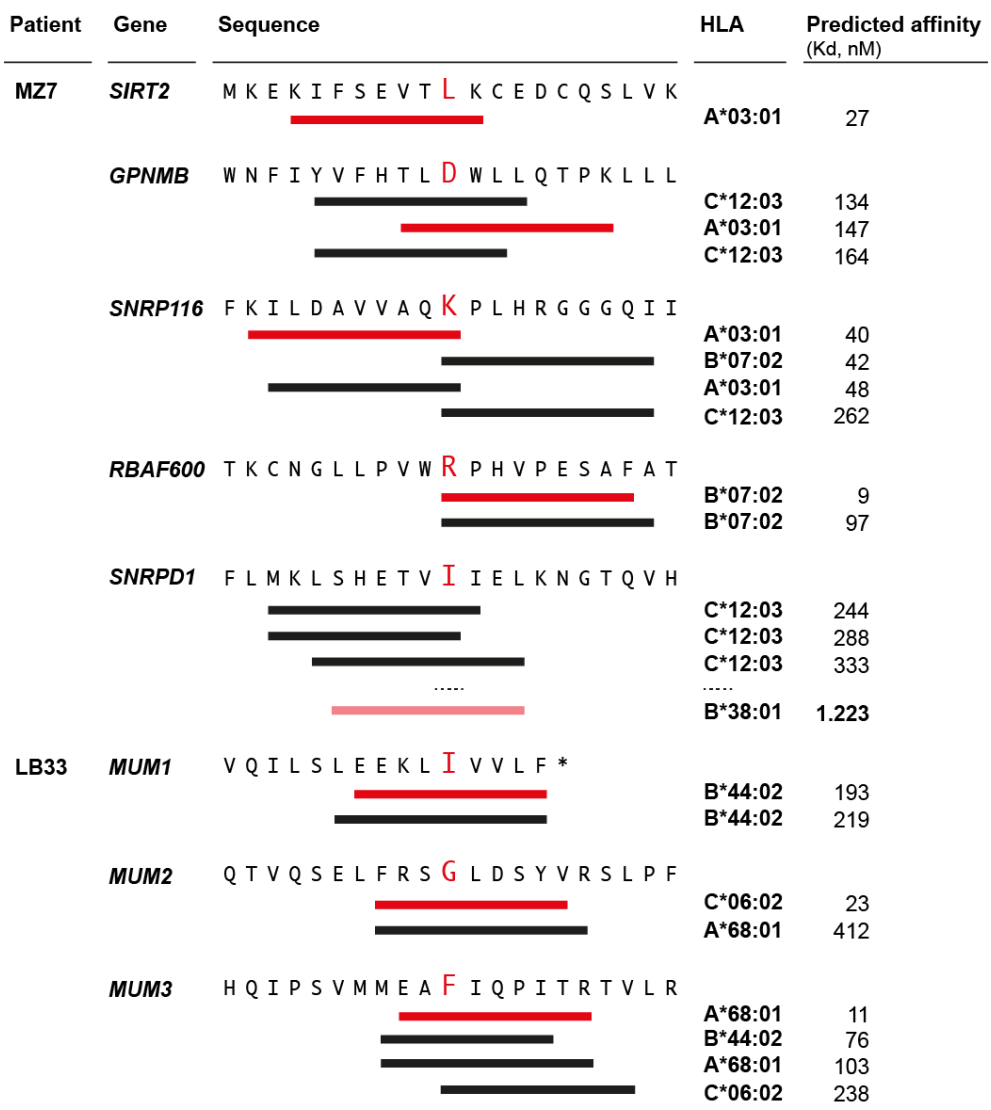

Figure 2-27. HLA-binding predictions for mutant antigens of 2 metastatic melanomas.

For each mutant precursor peptide we indicate the peptides of 9 or 10 amino acids predicted by NetMHC to bind to any HLA class I molecule of the patient with a Kd ≤500 nM. They are listed by decreasing binding affinity. The peptides recognized by the antitumor CTLs are indicated in red. All 5 HLA class I alleles of patient MZ7 could be used for prediction while only 4 out of 6 alleles of patient LB33 were present in NetMHC (B*13:02 and C*07:02 were missing).

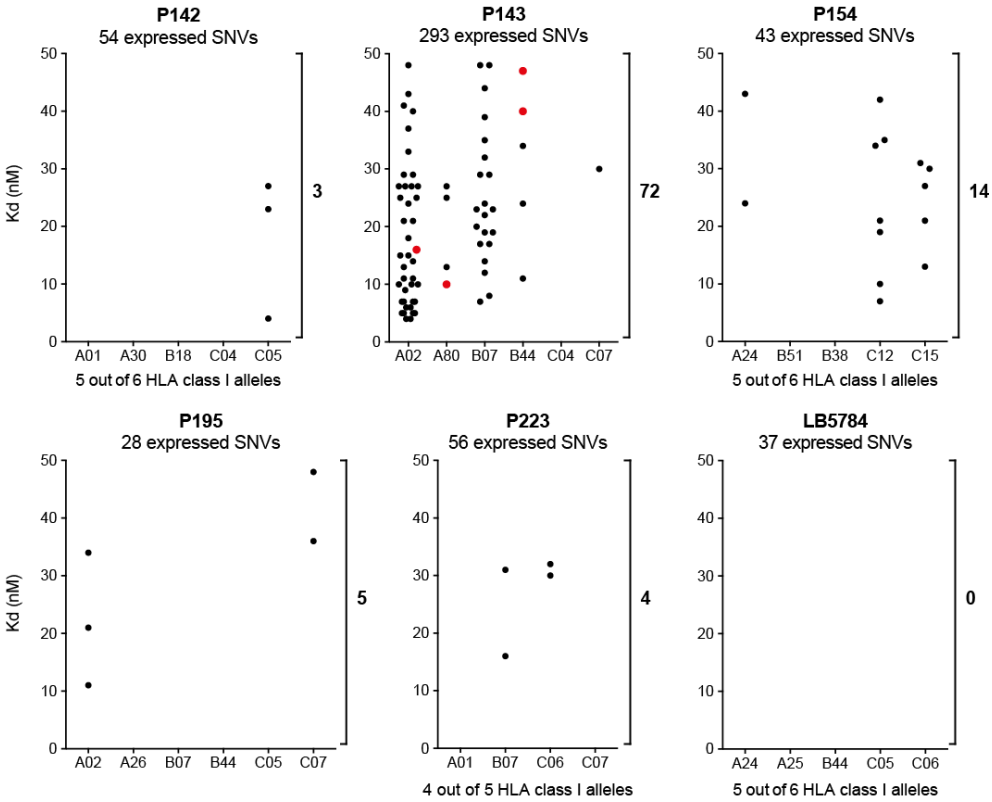

Figure 2-28. Predicted HLA class I-binding mutant peptides for the 6 tumors.

We used for prediction missense SNVs that were found in expressed genes. Genes were defined as expressed when the expression of the gene was equal to or higher than the median expression of all protein-coding genes.

NetMHC was used to predict mutant antigenic peptides of 9 or 10 amino acids with the highest predicted HLA class I-binding affinity within the set of all peptides derived from the same precursor and with a Kd ≤ 50 nM.

For tumors P142, P154, P223 and LB5784, one of the HLA class I alleles was absent from NetMHC.

For P143, the red dots indicate the peptides recognized by the TIL clones.

Antigen processing is a multi-step process (Figure 2-29): cytoplasmic proteins are degraded in peptides of 3-22 amino acids by the (immuno)proteasome, these peptides are transported in the endoplasmic reticulum (ER) by the transporter associated with antigen processing (TAP) and peptides of 8-11 amino acids bind on HLA class I molecules[133]. Proteases of the cytoplasm or the ER can trim peptides from their N-terminus to generate the optimal length for HLA class I binding. Several of these steps restrict the diversity of presented peptides, notably through the internal cleavage of potential antigenic peptides or the failure (usually of the proteasome) to generate an appropriate C-terminus of the peptide prior to entry in the ER. It is usually admitted that the C-terminus of a peptide is very important for HLA class I binding (C-ter residues are very often anchor residues) and that ER-resident proteases or peptidases do not trim C-termini of peptides. It is not yet possible to predict the products of this antigen processing machinery.

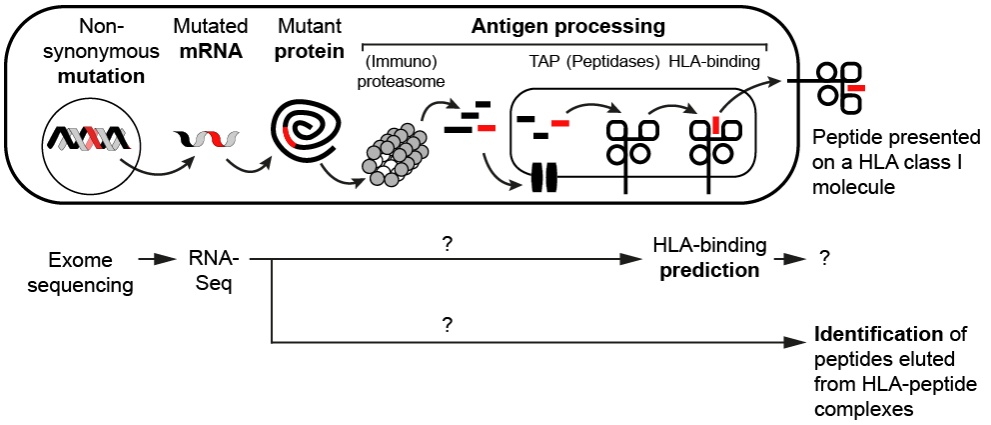

Figure 2-29. Antigen processing and presentation.

Can we estimate the proportion of predicted antigenic peptides that is actually displayed on the tumor cell surface, presented by HLA class I molecules? This proportion can be deduced from experiments in which antigenic peptides are directly eluted from surface HLA class I molecules, and identified by mass spectrometry. Such experiments generate what is often called the 'HLA ligandome'. HLA-peptide complexes of a cell line or tissue are immuno-

precipitated and the presented peptides, *i.e.* ligands, are eluted off the HLA by acid treatment. Then the peptides are purified and identified with mass spectrometry (LC-MS/MS). Exome sequencing is used to identify the mutant peptides in the HLA ligandome[134]. One difficulty however is the sensitivity of the approach (approximately 30% of HLA class I-bound peptides can be identified[134]).

Yadav *et al.* identified 1,290 nonsynonymous SNVs in the expressed genes of the murine colon carcinoma cell line MC-38[135]. With NetMHC they predicted that 25 peptides (9-mers only) bound HLA class I molecules with a Kd ≤50 nM. Four of these 25 peptides were present in the HLA ligandome (among 6,239 peptides). Thus here the proportion of predicted peptides that are detected in the ligandome is 16%. The antigen processing machinery appears therefore to actually produce 10-20% of the mutant peptides that can be predicted with DNA/RNA sequencing and HLA binding algorithms.

Therefore, in tumor P143 the 11% of predicted mutant peptides that are recognized by CTLs might represent the majority of all mutant peptides presented on surface HLA class I molecules. In other words, the CTL response of patient P143 covered not some of, but most of the mutant antigens of the tumor.

If we apply the same reasoning to the other 5 tumors that we have analyzed, the numbers of antigens are much lower than in tumor P143. The numbers of predicted peptides are shown on Figure 2-28. With a conservative estimation of 20% efficiency of the antigen processing machinery, the numbers of antigenic mutations range from 0 in tumor LB5784 to about 1 in tumors P142, P195 and P223 and about 3 in tumor P154. Thus, the antigenicity of these tumors might be much lower than anticipated, explaining the absence of detectable tumor-specific T cells. It has important consequences for the development of immunotherapy against such tumors.

2.7 Tumor resistance

2.7.1 Gene expression analysis of immunosuppressive mechanisms

We looked for other mechanisms that could explain the absence of detected tumor-specific CD8 TIL clones in the non-P143 tumors. In the RNA-Seq data we did not find genes expressed selectively in the non-P143 tumors and involved in tumor resistance mechanisms.

On the contrary, genes encoding inhibitory receptors, mostly LAG-3 and to a lesser extend PD-1, were expressed at higher levels in tumor P143 than in the other tumors (Figure 2-30). Those receptors are expressed on activated T cells[13,136-138], and on NK cells and some myeloid cells[13,139]. LAG-3 and PD-1 tissue staining would be very useful to identify the LAG-3 and PD-1 expressing cells.

We observed an IFNγ signature in tumor P143, with IFNγ-regulated genes *CXCL9*, *CXCL10*, *CXCL11*, *IDO1*, *TAP1*, *PSMB8* (immunoproteasome subunit ß5i) and *PSMB9* (immunoproteasome subunit ß1i). *CXCL9*, *CXCL10* and *CXCL11* encode chemokines that attract T cells and NK cells[140]. *IDO1* encodes the immunosuppressive enzyme IDO which catabolizes tryptophan, and depletion of this essential amino acid results in T cell anergy and apoptosis[141]. Are PD-L1 and IDO expressed on neighbor cells of CD8 TILs? It would be interesting to analyse by IHC the relative localizations of CD8 T cells, PD-L1-expressing cells, and IDO-expressing cells.

Our data are reminiscent of the upregulation of IFNγ, IDO, PD-1, LAG-3 and PD-L1 encoding genes in microsatellite unstable (MSI) colorectal tumors as compared to microsatellite stable (MSS) colorectal tumors[142]. The MSI tumors are highly infiltrated by T cells, mostly CD8 T cells, and PD-1 and LAG-3 expression on lymphocytes was shown by IHC.

Our interpretation of these results is what is often referred to as 'adaptive resistance'. Activated T cells express inhibitory receptors and secrete cytokines such as IFNγ that contribute to a negative feedback of the T cell response through the expression of membrane ligands for the inhibitory receptors or through a local decrease of nutrients such as tryptophan. It is possible but not certain that adaptive resistance alone explains the absence of tumor rejection by the CD8 tumor-specific T cells.

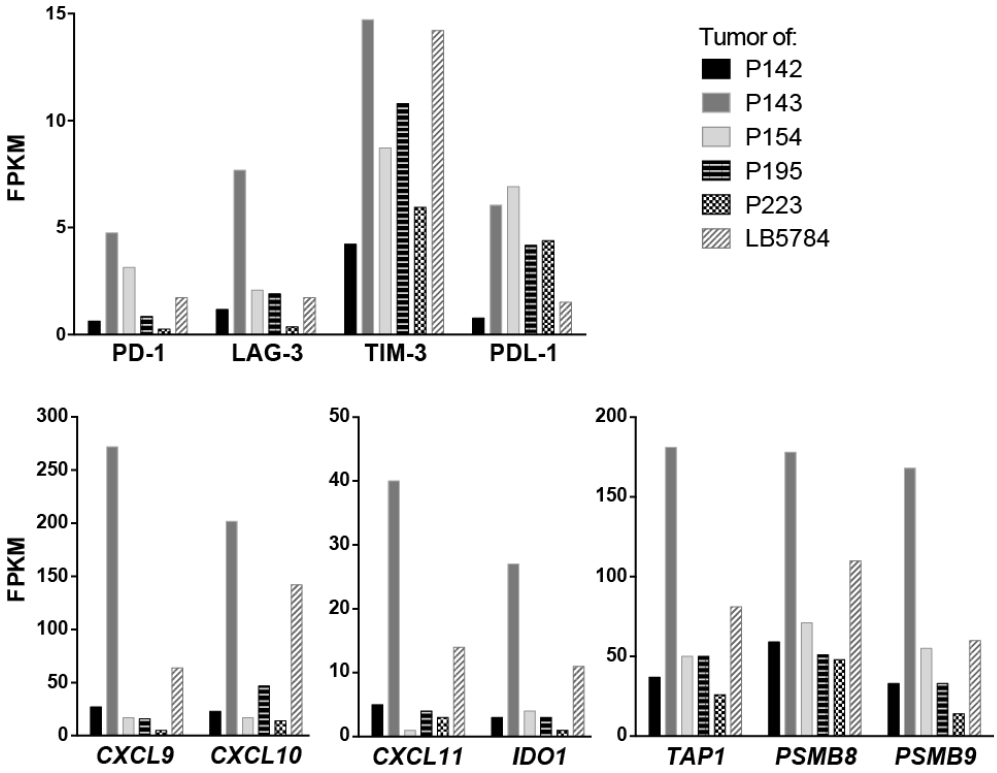

Figure 2-30. Expression of selected genes in the tumor of P143.

2.7.2 Expression of HLA class I and ß2-microglobulin

Another mechanism of tumor resistance to antitumor CD8 T cells is the loss of presentation of the recognized antigen caused by a downregulation or loss of expression of HLA class I alleles or ß2-microglobulin[59,143].

Immunohistochemical analysis of tumor P143, P142 and LB5784 showed the presence of HLA class I molecules and of ß2-microglobulin in tumor cells (Figure 2-31).

Noteworthily, we observed a strong decrease and possible absence of surface staining for HLA class I and ß2-microglobulin on tumor cells of P154 and P195, and on a fraction of the tumor cells of P223. It was associated with a decreased cytoplasmic staining when compared to the stromal cells. In the exomes of the tumors we found no mutation in the HLA class I, *TAP1*, *TAP2* or *B2M* genes that could explain these observations. HLA class I antigen processing or presentation defects in these tumor cells suggest prior recognition by tumor-specific CD8 T cells. We did not detect tumor-specific CD8 T cells among the TILs of these tumors, but after antigen loss they might be present at much lower frequencies or they might have disappeared. Another possibility is the recognition of tumor antigens that were not included in our assays. Identifying such antigens, possibly of a new type, might be very interesting for the immunotherapy of breast cancer.

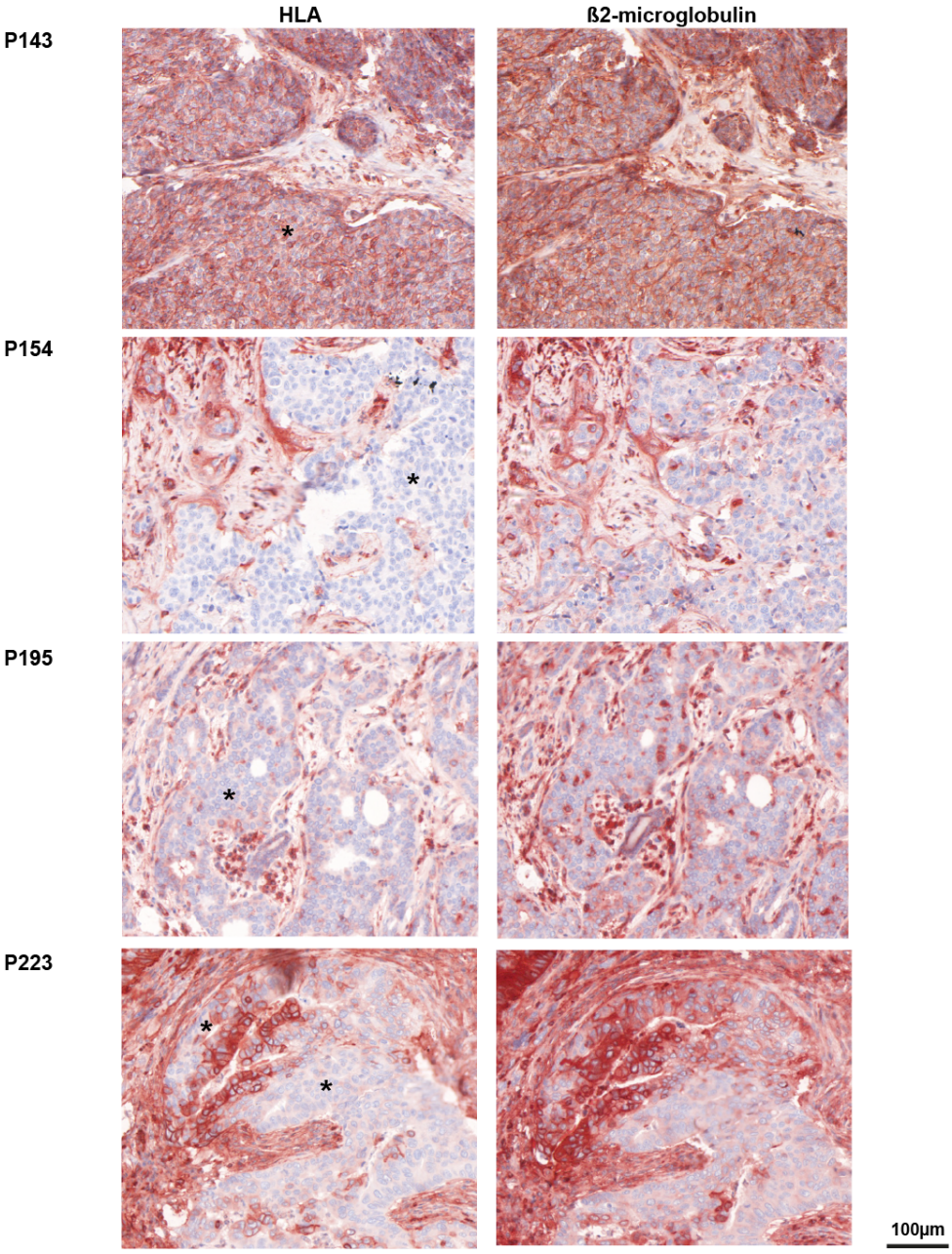

Figure 2-31. HLA class I and ß2-microglobulin staining in IHC.

Asterisks mark areas of tumor cells. In tumors P154 and P195, stained stromal cells infiltrate the tumor. In tumor P223, some tumor cells display membrane staining (upper part) while others do not.

3 Discussion and perspectives

The positive association between the presence of tumor-infiltrating T cells and a more favorable clinical outcome of patients with breast cancer suggests that at least some of these patients mount spontaneously antitumor T cell responses and that some of these T cells infiltrate the primary tumors. The immunogenicity of primary breast carcinoma is important insofar as it influences the choice of immunotherapies that can be proposed to the patients. Spontaneously immunogenic tumors can be treated with immunostimulatory antibodies such as those that target the PD-1 pathway. Non-immunogenic but antigenic tumors should be treated by active (vaccines, T-VEC) or passive (adoptive transfer of antitumor T cells, including CAR T cells) immunizations, which can be combined with immuno-stimulatory antibodies.

Here we have documented the spontaneous immunogenicity towards CD8 T cells of six primary breast carcinomas corresponding to the various subtypes of breast tumors (2 $ER^{+}HER2^{-}$, 2 $HER2^{+}$, 2 triple-negative).

3.1 Testing the immunogenicity of breast tumors

In the past, the immunogenicity of breast tumors was very difficult to test because stable autologous tumor cell lines were necessary to identify *in vitro* tumor-specific T cells. Tumor-specific CD8 T cells were expanded from PBMCs or TILs by mixed lymphocyte-tumor cell cultures and identified by their recognition of tumor cells, usually in lysis assays. The genes encoding the antigens recognized by these tumor-specific cells were identified by testing the recognition of HLA-matched cells transfected with cDNA libraries prepared from the tumor. This approach enabled the discovery of the MAGE-type antigens and of the first mutated genes that encoded tumor-specific antigens[6,79].

Unfortunately, it is almost impossible, with current methods, to derive tumor cell lines from breast tumors. Only a few breast tumor cell lines exist worldwide. However, what has become possible is to use exome and RNA sequencing data from a small fragment of tumor to propose candidate tumor-specific antigens for each tumor, bypassing the need for autologous tumor cell lines. As a source of tumor-specific T cells we selected TILs, which are likely to be greatly enriched in tumor-specific T cells as compared to blood lymphocytes. We have limited our analysis to CD8 T cells, the main effector T cells against a tumor. TIL clones were used in order to be able to completely characterize the target antigens, the

functions and the TCR of the antitumor T cells. Finally, we screened the CD8 TIL clones for recognition of candidate tumor antigens: encoded by genes that are mutated in the autologous tumor, by cancer-germline genes expressed in the tumor and by gene *ERBB2* if overexpressed in the tumor. Antigens were presented by autologous EBV-B cells to test the recognition of antigens on all HLA class I alleles and we decided not to use HLA-binding prediction algorithms in order to avoid potential biases of peptide selection (*e.g.* some HLA class I alleles are absent from NetMHC).

Other groups have also used exome sequencing to detect TILs recognizing candidate mutant antigens and they have found tumor-specific T cells in the tumor or in the blood of patients with metastatic melanoma, metastatic gastrointestinal carcinoma, chronic lymphocytic leukemia and ovarian carcinoma[11,63,66,67,69].

The method followed here does not allow the detection of tumor-specific CD8 T cells that are present at low frequencies (<1%) among CD8 TILs or that cannot be amplified *in vitro* under our conditions. In addition, neither antitumor CD8 T cells recognizing other antigens than those listed above, nor antitumor CD4 T cells, could be detected in our experiments.

3.2 Presence of repeated clones in sets of clones

We observed repeated clones (clonotypes represented by more than one clone) in all sets of CD8 TIL clones. Why did we find such clonotypes in all sets?

These repeated clones are probably virus-specific memory CD8 T cells like tissue-resident CMV- and EBV-specific CD8 T cells that have been observed in the liver of healthy donors[144]. For all sets of TIL clones, we observed clones that were activated in all cocultures containing autologous EBV-B cells, with proportions ranging from 1 to 14% of all clonotypes (data not shown). We surmise that these clones recognize EBV antigens, but have not carried out tests to confirm this possibility. Moreover we found EBV-specific T cells among the repeated clones in 5 out of 6 sets of TIL clones, suggesting that the repeated clones are virus-specific CD8 T cells. Finally, we found repeated clones also in the 3 sets of CD8 clones derived from normal breast tissue, indicating that repeated clones exist in the breast tissue. This explains why we found them in breast tumors.

3.3 Some breast tumors are immunogenic

A spontaneous tumor-specific CTL response was observed in one out of the 6 tested tumors. In tumor P143, 6 different tumor-specific CTLs recognized 4 antigens that were encoded by different missense point mutations. These four mutant antigenic peptides were presented by three out of 6 HLA class I alleles. We therefore demonstrate that some breast carcinomas are highly immunogenic.

Triple-negative (TN) and $HER2^+$ tumors are considered immunogenic in the literature based on the positive association between the presence of TILs and a more favorable clinical outcome of patients with tumors of these subtypes. We demonstrated that an ER^+HER2^- breast carcinoma with pathological surrogate markers of luminal B tumors (high tumor cell proliferation) is spontaneously immunogenic. Interestingly, gene expression analyses did not show that potentially immunogenic tumors are limited to TN and $HER2^+$ breast tumors. Furthermore, the gene expression analysis of Dedeurwaerder *et al.* suggested that some luminal B tumors are immunogenic and we confirm their hypothesis[41]. Thus the immunogenicity of breast carcinomas is not restricted to TN and $HER2^+$ tumors. Although the immunogenicity is not restricted to TN tumors, the JAVELIN trial showed that mostly patients with TN tumors responded to an anti-PD-L1 antibody. The response rate was 9% for TN tumors (5/58), 4% for $HER2^+$ tumors (1/26) and 3% for ER^+HER2^- tumors (2/72)[98,99]. Even if the response rate with ER^+HER2^- tumors was low, some tumors responded and they should be studied in detail to understand their response to the anti-PD-L1 antibody. Thus it would be interesting to include patients with ER^+HER2^- tumors in trials with PD-1 pathway inhibitors, although most ongoing studies are restricted to TN or $HER2^+$ tumors, and to associate the clinical response with an analysis of genetic and immune markers.

Why are TN breast carcinomas more immunogenic? A major difference between the tumor P143 and the other five tumors was the higher number of missense SNVs in tumor P143. As expected the number of missense mutations impacts the number of mutant antigenic peptides. A higher number of mutations should therefore lead to a higher probability of priming a tumor-specific T cell response. A higher antigenicity may explain why triple-negative tumors are more immunogenic than the other breast tumor subtypes. Indeed in the study of Nik-Zainal *et al.*, the median number of SNVs was 4 times higher in basal-like and 2

times higher in HER2-overexpressing or luminal B tumors than in luminal A tumors (Figure 3-1)[74]. Interestingly, tumors with a very high number of mutations ('hypermutated' tumors) were found in all intrinsic subtypes and it suggests that immunogenic tumors exist in all breast tumor subtypes. In addition to the higher expected antigenicity of triple-negative tumors with antigens encoded by mutations, the proportion of tumors that express MAGEA3 and MAGEA6 is higher in ER^- negative tumors[80], suggesting that triple-negative and $HER2^+ER^-$ tumors are also more antigenic by presenting more often MAGE-type antigens. It is therefore possible that it is only the high antigenicity of triple-negative tumors that explains their higher immunogenicity. Like tumor P143 the presence of 'hypermutated' tumors in the other breast tumor subtypes explains why immunogenic tumors also exist in the other subypes but at lower frequency.

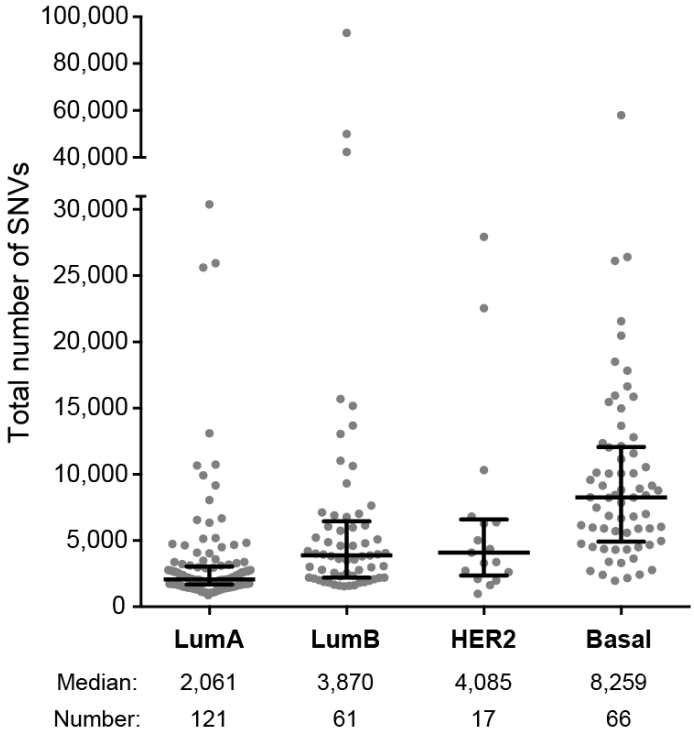

Figure 3-1. Number of SNVs according to the intrinsic subtypes.

Total number of SNVs for each breast tumor. The tumors are classified according to their intrinsic subtype. Whisker plots show for each subtype the median with inter-quartile range. Data from the supplemental data of Nik-Zainal and colleagues[74].

3.4 Tumor resistance to tumor-specific CTLs of P143

The antitumor T cell response in tumor P143 was significant. One tumor-specific clonotype was the most frequent clonotype in the TCRBV repertoire analysis of this tumor, corresponding to 5% of all T cells (CD4 and CD8) in the tumor. Two other tumor-specific clonotypes were among the 10 most frequent clonotypes (corresponding to 1% and 2% of all TILs). The total frequency of tumor-specific T cells in the TCRBV repertoire of tumor P143 was 9% of all TILs. Interestingly, tumor-specific CD8 T cells (recognizing MAGE-type antigens and a mutant antigen) were found at a similar total frequency (11% of all CD8 T cells) in a regressing cutaneous metastasis of a patient with metastatic melanoma who experienced tumor regression following *MAGEA3*-based vaccination[10]. This suggests that the proportion of tumor-specific T cells in tumor P143 could be sufficient to mediate tumor regression.

However tumor resistance to the spontaneous antitumor T cell response is obvious as the tumor was growing at tumor resection. The exome sequencing data of tumor P143 also suggests that the tumor-specific CTLs have not significantly eliminated the tumor cells. The allele frequency of the 'immunogenic' mutations was one third lower or identical to that of the putative driver mutation in *TP53*, which indicates that the proportion of antigenic tumor cells ranged from 65% to 100%, assuming that all those mutations are heterozygous and that the *TP53* mutation is present in all tumor cells.

The high number of stromal cells extracted from the tumor sample as well as the high proportion of CD8 TILs by flow cytometry indicate a high number of CD8 TILs within the tumor. A CD3 and CD8 IHC analysis is ongoing to confirm the high infiltration of CD8 TILs and we will characterize the localisation of these CD8 TILs. Are CD8 TILs of P143 in close proximity to tumor cells within the tumor parenchyma? Do CD8 TILs remain at the tumor margin in the other 5 tumors?

We checked if a loss of antigen presentation could be responsible for tumor P143 resistance. We did not observe any loss of staining for HLA class I molecules or ß2-microglobulin in a tumor section.

The analysis of RNA-Seq data revealed a significant IFNγ-signature (*CXCL9*, *IDO1*,..) in tumor P143 compared with the other 5 tumors. This differential expression suggests that the tumor-specific T cells in tumor P143 secrete IFNγ and induce IDO

expression. We also observed an upregulation of the inhibitory T cell receptors LAG-3 and PD-1 that are expressed on activated T cells. PD-L1, a ligand of PD-1, was not specifically upregulated in tumor P143 but the IFNγ signature in tumor P143 suggests the expression of PD-L1 on tumor and stromal cells. Thus we observed signs of T cell activation that lead to a negative feedback of the activated T cells, a process that is called 'adaptive resistance'.

In the absence of other detected mechanisms of tumor resistance to antitumor T cells, we tentatively conclude that this 'adaptive resistance' suppresses the capacity of tumor-specific T cells to eliminate tumor cells.

We started an IHC analysis of CD3, CD8, IDO and PD-L1 to confirm the observations of gene expression analysis. Furthermore, we will compare the localization of CD8 TILs with IDO-expressing cells and PD-L1-expressing cells to examine wether the expression of IFNγ-induced IDO and PD-L1 is in contact to CD8 T cells. In addition, we will add the staining of PD-1 and LAG-3 in order to confirm that CD8 T cells express LAG-3 and PD-1.

3.5 Cancer immunotherapy for patient P143

The tumor P143 exhibited an immune profile (numerous CD8 TILs, IFNγ signature, upregulated expression of IDO, PD-1, LAG-3 and IDO) similar to that which exists in MMR-deficient colorectal carcinomas[142]. Interestingly, a small study recently showed that most MMR-deficient colorectal cancers and other MMR-deficient cancers respond to the anti-PD-1 antibody pembrolizumab while no response was observed in MMR-proficient colorectal cancers (objective response rates of 40%, 71% and 0%, respectively; 10, 7 and 18 patients per cancer type)[4]. Therefore blocking the PD-1 pathway has the potential to revert the immune suppression that likely existed in tumor P143. This small study showed the great promise of anti-PD-1 antibodies in MMR-deficient tumors, although most responses were partial (1 complete response out of 9), which indicates persistent mechanisms of immune suppression.

Combined blocking of the PD-1 and another immunosuppressive pathway has the potential to increase the proportion of responding tumors and the proportion of complete tumor responses. Such candidates are LAG-3 and IDO based on the immune profile of tumor P143. A combination therapy of anti-PD-1 and anti-LAG-

3 antibodies has been shown superior to single anti-PD-1 therapy in 2 tumor mouse models[145]. The combination of an IDO inhibitor and a PD-L1 inhibitor delayed tumor growth more than each single inhibitor in another tumor mouse model[146]. Trials of those combinations are ongoing (*e.g.* NCT01968109 and NCT02073123, clinicaltrials.gov) and premiminary results of combined IDO/PD-1 blockade are promising (radiologically documented tumor response in 10/19 patients with various advanced or metastatic cancers)[147].

3.6 Which tumors will respond to blockade of the PD-1 pathway?

To date, validated predictive markers of response to PD-1 pathway inhibitors are lacking although several markers have been associated with response to those inhibitors.

Studies in advanced NSCLC, metastatic melanoma and in MMR-deficient/proficient tumors have shown that the number of nonsynonymous mutations is associated with the clinical benefit of anti-PD-1 antibodies[4,148,149]. Furthermore patients with tumors containing high number of nonsynonymous mutations due to mutations in genes *POLE* and *POLD1* encoding DNA polymerases δ and ε, respectively, respond also to anti-PD-1 antibodies[148,150]. Thus a higher number of mutations results in increased immunogenicity which leads to an increased likelihood to respond to anti-PD-1 antibodies. Yet some tumors with a low number of mutations have also responded and some tumors with a high number of mutations did not respond (Figure 3-2). The number of mutations is therefore not suitable for selecting patients who could benefit from anti-PD-1 or anti-PD-L1 antibodies. It is possible that tumors with a low number of mutations and response to anti-PD-1 antibodies contain TILs that recognize non-mutant tumor antigens such as MAGE-type antigens. Tumors with a high number of mutations and no response do probably contain an immunosuppressive microenvironment that cannot be overcome by blocking the PD-1 pathway. Further analyses are necessary to test these hypotheses.

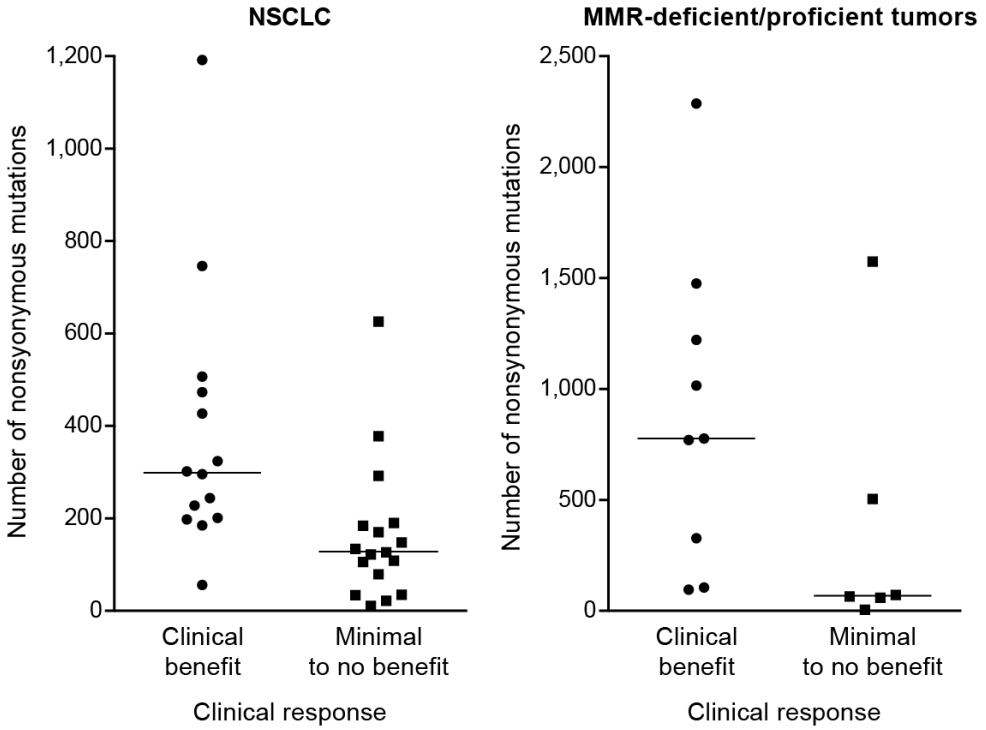

Figure 3-2. Number of nonsynonymous mutations in tumors of patients with or without response to an anti-PD-1 antibody.

The number of nonsynonymous mutations per tumor is indicated for patients with clinical benefit and for patients with no or minimal benefit to the anti-PD-1 antibody. Data from Le *et al.* (MMR-proficient colorectal, MMR-deficient colorectal tumors and other MMR-deficient tumors)[4] and Rizvi *et al.* (NSCLC)[148] are shown. Nonsynonymous mutations were identified with different variant calling algorithms in the 2 studies.

TIL markers in pre-treatment tumor samples have been shown to be associated with tumor response to anti-PD-1 or anti-PD-L1 antibodies. These T cell markers suggest the existence of an antitumor T cell response in the tumor and may therefore predict response to PD-1 blockade. CD8 TILs have been associated with response to the anti-PD-1 antibody pembrolizumab in advanced melanoma and other tumors[4,12]. However, Herbst *et al.* did not find a significant association between the number of CD8 TILs and the response to an anti-PD-L1 antibody in their study in several cancer types (melanoma, kidney, lung, head and neck and colorectal tumors)[53]. They observed clusters of CD8 TILs in tumors of patients without reponse to an anti-PD-L1 antibody and these tumors did not display

upregulation of cytolytic markers or IFNγ signature during therapy whereas the tumors of responders did. Markers of T cell activity such as IFNγ signature[12,53] or T cell activation marker (PD-1[12,15]) may be more precise to predict response to cancer immunotherapy. An IFNγ signature has been found associated with response to anti-PD-1 or anti-PD-L1 antibodies in two small studies (mostly in metastatic melanoma) but another small study (patients with metastatic melanoma treated with an anti-PD-1 antibody) did not confirm this association[149]. Finally, the most analysed marker to predict clinical response to PD-1 blockade is PD-L1 but its predictive value is not clear. PD-L1 expression on tumor cells and stromal cells is associated with response in most cases, but some patients with PD-L1 negative tumors respond also to anti-PD-1 or anti-PD-L1 antibodies[3].

None of these markers are validated and the search for predictive biomarkers of response to anti-PD-1 or anti-PD-L1 antibodies is ongoing.

3.7 Perspectives

The immunogenicity of metastatic human melanomas has been studied extensively by several groups. These tumors bear multiple tumor-specific and tumor-associated antigens that can be recognized by autologous CD8 T cells, and such antitumor T cells can be detected in the tumors and in the blood of most if not all melanoma patients. Thus metastatic melanoma is antigenic and spontaneously immunogenic. In this work we have shown that the situation is quite different for primary invasive breast carcinomas. Antitumor CD8 T cells could be observed in only one out of six breast tumors. This immunogenic tumor displayed a DNA mismatch repair deficiency and contained 4 to 7 times more missense SNVs than the other five tumors. Our estimation of tumor antigenicity suggests that the other five breast tumors present few if any mutant antigens to CD8 T cells, which could explain why we did not find tumor-specific CD8 T cells in these tumors.

We did not find anti-MAGE CD8 T cells in the four tumors that express cancer-germline genes. It is possible that the display of MAGE-type antigens on thymic medullary epithelial cells leads to some level of central T cell tolerance to these antigens. However this tolerance is not present in all individuals as many melanoma patients were shown to have mounted anti-MAGE T cell responses. We have not tried to determine the frequencies of naive anti-MAGE T cells in the

blood of the six patients of this study. MAGE-type antigens remain interesting targets for cancer immunotherapy and our results suggest that in breast cancer patients they should be used in vaccines capable to prime CD8 T cell responses or through the adoptive transfer of MAGE-specific T cells.

The low antigenicity of primary invasive breast carcinomas could result from prior immunoselection by tumor-specific T responses induced at an earlier stage of tumor development. Ductal carcinoma *in situ* (DCIS) is an intraductal proliferation of tumor cells that do not cross the basement membrane as opposed to invasive carcinoma, and is often associated with primary invasive breast carcinomas[151]. Untreated DCIS evolves to invasive ductal carcinoma in 14-75% (average of 43%) of patients[152] and DCIS is considered to be a non-obligate precursor of invasive carcinoma[151]. The mechanisms of progression from *in situ* to invasive ductal carcinoma are not understood. Intriguingly, lymphocytes are present in DCIS and at their margins[153,154], suggesting that tumor-specific T cells may contribute to control tumor progression at this very early stage. The antigenicity of DCIS is expected to be similar to that of invasive ductal carcinoma because *in situ* and invasive components of the same tumor are similar at the genomic and transcriptomic levels[151,155,156]. However some genomic differences have been observed and clonal selection of tumor cells in DCIS leading to invasive tumor has been suggested[155,156]. This clonal selection could also be caused by tumor-specific T cells, with a resulting lower antigenicity of tumor cells of invasive primary tumors than of DCIS tumor cells. We will explore the tumor-specificity of T cells infiltrating DCIS.

How can we use immunotherapy for poorly antigenic tumors? Of course T cell-mediated immunotherapy is not applicable to non-antigenic tumors and chemotherapy or targeted therapy are the systemic treatments of choice for patients with those tumors. However using NK cells remains a possibility and NK activating receptors can be transduced into T cells in adoptive transfer approaches[157]. If very few different antigens are present on a tumor, they can be targeted with vaccines or adoptively transfered T cells. It requires the identification of these antigens. The antigenicity of tumors could be predicted by combining exome and RNA sequencing with HLA-binding predictions. This approach would however probably overestimate the number of antigenic tumors. Nevertheless this approach could already identify tumors without any predicted mutant antigenic peptides and without any MAGE-type antigens. Another

approach would be to identify the HLA ligandome. This technique is currently laborious and needs 1 g of tissue[158]. In addition, the current detection rate of 30% underestimates the antigenicity of tumors[134]. The identification of the HLA ligandome will certainly improve in the future and hopefully require less tumor tissue. It would be very interesting to combine these two approaches in a study that tests for the presence of tumor-specific TILs in some tumors, and to analyse the correlation between predicted tumor antigens, detected tumor antigens in the HLA ligandome and the presence of tumor-specific TILs.

Considering all primary breast carcinomas, which modalities of immunotherapy are likely to be used in the next few years ? As discussed above, spontaneously immunogenic tumors should be treated with blocking anti-PD-1 or anti-PD-L1 antibodies that can also be used in combination with inhibitors of other immunosuppressive pathways (LAG-3, IDO or CTLA-4[159]). The adoptive transfer of TILs may be performed as a last option which requires an intensive *in vitro* work and remains limited to few clinical centers in the world. TIL cultures are derived from a resected metastasis, amplified *in vitro*, and administered back into the patient with high dose IL-2 after lymphodepleting regimens. Tumor-specific T cells have been observed in these TIL products and probably mediate tumor regression[66,160]. In metastatic melanoma, this therapy has shown promising results: up to 72% of response rate with 22% of complete response[161].

Antitumor T cell responses should be induced against antigenic tumors without spontaneous antitumor T cell response by active or passive immunization. Vaccination with tumor antigens is the first choice of active immunization. So far, vaccines based on single proteins have been disappointing[162]. A key issue is the lack of efficient CD8 T cell immunization by current vaccines. Another issue is the choice of antigens. MAGE-type antigens and tumor-associated antigens have been used. Nowadays, a combination of whole-exome sequencing, gene expression profiling and HLA-binding prediction can be used to predict mutant antigenic peptides[163], although it is not known if mutant antigens are superior to other tumor antigens as therapeutic targets[164]. Best responses are expected with a combination of several antigens to reduce the risk of tumor evasion. Encouraging results have been published in advanced melanoma with a combination therapy of autologous dendritic cells expressing shared tumor antigens and the anti-CTLA-4 antibody ipilimumab. The combination led to an objective tumor response rate of 38%, including 20% of complete response[165].

A second option for active immunization is the oncolytic virus talimogene laherparepvec (T-VEC). It is an herpes simplex type I virus (HSV1) in which the genes *ICP34.5* and *ICP47* were deleted. Gene *ICP34.5* encodes for a protein that blocks the PKR protein. PKR (double stranded RNA-activated protein kinase) is activated in infected cells during virus replication and inhibits protein translation and therefore virus replication[166,167]. The deletion of *ICP34.5* prevents virus replication in normal cells with PKR activity but leads to virus replication in tumor cells with a dysfunctional PKR pathway[167,168]. The deletion *ICP47* improves the lytic activity of the virus and increases antigen processing, because the encoded protein binds to TAP and prevents translocation of peptides into the ER[169]. Furthermore, the gene encoding GM-CSF was inserted into the virus to increase dendritic cell maturation and T cell immunization. Intratumoral T-VEC injection lead to regressions of injected and non-injected metastases, indicating systemic activity of T-VEC[170]. It is unknown if T-VEC induces new T cell responses or amplifies existing ones and studies are ongoing to dissect the underlying immune responses. Nevertheless, T-VEC has the potential to induce antitumor T cell responses.

Active immunization could be combined with anti-PD-1 or anti-PD-L1 antibodies to prevent subsequent immune suppression of induced antitumor T cell responses. A trial is ongoing to test the combination of T-VEC and pembrolizumab.

Passive immunization is the adoptive transfer of autologous TILs or of autologous T cells transduced with a tumor-specific TCR or a chimeric antigen receptor (CAR)[171]. TCRs or CARs are inserted *in vitro* into T cells of a patient and engineered T cells are amplified and administered back to the patient. 45% of patients with metastatic melanoma (3 partial and 2 complete responses) and 67% of patients with synovial cell sarcoma responded to the adoptive transfer of autologous T cells transduced with an affinity-enhanced NYESO1.A02-specific TCR[172]. Although very promising, affinity-enhanced TCR-engineered T cell therapy can be fatal when the engineered T cells cross-react with self antigens[173]. T cells undergo negative selection in the thymus to prevent recognition of self antigens and engineered TCRs bypass this selection. The key issue is currently the difficulty to identify tumor-specific TCRs for a given patient. The number of currently available antitumor TCRs is limited to shared tumor antigens (*e.g.* MAGE-type or gp100) and common HLA alleles (*e.g.* HLA-A*02). Two approaches exist to extend the use of TCR-engineered T cells to mutant and other tumor antigens. Antitumor TCRs

can be identified in the pool of naive T cells from HLA-matched healthy donors by screening their PBMCs for recognition of tumor antigens[174]. The drawback of this procedure is the restriction to some of the HLA class I alleles. Screening autologous naive T cells for tumor antigen specificity is the other option. After identification of antitumor TCRs, T cells transduced with such TCR must be tested on cells expressing genes encoding the relevant HLA and antigen to confirm antigen processing. Otherwise these engineered T cells are useless.

The adoptive transfer of chimeric antigen receptor (CAR) T cells may be used in the future for the treatment of solid tumors. A CAR contains an extracellular antigen-recognition domain and one or several intracellular T cell signalling domains (CD3ξ, CD28 or CD137). The single chain of the variable part of an antibody (scFv) is used in most CARs for antigen recognition[175]. CAR T cells have the advantage to target surface molecules such as CD19, and not HLA-peptide complexes. Thus they may even be used for tumors that have lost HLA expressiong. CAR T cells are very efficient against B cell malignancies ($CD19^+$ acute lymphoblastic leukemia)[176]. A key issue is their toxicity on normal cells that express the target surface molecule (on-target off-tumor toxicity). The induced B cell aplasia of anti-CD19 CAR T cell therapy is clinically manageable by immunoglobulin replacement. For solid tumors, validated target surface molecules are lacking. First trials with PSMA- or mesothelin-specific CAR T cells are ongoing in patients with solid tumors[175].

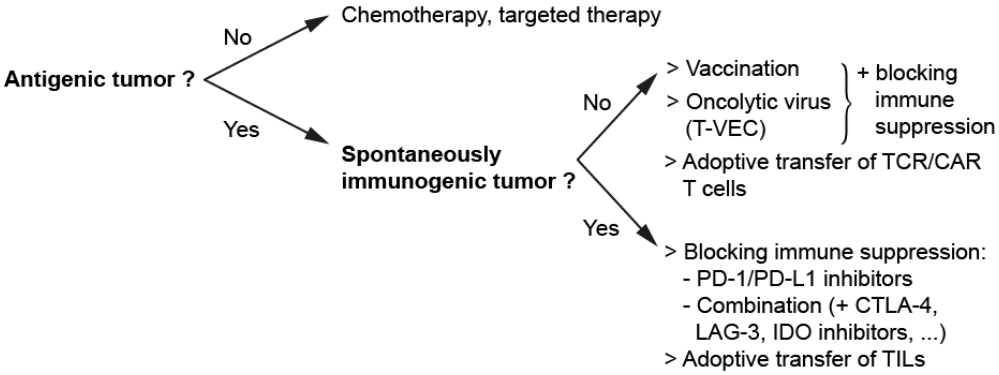

Figure 3-3. A proposed guide of T cell-mediated immunotherapy in oncology.

4 Materials and Methods

4.1 Patients and their samples

Patients with stage 2-3 breast carcinoma, a minimal tumor size of 2cm and without neoadjuvant chemotherapy were selected for the analysis of tumor tissues. Two patients undergoing breast reduction surgery and one patient with the resection of a benign breast tumor were selected for the study of normal breast tissue. Patients enrolled in this study gave written informed consent for the use of their blood and tissue samples (ONCO2008/01 trial, tumor tissue bank of Cliniques universitaires de Saint Luc, study on normal breast tissue). The Ethics Review Committee of the Faculty of Medicine of the Catholic University of Louvain approved the experimental protocols. Tissue samples were obtained from surplus material of resected primary breast carcinoma or normal breast tissue (breast reduction or near to a benign breast tumor). Blood samples were taken before or at the day of tissue resection and at different time points after resection for patients enrolled in the ONCO2008/01 trial. Peripheral blood mononuclear cells (PBMC) were extracted from venous blood samples by density gradient (Lymphoprep, Axis-Shield, Oslo, Norway) and cryopreserved in Iscove's Modified Dulbecco's Medium (IMDM, Invitrogen) supplemented with 10% human serum (HS) and 10% DMSO until further use. HS was prepared from pools of plasma from unselected ABO donors. Plasma was supplemented with CaCl2 and bovine thrombin (MP Biomedicals, Santa Ana, CA) and allowed to clot for 1 h at 37°C. After centrifugation, serum was decomplemented (45 min at 56°C) and irradiated. Autologous EBV-transformed B lymphocytes (EBV-B cells) were generated for each patient by infecting PBMCs with the Ebstein-Barr virus (EBV, B95.8 strain) in presence of the murine cell line 3T6 stably transfected with CD40L.

4.2 Isolation and cloning of CD8 T cell clones

For each tumor or normal breast tissue sample, a part was frozen at -80°C within 1 hour following resection. The remaining fresh sample was weighed and T cells were extracted on the same day or the day after (tissue sample kept as pieces of 1-2 mm at 4°C overnight in cell culture medium). The fresh tissue samples were minced under sterile conditions and cells were extracted from the tissue by mechanical disruption and by enzymatic digestion according to the MACS human tumor dissociation kit protocol (Miltenyi Biotec, Bergisch Gladbach, Germany). The resulting cell suspensions were washed with RPMI 1640 medium (Invitrogen)

supplemented with 2% of HS, stained for cell sorting of CD8 T cells with a mix of fluorochrome-conjugated antibodies (different mixes were used during the project, see Table 4-1) during 30 minutes at 4°C in 0,5-1 mL of locally produced Hanks' balanced salt solution supplemented with 1% of HS (staining medium), and washed once. A viability dye was used additionnally for some cell suspsensions. Living $CD3^+CD8^+CD4^-$ cells were sorted on a FACS Aria III (BD Biosciences, New Jersey, NJ) as one cell per well in a 96-well plate (Costar). All analyses of flow cytometry data have been done with FlowJo (Ashland, OR).

Antibody	**Staining of tissue cell suspension from**		
	P142, P143, P154	**P195, LB3410, LB3466 and LB5673**	**P223 and LB5784**
Anti-CD3	APC, 1 µg/mL, UCHT1 clone, Biolegend #300412	FITC, 5 µg/mL, UCHT1 clone, Biolegend #300406	FITC, 1 µg/mL, UCHT1 clone, Biolegend #300406
Anti-CD8a	FITC, 1.8-3.5 µg/mL, B9.4.1 clone, in-house production	APC-H7, 2 µg/mL, SK1 clone, BD Biosc. #641400	PE, 0.1 µg/mL, SK1 clone, Biolegend #344706
Anti-CD4		PE, 0.5 µg/mL, RPA-T4 clone, Biolegend #300508	APC-Cy7, 1 µg/mL, RPA-T4 clone, Biolegend #300518
Viability dye	No	To-Pro-3, 10 nM, Invitrogen	7-AAD, 0.5 µg/mL, ThermoFischer Scientific

Table 4-1. Staining of TILs.

Final concentration of antibodies or viability dies is indicated. Allophycocyanin, APC; fluorescein isothiocyanate, FITC; phycoerythrin, PE; BD Biosciences, BD Biosc.

Sorted CD8 T cells clones were next expanded with a non-specific T cell stimulation in 200 µL of complete T cell culture medium consisting of IMDM supplemented with 10% of HS, L-arginine (0.55 mM), L-asparagine (0.24 mM), L-glutamine (1.5 mM), mercaptoethanol (0.05 mM), 1-methyl-L-tryptophan (0.1 mM), penicillin (100 U/mL) and streptomycin (0.1 mg/mL). Clones from P142, P143, P154 and LB3410 were expanded with the old protocol and clones from P195, P223, LB3466, LB5673 and LB5784 with the new protocol (Table 4-2). The clone stimulation was repeated without gentamycin at day 9-10 for both

protocols and at day 19-21 for the old protocol. Clones were passed from 96-well plates to 48-well and 24-well plates when needed. Clones at sufficient cell number (>0.5 x 10^6 cells) were frozen at least 7 days following the last stimulation.

	Old protocol	New protocol
Allogenic irradiated EBV-B cell line	10^4 cells/well	6 x 10^4 cells/well
Allogenic irradiated PBMCs from different donors	2 x 10^4 cells/well	3 x 10^5 cells/well
Anti-CD3 monoclonal antibody	1 µg/mL	40 ng/mL
IL-2, IL-7	50 U/mL, 10 ng/mL	50 U/mL, 10 ng/mL
Gentamycin	50 µg/mL	50 µg/mL

Table 4-2. Old and new clone stimulation.

Anti-CD3 monoclonal antibody: OKT3 clone (Janssen-Cilag, Berchem, Belgium; or Bio X cell, West Lebanon, NH)

4.3 CDR3 sequencing of TCRß

Method was adapted from Warren *et al.*[177] RNA from each T cell clone was extracted using the MagMax-96 Total RNA isolation kit (Ambion) and eluted in 50µL. Reverse transcription was performed in 10.5µL. 100 units of SmartScribe Reverse Transcriptase (Clontech Laboratories), 2µM of universal primer matching the Cß1 and Cß2 sequences (5'-CACGTGGTCGGGGWAGAAGC-3'), 1mM deoxyNTP mix (Clontech), 2mM DTT (Clontech) and 10 units of RNAse Ribolock were added to 3.5µL of RNA. 2µM of the target-switching oligonucleotide (5'-AAGCAGTGGT AACAACGCAGAGTACGCGGG-3') was added to create a 5' template for RACE. After reaching the 5' end of the TCRß mRNA, the reverse transcriptase adds a few deoxy-C nucleotides to the cDNA molecule. The poly-G sequence at the 3' end of the target-switching oligonucleotide anneals to the stretch of deoxy-C and serves as an extended template for the reverse transcriptase. The resulting cDNA molecule is complementary to the TCRß transcript and to the target-switching oligonucleotide at its 5' end. After 75 minutes of extension at 72°C and inactivation at 70°C for 10 minutes, RNA was digested with 1 unit of Ribonuclease H (Invitrogen or Affymetrix) and cDNA was purified with AMPure XP paramagnetic

beads (Agencourt). One sixth of cDNA was used as a template in PCR amplification using 2 units of Phusion high-fidelity Hot-Start DNA polymerase (New England BioLabs or Thermo Fischer Scientific) for 32 cycles with annealing at 68°C. 3 primers were used simultaneously in the PCR amplification. A first primer is composed of a sequence identical to a part of the target-switching oligonucleotide at its 3' end and of a new sequence at its 5' end (0.16µM, 5'-CTAATACGACTCACTATAGGGCAAGCAGTGGTAACAACGCAGAGT-3'). The second primer is complementary to the new sequence ot the first primer (0.8µM, 5'-CTAATACGACTCACTATAGGGC-3'). The third primer is an internal primer of the Cß (0.8µM, 5'-TCTCTGCTTCTGATGGCTCAAAC-3'). PCR amplification was performed in 50µL. PCR products were purified and sequenced in-house or by Beckman-Coulter Genomics with a primer matching the Cß. V gene, J gene and CDR3 of the TCR ß chain were identified using IMGT/V-QUEST[178].

4.4 RNA and DNA extraction for NGS analysis

Slices of 7µm and 20-30µm were cut with a cryotome from the frozen tumor sample embedded in optimal cutting temperature compound. The presence of infiltrating tumor cells was verified by a pathologist (C Galant) on the 7µm-thick hematoxylin and eosin-stained tumor slices (~40-50% of tumor cells in the tumor of P142 and P143, ~20-30% in the tumor of P154, ~70% in the tumor of P195, P223 and LB5784). Several 20-30µm slices of each tumor were stored at -80°C until further DNA/RNA extraction. GITC/CsCl method was used to isolate tumor DNA and RNA from the same tumor slices and DNA/RNA was purified using purification columns. Briefly, several 20-30µm tumor slices were lysed in 1.5ml of 4M guanidinium isothiocyanate (GITC) and supernatant was collected after centrifugation (10min, 4°C, 11000 rcf). Supernatant was added carefully to ultracentrifugation tubes containing 1ml of 5.7M Cesium Chloride (CsCl) in the lower part and 1.5ml of GITC in the upper part. Ultracentrifugation was performed for 16h at $2.26x10^5$ rcf on an Optima LE-80K ultracentrifuge (Beckman Coulter, Palo Alto, CA). GITC fraction was discarded, DNA was collected in CsCl fraction and RNA pellet was resuspended and purified with the NucleoSpin RNA purification kit (NucleoSpin RNA, Macherey-Nagel, Düren, Germany). RNA was washed, DNase-treated and resuspended according to the NucleoSpin RNA kit protocol. For DNA, pure ethanol was added to the DNA/CsCl fraction, DNA

washed and resuspended subsequently according to the NucleoSpin Tissue kit protocol (Macherey-Nagel). If RNA was detected in the DNA (measured by fluorometric quantification assay Qubit (Invitrogen)), the DNA was treated with 20 mg/mL of RNase A and washed again according to the NucleoSpin Tissue kit protocol. DNA of frozen autologous EBV-B cell pellet was extracted following NucleoSpin Tissue kit protocol including RNase treatment.

4.5 Whole-exome sequencing

Whole exome-sequencing was performed on tumor DNA and matched normal DNA (extracted from EBV-B cells for all patients except from PBMC for LB5784). The library of samples from P142 and P143 were prepared with the Nextera Rapid Capture Exome kit (37Mb, Illumina) and sequenced by AROS Applied Biotechnology (Aarhus, Denmark). The library of samples from P154, P195, P223 and LB5784 were prepared with the SureSelect Human All Exon kit (version 5, Agilent) and sequenced by Beckman-Coulter Genomics. Paired-end sequencing was performed on an Illumina HiSeq 2000 (2x100bp for all samples except 2x125bp for the samples of LB5784). Reads of tumor and normal exomes were aligned to the reference human genome GRCh38 (Ensemble[179], version 79 from March 2015) using the Burrows-Wheeler Aligner software with MEM algorithm[180] (version 0.7.12). Average depth was 390x for tumor samples of P142 and P143, 180x for normal samples of P142 and P143, 120-160x for tumor samples of P154, P195, P223, LB5784 and normal sample of LB5784 and 40-60x for normal samples of P154, P195 and P223. Picard tools (version 1.101, http://broadinstitute.github.io/picard) were used to sort SAM files by genomic coordinates, to convert SAM to BAM files and to sort out duplicate reads. Reads were locally realigned around germline indels using RealignerTargetCreator and IndelRealigner of the GATK tools[181] (version 3.3-0). Somatic single nucleotide variants (SNV) were called with Mutect[107] (version 1.1.7) and somatic indels were called with VarScan2[108] (version 2.3.7, http://varscan.sourceforge.net). Functional effect of identified variants was predicted with SnpEff[109] (version 4.1 for SNVs and version 3.6 for indels). Peptide of 19 amino acids with mutated peptide at the center was predicted for each SNV with SnpEff v3.6 ('-a' option). All tools and algorithms were run by default parameters if not otherwise stated.

4.6 mRNA sequencing

mRNA sequencing was performed with tumor RNA by Beckman-Coulter Genomics (Danvers, MA). Automated Illumina TruSeq RNA Library Construction using polyA capture for total RNA samples was performed and paired-end 100bp or 125bp reads were sequenced on an Illumina HiSeq. Reads were aligned to the reference human genome GRCh38 (Ensemble[179], version 79 from March 2015) using Bowtie2[182] (version 2.2.5) and TopHat[183] (version 2.0.13). Mate inner-distance was set to 100bp. 15-20 million read pairs were aligned per sample. Transcript abundance estimation was performed by Cufflinks program[184] (version 2.1.1) using SAMtools[185] (version 0.1.19). Gene annotation for each gene was added with Excel (Microsoft Excel for Mac 2011) using the Ensembl gene annotation of GRCh38.v79.

4.7 Peptides

Peptides with purity higher than 70% were synthesized by ProteoGenix (Schiltigheim, France) or by local facility (Ludwig Institute for Cancer Research, Brussels Branch, V. Stroobant), suspended in DMSO at 10mM and cryopreserved. The use of purified peptides is mentioned if used.

4.8 Transduction of EBV-B cells with cancer-germline genes or *ERBB2*

Autologous EBV-B cells were transduced with the coding sequence of selected cancer-germline genes and *ERBB2*. Briefly, coding sequences were extracted from pcDNA1 (*MAGEA3*, *MAGEA4, MAGEA10, MAGEA12 and NYESO1*) or pcDNA3 (*MAGEA6*, *ERBB2*) plasmids and inserted in the lentiviral vector pTM898 for *MAGEA3* or pLenti6/V5-D-TOPO for *MAGEA4, MAGEA6*, *MAGEA10, MAGEA12, NYESO1* and *ERBB2* (Invitrogen, Carlsbad, CA). Plasmids containing cancer-germline genes were a gift from the Brussels Branch of Ludwig Institute for Cancer Research. ERBB2 plasmid was a gift from Mien-Chie Hung[186] (Addgene plasmid # 16257). pTM898 vector was a gift from T. Michiels (de Duve Institute, Belgium). Lentiviral vectors were amplified and the sequence of the inserted coding sequence controlled by Sanger sequencing before the virus assembly in the 293 T cell line. The lentiviral vector contained an antibiotic resistance gene and

transduced EBV-B cells were selected with the corresponding antibiotic. Expression of MAGE-like genes was controlled by RT-PCR. The antigenic processing of MAGEA3-transduced EBV-B cells from P142 and P223 were tested at the beginning and at the end of the CD8 TIL clone screening with their recognition by a MAGEA3.A1 specific T cell clone. The expression of *ERBB2* was analysed by flow cytometry with an anti-HER2/PE antibody (1µg/mL, clone 24D2, Biolegend #324405) and HER2-positive cells were sorted by flow cytometry (FACS Aria III). Persistence of *ERBB2* expression was controlled by flow cytometry during CD8 TIL clone screening and compared with the HER2-overexpressing human ovary adenocarcinoma cell line SK-OV-3 (Cell Lines Service). Transduced and not transduced EBV-B cells were cultured in EBV-B cell medium consisting of IMDM supplemented with 10% fetal bovine serum (Gibco, Paisley, United Kingdom), L-arginine (0,55 mM), L-asparagine (0,24 mM), L-glutamine (1,5 mM), mercaptoethanol (0,05 mM), penicillin (100 U/mL) and streptomycin (0,1 mg/mL).

4.9 CD8 TIL clone screening

The clones were thawed 2 weeks before screening and amplified in 2 wells of a M24 plate filled with 2ml of T cell culture medium, allogenic irradiated EBV-B cell line (10^6 cells), irradiated allogenic PBMC from different donors (5.10^6 cells), anti-CD3 monoclonal antibody (40 ng/mL), IL-2 (50 U/mL) and IL-7 (10 ng/mL). At day 4, clones were washed and resuspended in same medium supplemented with cytokines at the same concentration. Wells were divided or half of supernatant replaced when necessary. At the first day of screening, 20,000 autologous EBV-B cells were incubated with peptides either individually (poorly soluble peptides) or in pools of 2-4 peptides at a concentration of 40 µM for 2 hours in M96 round-bottom microtiter plates filled with 100 µL IMDM supplemented with 1% of HS, penicillin (100 U/mL) and streptomycin (0.1 mg/mL). For the the TIL clones of P142, all peptides were tested with pools of 5-7 peptides at 20 µM. Clones were washed 3 times, counted and resuspended at 10^5 cells/mL in complete T cell culture medium supplemented with IL-2 at 7.5 or 15 U/mL (30 U/mL for P142 TIL clones). Then, 10,000 cells were added on the 20,000 'peptide-pulsed', transduced and non-transduced EBV-B cells. 5,000 human T-Activator CD3/CD28 beads (Dynabeads, Thermo Fischer Scientific) were used to test the ability of each clone to secrete detectable cytokines. All conditions were tested in triplicates.

After overnight co-culture (day 2), 130µL of supernatant were collected, frozen, thawed and 50µL added on 3-times-washed M-07e cells (20,000 cells in 50µL EBV-B cell medium). The day after (day 3), 20µL of [Methyl-^{3}H]-Thymidine 25µCi (PerkinElmer, Waltham, MA) was added and incorporation of tritiated thymidine in DNA was measured on day 4. Cells were lysed and DNA transferred to 96-well UniFilter GF/C plates (PerkinElmer) with a cell harvester FilterMate 196 (Packard Bioscience, CT). 30µL of MicroScint-O solution (PerkinElmer) was added on the filter and scintillation measured with a Top Count NXT (PerkinElmer) microplate scintillation counter (Perkin Elmer). Results are expressed as counts per minute (cpm). For each clone, the proportion of maximal activation was calculated as follow: 100 x cpm of condition / cpm of condition with maximal count. If not otherwise stated, all tests with the M-07e assay were performed in the same way. Further tests with CD8 T cell clones were performed as described above if not otherwise stated.

4.10 MHC class I typing

MHC class I allele typing was performed with ATHLATES[187] on whole-exome sequencing and RNA-seq data. Low-confidence and homozygous MCH alles were confirmed with sequence-specific primer PCR by a clinical laboratory (Cliniques universitaires Saint Luc).

4.11 ^{51}Cr-release assay

The cytolytic activity of T cell clones was assessed in a standard 4-hour ^{51}Cr-release assay. Target cells (P143-EBV, K562) were charged with 0.2mCi of ^{51}Cr (Perkin Elmer) at 37°C during 1 hour. Target cells were washed twice and P143-EBV were pulsed or not with 10µM of the mutant or wild-type 9-10mer peptide during 30 minutes (purified for mutant peptide, non-purified for normal peptide). After a third wash, 1,000 ^{51}Cr-labeled target cells per well were co-cultured with 100 to 30,000 CD8^{+} TIL clones during 4h (effector-target ratio of 0.1-0.3-1-3-10-30). ^{51}Cr-release in the supernatant was revealed using solid scintillator coated LumaPlates (Perkin Elmer) and the scintillation was measured with a Top Count NXT microplate scintillation counter (Perkin Elmer). All conditions were tested in triplicates. The percentage of specific lysis was calculated as follow: 100 x (Mean

observed ^{51}Cr-release – Mean spontaneous ^{51}Cr-release) / (Mean maximal ^{51}Cr-release – Mean spontaneous ^{51}Cr-release). Maximum ^{51}Cr-release was determined by treating target cells with 0.5% triton and spontaneous release was determined by incubating target cells in medium alone.

4.12 Bioplex assay

P143-EBV cells were pulsed for 1 hour at 37°C with 20µM of mutant or wild-type peptide (purified for mutant peptide, non-purified for normal peptide) and washed once. Per well, 20,000 of peptide-pulsed P143-EBV cells were co-cultured overnight with 10,000 autologous antitumor CD8 TIL clones and the supernatant was collected the day after. Cytokines of the supernatant were measured with the Bio-Plex Pro Human Cytokine 17-plex assay (Biorad) on a Bio-Plex 200 system according to the protocol, except that the antibody-coupled beads and detection antibodies were diluted 0.5 times.

4.13 Minigene transfection

Minigenes corresponding to 303-318bp of the mutated or the wild-type coding sequence of *PRR12*, *ATP2A2*, *NOC2L* and *TKT* were designed (wild-type or mutated nucleotide at the center). De-novo synthesis of those minigenes was performed by Integrated DNA Technologies. The minigenes were cloned in a pmaxGFP vector (Lonza) in phase with GFP and linked through a P2A sequence (porcine Teschovirus-1). Tumor cells were transfected with the minigene-containing plasmids using Transit-LT1 transfection reagent (Mirus). For the experiments with *TKT*, 293T cells were cotransfected with a HLA-A*80:01 plasmid that was cloned from EBV-B cells of the patient P143. 2 days after transfection, cells were harvested and the transfection efficiency measured with the expression of the maxGFP reporter by flow cytometry. As control, cells were pulsed with 10µM of the antigenic peptide and washed twice after 1h of incubation with the peptide. Coculture of 10,000 T cells and 10,000 target cells (peptide-pulsed or not) was started and supernatant collected the day after. Cytokine secretion was measured with the M-07e assay.

4.14 *Ex-vivo* staining, MLPC and multimer staining

PBMC were thawed in complete T cell medium with 10µg/mL of DNase I (Roche), resuspended in the same medium with 10µg/mL of DNase I and counted. Two samples of 0.5-1x10^6 living cells were used for the ex-vivo staining and incubated with 50nM of dasatinib (Axon Medchem) for one hour at room temperature. Cells were resuspended in PBS with 50nM of dasatinib and stained with a pair of tetramers or dextramers. The pair of tetramers contained a NOC2L.A02 tetramer (coupled to PE, final concentration of 10nM) and a BMFL1.A02 tetramer (coupled to APC, final concentration of 10nM). Both tetramers were produced by D. Colau at the Brussels Branch of the Ludwig Institute for Cancer Research. The pair of dextramers contained a PRR12.B44 dextramer (coupled to PE, Immudex, 0.025 times diluted) and an ATP2A2.B44 dextramer (coupled to APC, Immudex, 0.025 times diluted). Dextramers were added in 2 separate steps according to the protocol of Immudex. After 15 minutes of incubation at room temperature, an anti-CD8a antibody (coupled to FITC, B9.4.1 clone, in-house production, final concentration of 1µg/mL) and an anti-CD4 antibody (coupled to APC-Cy7, RPA-T4 clone, Biolegend, final concentration of 1µg/mL) were added and incubated for 20 minutes at room temperature for tetramer-stained cells and at 4°C for dextramer-stained cells. Cells were washed once in PBS supplemented with 1% of Bovine serum albumin (BSA, w/v, Sigma-Aldrich) and resuspended in PBS-1%BSA for flow cytometry analysis on a LSRFortessa (BD Biosciences). The remaining PBMCs were split in two equal parts and resuspended in IMDM supplemented with 1% HS. The first part was incubated with 10µM of the purified antigenic peptide of ATP2A2.B44 and the second part with 10µM of the purified antigenic peptides of PRR12.B44 and NOC2L.A02. After 1 hour of incubation, PBMCs were washed once, resuspended in complete T cell medium supplemented with 10ng/mL of IL-7 and 20U/mL of IL-2 and distributed in a microtiter plate (90,000 to 120,000 PBCMs per well for the 3 MLPCs, volume of 200µL). Cells were re-stimulated with 10µM of peptides at day 8 and analysed by flow cytometry at day 15. All wells were split into 2 wells at day 9 or 10 and half of the cell medium was resupplemented with complete T cell medium supplemented with 10ng/mL of IL-7 and 20U/mL of IL-2 when needed. As for the *ex-vivo* analysis, cells were stained with dasatinib, split in two parts and each part was stained with the pair of tetramers or dextramers (diluted x 0.05) before staining with 1µg/mL of the anti-CD8a antibody (coupled to FITC, B9.4.1 clone). For the cell sorting of multimer-positive CD8 T cells on the

FACS Aria III, cells were stained at day 16 without dasatinib. After adding the NOC2L.A02 tetramer (10nM), the PRR12.B44 or the ATP2A2.B44 dextamer (diluted x 0.067), the anti-CD8a/FITC were added after as described above (1µg/mL).

4.15 TCRBV repertoire by massive parallel sequencing

Briefly, RNA was extracted from frozen tumor sections or frozen PBMC and a reverse transcription was primed with an oligonucleotide specific to the Cß1 and Cß2 segments from the TCRß genes. This primer included a short random sequence that uniquely identified each synthesized cDNA molecule and that was referred as unique molecular identifier or UMI. TCRß cDNA molecules were then amplified by 2 consecutive nested multiplex PCR specific for all Vß genes. Adapters for sequencing on a Miseq (Illumina) platform were added before sequencing. Generated reads were engaged in an algorithm to identify V, D, J gene segments and the CDR3 region of rearranged TCRß genes. Compilation of reads by their UMI allowed to quantify sequenced TCRß molecules and to correct amplification bias as well as the sequence errors introduced during the library construction. Identical rearranged TCRß molecules characterizing each T cell clonotype were enumerated allowing a quantitative view of the T cell repertoire present in the sample and the accurate evaluation of individual clonotypes frequency in this repertoire.

4.16 Detection of MSI instability and loss of MSH2 in IHC

DNA of the 6 tumor-matched samples were used for detection of microsatellite instability (MSI Analysis System, Promega) and performed by the Institut de Pathologie et de Génétique (Gosselies, Belgium). IHC for MSH2, MSH6, MLH1 and PMS2 were performed on formaldehyde fixed paraffin embedded tumor (FFPE) tumor section by the pathology department of Cliniques Universitaires Saint-Luc and by the Institut de Pathologie et de Génétique.

4.17 Immunohistochemistry

Five µm-thick sections were obtained from FFPE tumors samples. Endogenous peroxidase activity was blocked with Peroxidase Blocking Reagent (Dako

Cytomation) and nonspecific protein binding was prevented with tris-buffered saline supplemented with 2% of milk, 5% of bovine serum albumin, 1% of human immunoglobulins and 0.15% of Tween20. Sections were stained with an unlabelled primary MHC class I or ß-2-microglobuline (B2M) monoclonal antibody (MHC class I: clone EMR8-5, mouse, Abcam, 0.002x dilution; B2M: clone D8P1H, rabbit, Cell Signaling Technology, 0.008x dilution) for 30 minutes, washed, and incubated for 60 minutes with a secondary polyclonal goat anti-mouse or anti-rabbit antibody coupled to horseradish peroxidase (Dako Cytomation). After washing, bound antibodies were detected with 3-amino-9-ethylcarbazole and sections were counterstained with hematoxylin.

5 References

1. Robert C, Thomas L, Bondarenko I, O'Day S, Weber J, Garbe C, Lebbe C, Baurain JF, Testori A, Grob JJ, Davidson N, Richards J, Maio M, Hauschild A, Miller WH, Jr., Gascon P, Lotem M, Harmankaya K, Ibrahim R, Francis S, Chen TT, Humphrey R, Hoos A, Wolchok JD. Ipilimumab plus dacarbazine for previously untreated metastatic melanoma. N Engl J Med 2011;364:2517-26.
2. Robert C, Schachter J, Long GV, Arance A, Grob JJ, Mortier L, Daud A, Carlino MS, McNeil C, Lotem M, Larkin J, Lorigan P, Neyns B, Blank CU, Hamid O, Mateus C, Shapira-Frommer R, Kosh M, Zhou H, Ibrahim N, Ebbinghaus S, Ribas A, investigators K-. Pembrolizumab versus Ipilimumab in Advanced Melanoma. N Engl J Med 2015;372:2521-32.
3. Callahan MK, Postow MA, Wolchok JD. Targeting T Cell Co-receptors for Cancer Therapy. Immunity 2016;44:1069-78.
4. Le DT, Uram JN, Wang H, Bartlett BR, Kemberling H, Eyring AD, Skora AD, Luber BS, Azad NS, Laheru D, Biedrzycki B, Donehower RC, Zaheer A, Fisher GA, Crocenzi TS, Lee JJ, Duffy SM, Goldberg RM, de la Chapelle A, Koshiji M, Bhaijee F, Huebner T, Hruban RH, Wood LD, Cuka N, Pardoll DM, Papadopoulos N, Kinzler KW, Zhou S, Cornish TC, Taube JM, Anders RA, Eshleman JR, Vogelstein B, Diaz LA, Jr. PD-1 Blockade in Tumors with Mismatch-Repair Deficiency. N Engl J Med 2015;372:2509-20.
5. Nghiem PT, Bhatia S, Lipson EJ, Kudchadkar RR, Miller NJ, Annamalai L, Berry S, Chartash EK, Daud A, Fling SP, Friedlander PA, Kluger HM, Kohrt HE, Lundgren L, Margolin K, Mitchell A, Olencki T, Pardoll DM, Reddy SA, Shantha EM, Sharfman WH, Sharon E, Shemanski LR, Shinohara MM, Sunshine JC, Taube JM, Thompson JA, Townson SM, Yearley JH, Topalian SL, Cheever MA. PD-1 Blockade with Pembrolizumab in Advanced Merkel-Cell Carcinoma. N Engl J Med 2016;374:2542-52.
6. Coulie PG, Van den Eynde BJ, van der Bruggen P, Boon T. Tumour antigens recognized by T lymphocytes: at the core of cancer immunotherapy. Nat Rev Cancer 2014;14:135-46.
7. Lonchay C, van der Bruggen P, Connerotte T, Hanagiri T, Coulie P, Colau D, Lucas S, Van Pel A, Thielemans K, van Baren N, Boon T. Correlation between tumor regression and T cell responses in melanoma patients vaccinated with a MAGE antigen. Proc Natl Acad Sci U S A 2004;101 Suppl 2:14631-8.
8. Carrasco J, Van Pel A, Neyns B, Lethe B, Brasseur F, Renkvist N, van der Bruggen P, van Baren N, Paulus R, Thielemans K, Boon T, Godelaine D. Vaccination of a melanoma patient with mature dendritic cells pulsed with

MAGE-3 peptides triggers the activity of nonvaccine anti-tumor cells. J Immunol 2008;180:3585-93.
9. Germeau C, Ma W, Schiavetti F, Lurquin C, Henry E, Vigneron N, Brasseur F, Lethe B, De Plaen E, Velu T, Boon T, Coulie PG. High frequency of antitumor T cells in the blood of melanoma patients before and after vaccination with tumor antigens. J Exp Med 2005;201:241-28.
10. Lurquin C, Lethe B, De Plaen E, Corbiere V, Theate I, van Baren N, Coulie PG, Boon T. Contrasting frequencies of antitumor and anti-vaccine T cells in metastases of a melanoma patient vaccinated with a MAGE tumor antigen. J Exp Med 2005;201:249-57.
11. Tran E, Ahmadzadeh M, Lu YC, Gros A, Turcotte S, Robbins PF, Gartner JJ, Zheng Z, Li YF, Ray S, Wunderlich JR, Somerville RP, Rosenberg SA. Immunogenicity of somatic mutations in human gastrointestinal cancers. Science 2015;350:1387-90.
12. Tumeh PC, Harview CL, Yearley JH, Shintaku IP, Taylor EJ, Robert L, Chmielowski B, Spasic M, Henry G, Ciobanu V, West AN, Carmona M, Kivork C, Seja E, Cherry G, Gutierrez AJ, Grogan TR, Mateus C, Tomasic G, Glaspy JA, Emerson RO, Robins H, Pierce RH, Elashoff DA, Robert C, Ribas A. PD-1 blockade induces responses by inhibiting adaptive immune resistance. Nature 2014;515:568-71.
13. Nguyen LT, Ohashi PS. Clinical blockade of PD1 and LAG3--potential mechanisms of action. Nat Rev Immunol 2015;15:45-56.
14. Gros A, Parkhurst MR, Tran E, Pasetto A, Robbins PF, Ilyas S, Prickett TD, Gartner JJ, Crystal JS, Roberts IM, Trebska-McGowan K, Wunderlich JR, Yang JC, Rosenberg SA. Prospective identification of neoantigen-specific lymphocytes in the peripheral blood of melanoma patients. Nat Med 2016;22:433-8.
15. Gros A, Robbins PF, Yao X, Li YF, Turcotte S, Tran E, Wunderlich JR, Mixon A, Farid S, Dudley ME, Hanada K, Almeida JR, Darko S, Douek DC, Yang JC, Rosenberg SA. PD-1 identifies the patient-specific CD8(+) tumor-reactive repertoire infiltrating human tumors. J Clin Invest 2014;124:2246-59.
16. Gradishar WJ, Anderson BO, Balassanian R, Blair SL, Burstein HJ, Cyr A, Elias AD, Farrar WB, Forero A, Giordano SH, Goetz M, Goldstein LJ, Hudis CA, Isakoff SJ, Marcom PK, Mayer IA, McCormick B, Moran M, Patel SA, Pierce LJ, Reed EC, Salerno KE, Schwartzberg LS, Smith KL, Smith ML, Soliman H, Somlo G, Telli M, Ward JH, Shead DA, Kumar R. Invasive Breast Cancer Version 1.2016, NCCN Clinical Practice Guidelines in Oncology. J Natl Compr Canc Netw 2016;14:324-54.
17. Viale G. ESMO Factssheets on Biomarkers. 2016.
18. Perou CM, Sorlie T, Eisen MB, van de Rijn M, Jeffrey SS, Rees CA, Pollack JR, Ross DT, Johnsen H, Akslen LA, Fluge O, Pergamenschikov A, Williams C, Zhu

SX, Lonning PE, Borresen-Dale AL, Brown PO, Botstein D. Molecular portraits of human breast tumours. Nature 2000;406:747-52.
19. Carey L, Winer E, Viale G, Cameron D, Gianni L. Triple-negative breast cancer: disease entity or title of convenience? Nat Rev Clin Oncol 2010;7:683-92.
20. Wong E, Chaudhry S, Rossi M. Breast cancer. McMaster Pathophysiology Review.
21. Dawson SJ, Rueda OM, Aparicio S, Caldas C. A new genome-driven integrated classification of breast cancer and its implications. EMBO J 2013;32:617-28.
22. Sotiriou C, Pusztai L. Gene-expression signatures in breast cancer. N Engl J Med 2009;360:790-800.
23. Ruffell B, Au A, Rugo HS, Esserman LJ, Hwang ES, Coussens LM. Leukocyte composition of human breast cancer. Proc Natl Acad Sci USA 2012;109:2796-801.
24. Gu-Trantien C, Loi S, Garaud S, Equeter C, Libin M, de Wind A, Ravoet M, Le Buanec H, Sibille C, Manfouo-Foutsop G, Veys I, Haibe-Kains B, Singhal SK, Michiels S, Rothe F, Salgado R, Duvillier H, Ignatiadis M, Desmedt C, Bron D, Larsimont D, Piccart M, Sotiriou C, Willard-Gallo K. CD4(+) follicular helper T cell infiltration predicts breast cancer survival. J Clin Invest 2013;123:2873-92.
25. Aaltomaa S, Lipponen P, Eskelinen M, Kosma VM, Marin S, Alhava E, Syrjanen K. Lymphocyte infiltrates as a prognostic variable in female breast cancer. Eur J Cancer 1992;28A:859-64.
26. Alderson MR, Hamlin I, Staunton MD. The relative significance of prognostic factors in breast carcinoma. Br J Cancer 1971;25:646-56.
27. Denkert C, Loibl S, Noske A, Roller M, Muller BM, Komor M, Budczies J, Darb-Esfahani S, Kronenwett R, Hanusch C, von Torne C, Weichert W, Engels K, Solbach C, Schrader I, Dietel M, von Minckwitz G. Tumor-associated lymphocytes as an independent predictor of response to neoadjuvant chemotherapy in breast cancer. J Clin Oncol 2010;28:105-13.
28. Salgado R, Denkert C, Demaria S, Sirtaine N, Klauschen F, Pruneri G, Wienert S, Van den Eynden G, Baehner FL, Penault-Llorca F, Perez EA, Thompson EA, Symmans WF, Richardson AL, Brock J, Criscitiello C, Bailey H, Ignatiadis M, Floris G, Sparano J, Kos Z, Nielsen T, Rimm DL, Allison KH, Reis-Filho JS, Loibl S, Sotiriou C, Viale G, Badve S, Adams S, Willard-Gallo K, Loi S, International TWG. The evaluation of tumor-infiltrating lymphocytes (TILs) in breast cancer: recommendations by an International TILs Working Group 2014. Ann Oncol 2015;26:259-71.
29. Adams S, Gray RJ, Demaria S, Goldstein L, Perez EA, Shulman LN, Martino S, Wang M, Jones VE, Saphner TJ, Wolff AC, Wood WC, Davidson NE, Sledge GW, Sparano JA, Badve SS. Prognostic value of tumor-infiltrating lymphocytes in triple-negative breast cancers from two phase III randomized adjuvant

breast cancer trials: ECOG 2197 and ECOG 1199. J Clin Oncol 2014;32:2959-66.
30. Loi S, Michiels S, Salgado R, Sirtaine N, Jose V, Fumagalli D, Kellokumpu-Lehtinen PL, Bono P, Kataja V, Desmedt C, Piccart MJ, Loibl S, Denkert C, Smyth MJ, Joensuu H, Sotiriou C. Tumor infiltrating lymphocytes are prognostic in triple negative breast cancer and predictive for trastuzumab benefit in early breast cancer: results from the FinHER trial. Ann Oncol 2014;25:1544-50.
31. Loi S, Sirtaine N, Piette F, Salgado R, Viale G, Van Eenoo F, Rouas G, Francis P, Crown JP, Hitre E, de Azambuja E, Quinaux E, Di Leo A, Michiels S, Piccart MJ, Sotiriou C. Prognostic and predictive value of tumor-infiltrating lymphocytes in a phase III randomized adjuvant breast cancer trial in node-positive breast cancer comparing the addition of docetaxel to doxorubicin with doxorubicin-based chemotherapy: BIG 02-98. J Clin Oncol 2013;31:860-7.
32. Perez EA, Ballman KV, Tenner KS, Thompson EA, Badve SS, Bailey H, Baehner FL. Association of Stromal Tumor-Infiltrating Lymphocytes With Recurrence-Free Survival in the N9831 Adjuvant Trial in Patients With Early-Stage HER2-Positive Breast Cancer. JAMA Oncol 2016;2:56-64.
33. Dieci MV, Mathieu MC, Guarneri V, Conte P, Delaloge S, Andre F, Goubar A. Prognostic and predictive value of tumor-infiltrating lymphocytes in two phase III randomized adjuvant breast cancer trials. Ann Oncol 2015;26:1698-704.
34. Pruneri G, Vingiani A, Bagnardi V, Rotmensz N, De Rose A, Palazzo A, Colleoni AM, Goldhirsch A, Viale G. Clinical validity of tumor-infiltrating lymphocytes analysis in patients with triple-negative breast cancer. Ann Oncol 2016;27:249-56.
35. Dieci MV, Criscitiello C, Goubar A, Viale G, Conte P, Guarneri V, Ficarra G, Mathieu MC, Delaloge S, Curigliano G, Andre F. Prognostic value of tumor-infiltrating lymphocytes on residual disease after primary chemotherapy for triple-negative breast cancer: a retrospective multicenter study. Ann Oncol 2014;25:611-8.
36. Denkert C, von Minckwitz G, Brase JC, Sinn BV, Gade S, Kronenwett R, Pfitzner BM, Salat C, Loi S, Schmitt WD, Schem C, Fisch K, Darb-Esfahani S, Mehta K, Sotiriou C, Wienert S, Klare P, Andre F, Klauschen F, Blohmer JU, Krappmann K, Schmidt M, Tesch H, Kummel S, Sinn P, Jackisch C, Dietel M, Reimer T, Untch M, Loibl S. Tumor-infiltrating lymphocytes and response to neoadjuvant chemotherapy with or without carboplatin in human epidermal growth factor receptor 2-positive and triple-negative primary breast cancers. J Clin Oncol 2015;33:983-91.
37. Salgado R, Denkert C, Campbell C, Savas P, Nuciforo P, Aura C, de Azambuja E, Eidtmann H, Ellis CE, Baselga J, Piccart-Gebhart MJ, Michiels S, Bradbury I,

Sotiriou C, Loi S. Tumor-Infiltrating Lymphocytes and Associations With Pathological Complete Response and Event-Free Survival in HER2-Positive Early-Stage Breast Cancer Treated With Lapatinib and Trastuzumab: A Secondary Analysis of the NeoALTTO Trial. JAMA Oncol 2015;1:448-54.
38. Ali HR, Provenzano E, Dawson SJ, Blows FM, Liu B, Shah M, Earl HM, Poole CJ, Hiller L, Dunn JA, Bowden SJ, Twelves C, Bartlett JM, Mahmoud SM, Rakha E, Ellis IO, Liu S, Gao D, Nielsen TO, Pharoah PD, Caldas C. Association between CD8+ T-cell infiltration and breast cancer survival in 12,439 patients. Ann Oncol 2014;25:1536-43.
39. Mahmoud SM, Paish EC, Powe DG, Macmillan RD, Grainge MJ, Lee AH, Ellis IO, Green AR. Tumor-infiltrating CD8+ lymphocytes predict clinical outcome in breast cancer. J Clin Oncol 2011;29:1949-55.
40. Curtis C, Shah SP, Chin SF, Turashvili G, Rueda OM, Dunning MJ, Speed D, Lynch AG, Samarajiwa S, Yuan Y, Graf S, Ha G, Haffari G, Bashashati A, Russell R, McKinney S, Group M, Langerod A, Green A, Provenzano E, Wishart G, Pinder S, Watson P, Markowetz F, Murphy L, Ellis I, Purushotham A, Borresen-Dale AL, Brenton JD, Tavare S, Caldas C, Aparicio S. The genomic and transcriptomic architecture of 2,000 breast tumours reveals novel subgroups. Nature 2012;486:346-52.
41. Dedeurwaerder S, Desmedt C, Calonne E, Singhal SK, Haibe-Kains B, Defrance M, Michiels S, Volkmar M, Deplus R, Luciani J, Lallemand F, Larsimont D, Toussaint J, Haussy S, Rothe F, Rouas G, Metzger O, Majjaj S, Saini K, Putmans P, Hames G, van Baren N, Coulie PG, Piccart M, Sotiriou C, Fuks F. DNA methylation profiling reveals a predominant immune component in breast cancers. EMBO Mol Med 2011;3:726-41.
42. Finak G, Bertos N, Pepin F, Sadekova S, Souleimanova M, Zhao H, Chen H, Omeroglu G, Meterissian S, Omeroglu A, Hallett M, Park M. Stromal gene expression predicts clinical outcome in breast cancer. Nat Med 2008;14:518-27.
43. Burstein MD, Tsimelzon A, Poage GM, Covington KR, Contreras A, Fuqua SA, Savage MI, Osborne CK, Hilsenbeck SG, Chang JC, Mills GB, Lau CC, Brown PH. Comprehensive genomic analysis identifies novel subtypes and targets of triple-negative breast cancer. Clin Cancer Res 2015;21:1688-98.
44. Figenschau SL, Fismen S, Fenton KA, Fenton C, Mortensen ES. Tertiary lymphoid structures are associated with higher tumor grade in primary operable breast cancer patients. BMC Cancer 2015;15:101.
45. Martinet L, Garrido I, Filleron T, Le Guellec S, Bellard E, Fournie JJ, Rochaix P, Girard JP. Human solid tumors contain high endothelial venules: association with T- and B-lymphocyte infiltration and favorable prognosis in breast cancer. Cancer Res 2011;71:5678-87.

46. Cipponi A, Mercier M, Seremet T, Baurain JF, Theate I, van den Oord J, Stas M, Boon T, Coulie PG, van Baren N. Neogenesis of lymphoid structures and antibody responses occur in human melanoma metastases. Cancer Res 2012;72:3997-4007.
47. Chen J, Feng Y, Lu L, Wang H, Dai L, Li Y, Zhang P. Interferon-gamma-induced PD-L1 surface expression on human oral squamous carcinoma via PKD2 signal pathway. Immunobiology 2012;217:385-93.
48. Schildberg FA, Klein SR, Freeman GJ, Sharpe AH. Coinhibitory Pathways in the B7-CD28 Ligand-Receptor Family. Immunity 2016;44:955-72.
49. Cancer Genome Atlas Research N. Comprehensive molecular characterization of gastric adenocarcinoma. Nature 2014;513:202-9.
50. Green MR, Monti S, Rodig SJ, Juszczynski P, Currie T, O'Donnell E, Chapuy B, Takeyama K, Neuberg D, Golub TR, Kutok JL, Shipp MA. Integrative analysis reveals selective 9p24.1 amplification, increased PD-1 ligand expression, and further induction via JAK2 in nodular sclerosing Hodgkin lymphoma and primary mediastinal large B-cell lymphoma. Blood 2010;116:3268-77.
51. Roemer MG, Advani RH, Ligon AH, Natkunam Y, Redd RA, Homer H, Connelly CF, Sun HH, Daadi SE, Freeman GJ, Armand P, Chapuy B, de Jong D, Hoppe RT, Neuberg DS, Rodig SJ, Shipp MA. PD-L1 and PD-L2 Genetic Alterations Define Classical Hodgkin Lymphoma and Predict Outcome. J Clin Oncol 2016.
52. Kataoka K, Shiraishi Y, Takeda Y, Sakata S, Matsumoto M, Nagano S, Maeda T, Nagata Y, Kitanaka A, Mizuno S, Tanaka H, Chiba K, Ito S, Watatani Y, Kakiuchi N, Suzuki H, Yoshizato T, Yoshida K, Sanada M, Itonaga H, Imaizumi Y, Totoki Y, Munakata W, Nakamura H, Hama N, Shide K, Kubuki Y, Hidaka T, Kameda T, Masuda K, Minato N, Kashiwase K, Izutsu K, Takaori-Kondo A, Miyazaki Y, Takahashi S, Shibata T, Kawamoto H, Akatsuka Y, Shimoda K, Takeuchi K, Seya T, Miyano S, Ogawa S. Aberrant PD-L1 expression through 3'-UTR disruption in multiple cancers. Nature 2016;534:402-6.
53. Herbst RS, Soria JC, Kowanetz M, Fine GD, Hamid O, Gordon MS, Sosman JA, McDermott DF, Powderly JD, Gettinger SN, Kohrt HE, Horn L, Lawrence DP, Rost S, Leabman M, Xiao Y, Mokatrin A, Koeppen H, Hegde PS, Mellman I, Chen DS, Hodi FS. Predictive correlates of response to the anti-PD-L1 antibody MPDL3280A in cancer patients. Nature 2014;515:563-7.
54. Schalper KA, Velcheti V, Carvajal D, Wimberly H, Brown J, Pusztai L, Rimm DL. In situ tumor PD-L1 mRNA expression is associated with increased TILs and better outcome in breast carcinomas. Clin Cancer Res 2014;20:2773-82.
55. Ali HR, Glont SE, Blows FM, Provenzano E, Dawson SJ, Liu B, Hiller L, Dunn J, Poole CJ, Bowden S, Earl HM, Pharoah PD, Caldas C. PD-L1 protein expression in breast cancer is rare, enriched in basal-like tumours and associated with infiltrating lymphocytes. Ann Oncol 2015;26:1488-93.

56. Mittendorf EA, Philips AV, Meric-Bernstam F, Qiao N, Wu Y, Harrington S, Su X, Wang Y, Gonzalez-Angulo AM, Akcakanat A, Chawla A, Curran M, Hwu P, Sharma P, Litton JK, Molldrem JJ, Alatrash G. PD-L1 expression in triple-negative breast cancer. Cancer Immunol Res 2014;2:361-70.
57. Cancer Genome Atlas N. Comprehensive molecular portraits of human breast tumours. Nature 2012;490:61-70.
58. Coulie PG, Lehmann F, Lethe B, Herman J, Lurquin C, Andrawiss M, Boon T. A mutated intron sequence codes for an antigenic peptide recognized by cytolytic T lymphocytes on a human melanoma. Proc Natl Acad Sci USA 1995;92:7976-80.
59. Baurain JF, Colau D, van Baren N, Landry C, Martelange V, Vikkula M, Boon T, Coulie PG. High frequency of autologous anti-melanoma CTL directed against an antigen generated by a point mutation in a new helicase gene. J Immunol 2000;164:6057-66.
60. Chiari R, Foury F, De Plaen E, Baurain JF, Thonnard J, Coulie PG. Two antigens recognized by autologous cytolytic T lymphocytes on a melanoma result from a single point mutation in an essential housekeeping gene. Cancer Res 1999;59:5785-92.
61. Cohen CJ, Gartner JJ, Horovitz-Fried M, Shamalov K, Trebska-McGowan K, Bliskovsky VV, Parkhurst MR, Ankri C, Prickett TD, Crystal JS, Li YF, El-Gamil M, Rosenberg SA, Robbins PF. Isolation of neoantigen-specific T cells from tumor and peripheral lymphocytes. J Clin Invest 2015;125:3981-91.
62. Lennerz V, Fatho M, Gentilini C, Frye RA, Lifke A, Ferel D, Wolfel C, Huber C, Wolfel T. The response of autologous T cells to a human melanoma is dominated by mutated neoantigens. Proc Natl Acad Sci USA 2005;102:16013-8.
63. Linnemann C, van Buuren MM, Bies L, Verdegaal EM, Schotte R, Calis JJ, Behjati S, Velds A, Hilkmann H, Atmioui DE, Visser M, Stratton MR, Haanen JB, Spits H, van der Burg SH, Schumacher TN. High-throughput epitope discovery reveals frequent recognition of neo-antigens by CD4+ T cells in human melanoma. Nat Med 2015;21:81-5.
64. Lu YC, Yao X, Crystal JS, Li YF, El-Gamil M, Gross C, Davis L, Dudley ME, Yang JC, Samuels Y, Rosenberg SA, Robbins PF. Efficient identification of mutated cancer antigens recognized by T cells associated with durable tumor regressions. Clin Cancer Res 2014;20:3401-10.
65. Pritchard AL, Burel JG, Neller MA, Hayward NK, Lopez JA, Fatho M, Lennerz V, Wolfel T, Schmidt CW. Exome Sequencing to Predict Neoantigens in Melanoma. Cancer Immunol Res 2015;3:992-8.
66. Robbins PF, Lu YC, El-Gamil M, Li YF, Gross C, Gartner J, Lin JC, Teer JK, Cliften P, Tycksen E, Samuels Y, Rosenberg SA. Mining exomic sequencing data to

identify mutated antigens recognized by adoptively transferred tumor-reactive T cells. Nat Med 2013;19:747-52.
67. Rajasagi M, Shukla SA, Fritsch EF, Keskin DB, DeLuca D, Carmona E, Zhang W, Sougnez C, Cibulskis K, Sidney J, Stevenson K, Ritz J, Neuberg D, Brusic V, Gabriel S, Lander ES, Getz G, Hacohen N, Wu CJ. Systematic identification of personal tumor-specific neoantigens in chronic lymphocytic leukemia. Blood 2014;124:453-62.
68. Mandruzzato S, Brasseur F, Andry G, Boon T, van der Bruggen P. A CASP-8 mutation recognized by cytolytic T lymphocytes on a human head and neck carcinoma. J Exp Med 1997;186:785-93.
69. Wick DA, Webb JR, Nielsen JS, Martin SD, Kroeger DR, Milne K, Castellarin M, Twumasi-Boateng K, Watson PH, Holt RA, Nelson BH. Surveillance of the tumor mutanome by T cells during progression from primary to recurrent ovarian cancer. Clin Cancer Res 2014;20:1125-34.
70. Stolze B, Reinhart S, Bulllinger L, Frohling S, Scholl C. Comparative analysis of KRAS codon 12, 13, 18, 61, and 117 mutations using human MCF10A isogenic cell lines. Sci Rep 2015;5:8535-9.
71. van der Bruggen P, Strooban V, Vigneron N, Van den Eynde B. Peptide database: T cell-defined tumor antigens. Cancer Immun 2013.
72. Vogelstein B, Papadopoulos N, Velculescu VE, Zhou S, Diaz LA, Jr., Kinzler KW. Cancer genome landscapes. Science 2013;339:1546-58.
73. Ng SB, Turner EH, Robertson PD, Flygare SD, Bigham AW, Lee C, Shaffer T, Wong M, Bhattacharjee A, Eichler EE, Bamshad M, Nickerson DA, Shendure J. Targeted capture and massively parallel sequencing of 12 human exomes. Nature 2009;461:272-6.
74. Nik-Zainal S, Davies H, Staaf J, Ramakrishna M, Glodzik D, Zou X, Martincorena I, Alexandrov LB, Martin S, Wedge DC, Van Loo P, Ju YS, Smid M, Brinkman AB, Morganella S, Aure MR, Lingjaerde OC, Langerod A, Ringner M, Ahn SM, Boyault S, Brock JE, Broeks A, Butler A, Desmedt C, Dirix L, Dronov S, Fatima A, Foekens JA, Gerstung M, Hooijer GK, Jang SJ, Jones DR, Kim HY, King TA, Krishnamurthy S, Lee HJ, Lee JY, Li Y, McLaren S, Menzies A, Mustonen V, O'Meara S, Pauporte I, Pivot X, Purdie CA, Raine K, Ramakrishnan K, Rodriguez-Gonzalez FG, Romieu G, Sieuwerts AM, Simpson PT, Shepherd R, Stebbings L, Stefansson OA, Teague J, Tommasi S, Treilleux I, Van den Eynden GG, Vermeulen P, Vincent-Salomon A, Yates L, Caldas C, van't Veer L, Tutt A, Knappskog S, Tan BK, Jonkers J, Borg A, Ueno NT, Sotiriou C, Viari A, Futreal PA, Campbell PJ, Span PN, Van Laere S, Lakhani SR, Eyfjord JE, Thompson AM, Birney E, Stunnenberg HG, van de Vijver MJ, Martens JW, Borresen-Dale AL, Richardson AL, Kong G, Thomas G, Stratton MR. Landscape of somatic mutations in 560 breast cancer whole-genome sequences. Nature 2016;534:47-54.

75. Alexandrov LB, Nik-Zainal S, Wedge DC, Aparicio SA, Behjati S, Biankin AV, Bignell GR, Bolli N, Borg A, Borresen-Dale AL, Boyault S, Burkhardt B, Butler AP, Caldas C, Davies HR, Desmedt C, Eils R, Eyfjord JE, Foekens JA, Greaves M, Hosoda F, Hutter B, Ilicic T, Imbeaud S, Imielinski M, Jager N, Jones DT, Jones D, Knappskog S, Kool M, Lakhani SR, Lopez-Otin C, Martin S, Munshi NC, Nakamura H, Northcott PA, Pajic M, Papaemmanuil E, Paradiso A, Pearson JV, Puente XS, Raine K, Ramakrishna M, Richardson AL, Richter J, Rosenstiel P, Schlesner M, Schumacher TN, Span PN, Teague JW, Totoki Y, Tutt AN, Valdes-Mas R, van Buuren MM, van 't Veer L, Vincent-Salomon A, Waddell N, Yates LR, Australian Pancreatic Cancer Genome I, Consortium IBC, Consortium IM-S, PedBrain I, Zucman-Rossi J, Futreal PA, McDermott U, Lichter P, Meyerson M, Grimmond SM, Siebert R, Campo E, Shibata T, Pfister SM, Campbell PJ, Stratton MR. Signatures of mutational processes in human cancer. Nature 2013;500:415-21.
76. Helleday T, Eshtad S, Nik-Zainal S. Mechanisms underlying mutational signatures in human cancers. Nat Rev Genet 2014;15:585-98.
77. Foulkes WD. Inherited susceptibility to common cancers. N Engl J Med 2008;359:2143-53.
78. Shah SP, Roth A, Goya R, Oloumi A, Ha G, Zhao Y, Turashvili G, Ding J, Tse K, Haffari G, Bashashati A, Prentice LM, Khattra J, Burleigh A, Yap D, Bernard V, McPherson A, Shumansky K, Crisan A, Giuliany R, Heravi-Moussavi A, Rosner J, Lai D, Birol I, Varhol R, Tam A, Dhalla N, Zeng T, Ma K, Chan SK, Griffith M, Moradian A, Cheng SW, Morin GB, Watson P, Gelmon K, Chia S, Chin SF, Curtis C, Rueda OM, Pharoah PD, Damaraju S, Mackey J, Hoon K, Harkins T, Tadigotla V, Sigaroudinia M, Gascard P, Tlsty T, Costello JF, Meyer IM, Eaves CJ, Wasserman WW, Jones S, Huntsman D, Hirst M, Caldas C, Marra MA, Aparicio S. The clonal and mutational evolution spectrum of primary triple-negative breast cancers. Nature 2012;486:395-9.
79. Van Der Bruggen P, Zhang Y, Chaux P, Stroobant V, Panichelli C, Schultz ES, Chapiro J, Van Den Eynde BJ, Brasseur F, Boon T. Tumor-specific shared antigenic peptides recognized by human T cells. Immunol Rev 2002;188:51-64.
80. Ayyoub M, Scarlata CM, Hamai A, Pignon P, Valmori D. Expression of MAGE-A3/6 in primary breast cancer is associated with hormone receptor negative status, high histologic grade, and poor survival. J Immunother 2014;37:73-6.
81. Putti TC, El-Rehim DM, Rakha EA, Paish CE, Lee AH, Pinder SE, Ellis IO. Estrogen receptor-negative breast carcinomas: a review of morphology and immunophenotypical analysis. Mod Pathol 2005;18:26-35.
82. Wang RF, Johnston SL, Zeng G, Topalian SL, Schwartzentruber DJ, Rosenberg SA. A breast and melanoma-shared tumor antigen: T cell responses to

antigenic peptides translated from different open reading frames. J Immunol 1998;161:3598-606.
83. Fisk B, Blevins TL, Wharton JT, Ioannides CG. Identification of an immunodominant peptide of HER-2/neu protooncogene recognized by ovarian tumor-specific cytotoxic T lymphocyte lines. J Exp Med 1995;181:2109-17.
84. Zaks TZ, Rosenberg SA. Immunization with a peptide epitope (p369-377) from HER-2/neu leads to peptide-specific cytotoxic T lymphocytes that fail to recognize HER-2/neu+ tumors. Cancer Res 1998;58:4902-8.
85. Mittendorf EA, Holmes JP, Ponniah S, Peoples GE. The E75 HER2/neu peptide vaccine. Cancer Immunol Immunother 2008;57:1511-21.
86. Mittendorf EA, Clifton GT, Holmes JP, Schneble E, van Echo D, Ponniah S, Peoples GE. Final report of the phase I/II clinical trial of the E75 (nelipepimut-S) vaccine with booster inoculations to prevent disease recurrence in high-risk breast cancer patients. Ann Oncol 2014;25:1735-42.
87. Benavides LC, Gates JD, Carmichael MG, Patil R, Holmes JP, Hueman MT, Mittendorf EA, Craig D, Stojadinovic A, Ponniah S, Peoples GE. The impact of HER2/neu expression level on response to the E75 vaccine: from U.S. Military Cancer Institute Clinical Trials Group Study I-01 and I-02. Clin Cancer Res 2009;15:2895-904.
88. Morgan RA, Yang JC, Kitano M, Dudley ME, Laurencot CM, Rosenberg SA. Case report of a serious adverse event following the administration of T cells transduced with a chimeric antigen receptor recognizing ERBB2. Mol Ther 2010;18:843-51.
89. Jager D, Karbach J, Pauligk C, Seil I, Frei C, Chen YT, Old LJ, Knuth A, Jager E. Humoral and cellular immune responses against the breast cancer antigen NY-BR-1: definition of two HLA-A2 restricted peptide epitopes. Cancer Immun 2005;5:11.
90. Wang W, Epler J, Salazar LG, Riddell SR. Recognition of breast cancer cells by CD8+ cytotoxic T-cell clones specific for NY-BR-1. Cancer Res 2006;66:6826-33.
91. Brossart P, Heinrich KS, Stuhler G, Behnke L, Reichardt VL, Stevanovic S, Muhm A, Rammensee HG, Kanz L, Brugger W. Identification of HLA-A2-restricted T-cell epitopes derived from the MUC1 tumor antigen for broadly applicable vaccine therapies. Blood 1999;93:4309-17.
92. Vonderheide RH, Hahn WC, Schultze JL, Nadler LM. The telomerase catalytic subunit is a widely expressed tumor-associated antigen recognized by cytotoxic T lymphocytes. Immunity 1999;10:673-9.
93. Schwartzentruber DJ, Solomon D, Rosenberg SA, Topalian SL. Characterization of lymphocytes infiltrating human breast cancer: specific

immune reactivity detected by measuring cytokine secretion. J Immunother 1992;12:1-12.
94. Schwartzentruber DJ, Topalian SL, Mancini M, Rosenberg SA. Specific release of granulocyte-macrophage colony-stimulating factor, tumor necrosis factor-alpha, and IFN-gamma by human tumor-infiltrating lymphocytes after autologous tumor stimulation. J Immunol 1991;146:3674-81.
95. Dadmarz R, Sgagias MK, Rosenberg SA, Schwartzentruber DJ. CD4+ T lymphocytes infiltrating human breast cancer recognise autologous tumor in an MHC-class-II restricted fashion. Cancer Immunol Immunother 1995;40:1-9.
96. Baxevanis CN, Dedoussis GV, Papadopoulos NG, Missitzis I, Stathopoulos GP, Papamichail M. Tumor specific cytolysis by tumor infiltrating lymphocytes in breast cancer. Cancer 1994;74:1275-82.
97. Vonderheide RH, LoRusso PM, Khalil M, Gartner EM, Khaira D, Soulieres D, Dorazio P, Trosko JA, Ruter J, Mariani GL, Usari T, Domchek SM. Tremelimumab in combination with exemestane in patients with advanced breast cancer and treatment-associated modulation of inducible costimulator expression on patient T cells. Clin Cancer Res 2010;16:3485-94.
98. Dirix L, Takacs I, Nikolinakos P, Jerusalem G, Arkenau H-T, Hamilton E, von Heydebreck A, Grote H-J, Chin K, Lippman M. Abstract S1-04: Avelumab (MSB0010718C), an anti-PD-L1 antibody, in patients with locally advanced or metastatic breast cancer: A phase Ib JAVELIN solid tumor trial. Cancer Research 2016;76:S1-04.
99. Avelumab Effective in PD-L1-Positive Metastatic Breast Cancer. OncLive, 2015. at http://global.onclive.com/conference-coverage/sabcs-2015/avelumab-effective-in-pd-l1-positive-metastatic-breast-cancer.)
100. Emens LA, Braiteh FS, Cassier P, DeLord J-P, Eder JP, Fasso M, Xiao Y, Wang Y, Molinero L, Chen DS, Krop I. Abstract 6317: Inhibition of PD-L1 by MPDL3280A leads to clinical activity in patients with metastatic triple-negative breast cancer (TNBC). Presented at 2015 AACR Annual Meeting.
101. Nanda R, Chow LQ, Dees EC, Berger R, Gupta S, Geva R, Pusztai L, Pathiraja K, Aktan G, Cheng JD, Karantza V, Buisseret L. Pembrolizumab in Patients With Advanced Triple-Negative Breast Cancer: Phase Ib KEYNOTE-012 Study. J Clin Oncol 2016.
102. Anti-PD-L1 Agent MPDL3280A Shows Durable Responses in TNBC. 2015. at http://global.onclive.com/conference-coverage/aacr-2015/anti-pd-l1-agent-mpdl3280a-shows-durable-responses-in-tnbc.)
103. Eisenhauer EA, Therasse P, Bogaerts J, Schwartz LH, Sargent D, Ford R, Dancey J, Arbuck S, Gwyther S, Mooney M, Rubinstein L, Shankar L, Dodd L, Kaplan R, Lacombe D, Verweij J. New response evaluation criteria in solid tumours: revised RECIST guideline (version 1.1). Eur J Cancer 2009;45:228-47.

104. Rugo H, Delord J-P, Im S-A, Ott P, Piha-Paul S, Bedard P, Sachdev J, Le Tourneau C, van Brummelen E, Varga A, Saraf S, Pietrangelo D, Karantza V, Tan A. Abstract S5-07: Preliminary efficacy and safety of pembrolizumab (MK-3475) in patients with PD-L1–positive, estrogen receptor-positive (ER+)/HER2-negative advanced breast cancer enrolled in KEYNOTE-028. Cancer Research 2016;76:S5-07.
105. Immunotherapy for Breast Cancer: Early Lackluster Study Results yet Promise Remains. 2016. at http://www.ascopost.com/issues/january-25-2016/immunotherapy-for-breast-cancer-early-lackluster-study-results-yet-promise-remains/.)
106. Arstila TP, Casrouge A, Baron V, Even J, Kanellopoulos J, Kourilsky P. A direct estimate of the human alphabeta T cell receptor diversity. Science 1999;286:958-61.
107. Cibulskis K, Lawrence MS, Carter SL, Sivachenko A, Jaffe D, Sougnez C, Gabriel S, Meyerson M, Lander ES, Getz G. Sensitive detection of somatic point mutations in impure and heterogeneous cancer samples. Nat Biotechnol 2013;31:213-9.
108. Koboldt DC, Zhang Q, Larson DE, Shen D, McLellan MD, Lin L, Miller CA, Mardis ER, Ding L, Wilson RK. VarScan 2: somatic mutation and copy number alteration discovery in cancer by exome sequencing. Genome Res 2012;22:568-76.
109. Cingolani P, Platts A, Wang le L, Coon M, Nguyen T, Wang L, Land SJ, Lu X, Ruden DM. A program for annotating and predicting the effects of single nucleotide polymorphisms, SnpEff: SNPs in the genome of Drosophila melanogaster strain w1118; iso-2; iso-3. Fly (Austin) 2012;6:80-92.
110. Robinson JT, Thorvaldsdottir H, Winckler W, Guttman M, Lander ES, Getz G, Mesirov JP. Integrative genomics viewer. Nat Biotechnol 2011;29:24-6.
111. Thorvaldsdottir H, Robinson JT, Mesirov JP. Integrative Genomics Viewer (IGV): high-performance genomics data visualization and exploration. Brief Bioinform 2013;14:178-92.
112. Avanzi GC, Brizzi MF, Giannotti J, Ciarletta A, Yang YC, Pegoraro L, Clark SC. M-07e human leukemic factor-dependent cell line provides a rapid and sensitive bioassay for the human cytokines GM-CSF and IL-3. J Cell Physiol 1990;145:458-64.
113. Renauld JC, Van Snick J. Measurement of mouse and human interleukin 9. Curr Protoc Immunol 2002;Chapter 6:Unit 6.13.1-6..0.
114. Lundegaard C, Lamberth K, Harndahl M, Buus S, Lund O, Nielsen M. NetMHC-3.0: accurate web accessible predictions of human, mouse and monkey MHC class I affinities for peptides of length 8-11. Nucleic Acids Res 2008;36:W509-12.

115. Lundegaard C, Lund O, Nielsen M. Accurate approximation method for prediction of class I MHC affinities for peptides of length 8, 10 and 11 using prediction tools trained on 9mers. Bioinformatics 2008;24:1397-8.
116. Nielsen M, Lundegaard C, Worning P, Lauemoller SL, Lamberth K, Buus S, Brunak S, Lund O. Reliable prediction of T-cell epitopes using neural networks with novel sequence representations. Protein Sci 2003;12:1007-17.
117. Gonzalez-Galarza FF, Takeshita LY, Santos EJ, Kempson F, Maia MH, da Silva AL, Teles e Silva AL, Ghattaoraya GS, Alfirevic A, Jones AR, Middleton D. Allele frequency net 2015 update: new features for HLA epitopes, KIR and disease and HLA adverse drug reaction associations. Nucleic Acids Res 2015;43:D784-8.
118. Vita R, Overton JA, Greenbaum JA, Ponomarenko J, Clark JD, Cantrell JR, Wheeler DK, Gabbard JL, Hix D, Sette A, Peters B. The immune epitope database (IEDB) 3.0. Nucleic Acids Res 2015;43:D405-D12.
119. UniProt C. UniProt: a hub for protein information. Nucleic Acids Res 2015;43:D204-D12.
120. Uhlen M, Fagerberg L, Hallstrom BM, Lindskog C, Oksvold P, Mardinoglu A, Sivertsson A, Kampf C, Sjostedt E, Asplund A, Olsson I, Edlund K, Lundberg E, Navani S, Szigyarto CA, Odeberg J, Djureinovic D, Takanen JO, Hober S, Alm T, Edqvist PH, Berling H, Tegel H, Mulder J, Rockberg J, Nilsson P, Schwenk JM, Hamsten M, von Feilitzen K, Forsberg M, Persson L, Johansson F, Zwahlen M, von Heijne G, Nielsen J, Ponten F. Proteomics. Tissue-based map of the human proteome. Science 2015;347:1260419-1--9.
121. Monteith GR, McAndrew D, Faddy HM, Roberts-Thomson SJ. Calcium and cancer: targeting Ca2+ transport. Nat Rev Cancer 2007;7:519-30.
122. Lee WJ, Robinson JA, Holman NA, McCall MN, Roberts-Thomson SJ, Monteith GR. Antisense-mediated Inhibition of the plasma membrane calcium-ATPase suppresses proliferation of MCF-7 cells. J Biol Chem 2005;280:27076-84.
123. Wang L, Li W, Yang Y, Hu Y, Gu Y, Shu Y, Sun Y, Wu X, Shen Y, Xu Q. High expression of sarcoplasmic/endoplasmic reticulum Ca(2+)-ATPase 2b blocks cell differentiation in human liposarcoma cells. Life Sci 2014;99:37-43.
124. Heyne K, Forster J, Schule R, Roemer K. Transcriptional repressor NIR interacts with the p53-inhibiting ubiquitin ligase MDM2. Nucleic Acids Res 2014;42:3565-79.
125. Hublitz P, Kunowska N, Mayer UP, Muller JM, Heyne K, Yin N, Fritzsche C, Poli C, Miguet L, Schupp IW, van Grunsven LA, Potiers N, van Dorsselaer A, Metzger E, Roemer K, Schule R. NIR is a novel INHAT repressor that modulates the transcriptional activity of p53. Genes Dev 2005;19:2912-24.
126. Xu IM, Lai RK, Lin SH, Tse AP, Chiu DK, Koh HY, Law CT, Wong CM, Cai Z, Wong CC, Ng IO. Transketolase counteracts oxidative stress to drive cancer development. Proc Natl Acad Sci U S A 2016;113:E725-E34.

127. Forbes SA, Beare D, Gunasekaran P, Leung K, Bindal N, Boutselakis H, Ding M, Bamford S, Cole C, Ward S, Kok CY, Jia M, De T, Teague JW, Stratton MR, McDermott U, Campbell PJ. COSMIC: exploring the world's knowledge of somatic mutations in human cancer. Nucleic Acids Res 2015;43:D805-D11.
128. Lawrence MS, Stojanov P, Mermel CH, Robinson JT, Garraway LA, Golub TR, Meyerson M, Gabriel SB, Lander ES, Getz G. Discovery and saturation analysis of cancer genes across 21 tumour types. Nature 2014;505:495-501.
129. Helaers R, Vikkula M. Highlander: variant filtering made easy. 2016:In preparation.
130. Dudley JC, Lin MT, Le DT, Eshleman JR. Microsatellite Instability as a Biomarker for PD-1 Blockade. Clin Cancer Res 2016;22:813-20.
131. Kloor M, von Knebel Doeberitz M. The immune biology of microsatellite-unstable cancer. TRENDS in CANCER 2016;2:121-33.
132. Boland CR, Goel A. Microsatellite instability in colorectal cancer. Gastroenterology 2010;138:2073-87 e3.
133. Vigneron N, Van den Eynde BJ. Proteasome subtypes and regulators in the processing of antigenic peptides presented by class I molecules of the major histocompatibility complex. Biomolecules 2014;4:994-1025.
134. Rammensee HG, Singh-Jasuja H. HLA ligandome tumor antigen discovery for personalized vaccine approach. Expert Rev Vaccines 2013;12:1211-7.
135. Yadav M, Jhunjhunwala S, Phung QT, Lupardus P, Tanguay J, Bumbaca S, Franci C, Cheung TK, Fritsche J, Weinschenk T, Modrusan Z, Mellman I, Lill JR, Delamarre L. Predicting immunogenic tumour mutations by combining mass spectrometry and exome sequencing. Nature 2014;515:572-6.
136. Triebel F, Jitsukawa S, Baixeras E, Roman-Roman S, Genevee C, Viegas-Pequignot E, Hercend T. LAG-3, a novel lymphocyte activation gene closely related to CD4. J Exp Med 1990;171:1393-405.
137. Hastings WD, Anderson DE, Kassam N, Koguchi K, Greenfield EA, Kent SC, Zheng XX, Strom TB, Hafler DA, Kuchroo VK. TIM-3 is expressed on activated human CD4+ T cells and regulates Th1 and Th17 cytokines. Eur J Immunol 2009;39:2492-501.
138. Workman CJ, Rice DS, Dugger KJ, Kurschner C, Vignali DA. Phenotypic analysis of the murine CD4-related glycoprotein, CD223 (LAG-3). Eur J Immunol 2002;32:2255-63.
139. Anderson AC, Joller N, Kuchroo VK. Lag-3, Tim-3, and TIGIT: Co-inhibitory Receptors with Specialized Functions in Immune Regulation. Immunity 2016;44:989-1004.
140. Delves PJ, Martin SJ, Burton DR, Roitt IM. Roitt's essential immunology. 12th ed. Chichester, West Sussex ; Hoboken, NJ: Wiley-Blackwell; 2011.
141. Platten M, Wick W, Van den Eynde BJ. Tryptophan catabolism in cancer: beyond IDO and tryptophan depletion. Cancer Res 2012;72:5435-40.

142. Llosa NJ, Cruise M, Tam A, Wicks EC, Hechenbleikner EM, Taube JM, Blosser RL, Fan H, Wang H, Luber BS, Zhang M, Papadopoulos N, Kinzler KW, Vogelstein B, Sears CL, Anders RA, Pardoll DM, Housseau F. The vigorous immune microenvironment of microsatellite instable colon cancer is balanced by multiple counter-inhibitory checkpoints. Cancer Discov 2015;5:43-51.
143. Zaretsky JM, Garcia-Diaz A, Shin DS, Escuin-Ordinas H, Hugo W, Hu-Lieskovan S, Torrejon DY, Abril-Rodriguez G, Sandoval S, Barthly L, Saco J, Homet Moreno B, Mezzadra R, Chmielowski B, Ruchalski K, Shintaku IP, Sanchez PJ, Puig-Saus C, Cherry G, Seja E, Kong X, Pang J, Berent-Maoz B, Comin-Anduix B, Graeber TG, Tumeh PC, Schumacher TN, Lo RS, Ribas A. Mutations Associated with Acquired Resistance to PD-1 Blockade in Melanoma. N Engl J Med 2016.
144. Ward SM, Jonsson JR, Sierro S, Clouston AD, Lucas M, Vargas AL, Powell EE, Klenerman P. Virus-specific CD8+ T lymphocytes within the normal human liver. Eur J Immunol 2004;34:1526-31.
145. Woo SR, Turnis ME, Goldberg MV, Bankoti J, Selby M, Nirschl CJ, Bettini ML, Gravano DM, Vogel P, Liu CL, Tangsombatvisit S, Grosso JF, Netto G, Smeltzer MP, Chaux A, Utz PJ, Workman CJ, Pardoll DM, Korman AJ, Drake CG, Vignali DA. Immune inhibitory molecules LAG-3 and PD-1 synergistically regulate T-cell function to promote tumoral immune escape. Cancer Res 2012;72:917-27.
146. Spranger S, Koblish HK, Horton B, Scherle PA, Newton R, Gajewski TF. Mechanism of tumor rejection with doublets of CTLA-4, PD-1/PD-L1, or IDO blockade involves restored IL-2 production and proliferation of CD8(+) T cells directly within the tumor microenvironment. J Immunother Cancer 2014;2:3.
147. Gangadhar TC, Hamid O, Smith DC, Bauer TM, Wasser JS, Luke JJ, Balmanoukian AS, Kaufman DR, Zhao Y, Maleski J, Leopold L, Gajewski TF. Preliminary results from a Phase I/II study of epacadostat (incb024360) in combination with pembrolizumab in patients with selected advanced cancers. Journal for Immunotherapy of Cancer 2015;3:O7-O.
148. Rizvi NA, Hellmann MD, Snyder A, Kvistborg P, Makarov V, Havel JJ, Lee W, Yuan J, Wong P, Ho TS, Miller ML, Rekhtman N, Moreira AL, Ibrahim F, Bruggeman C, Gasmi B, Zappasodi R, Maeda Y, Sander C, Garon EB, Merghoub T, Wolchok JD, Schumacher TN, Chan TA. Cancer immunology. Mutational landscape determines sensitivity to PD-1 blockade in non-small cell lung cancer. Science 2015;348:124-8.
149. Hugo W, Zaretsky JM, Sun L, Song C, Moreno BH, Hu-Lieskovan S, Berent-Maoz B, Pang J, Chmielowski B, Cherry G, Seja E, Lomeli S, Kong X, Kelley MC, Sosman JA, Johnson DB, Ribas A, Lo RS. Genomic and Transcriptomic Features

of Response to Anti-PD-1 Therapy in Metastatic Melanoma. Cell 2016;165:35-44.
150. Mehnert JM, Panda A, Zhong H, Hirshfield K, Damare S, Lane K, Sokol L, Stein MN, Rodriguez-Rodriquez L, Kaufman HL, Ali S, Ross JS, Pavlick DC, Bhanot G, White EP, DiPaola RS, Lovell A, Cheng J, Ganesan S. Immune activation and response to pembrolizumab in POLE-mutant endometrial cancer. J Clin Invest 2016;126:2334-40.
151. Cowell CF, Weigelt B, Sakr RA, Ng CK, Hicks J, King TA, Reis-Filho JS. Progression from ductal carcinoma in situ to invasive breast cancer: revisited. Mol Oncol 2013;7:859-69.
152. Leonard GD, Swain SM. Ductal carcinoma in situ, complexities and challenges. J Natl Cancer Inst 2004;96:906-20.
153. Abba MC, Gong T, Lu Y, Lee J, Zhong Y, Lacunza E, Butti M, Takata Y, Gaddis S, Shen J, Estecio MR, Sahin AA, Aldaz CM. A Molecular Portrait of High-Grade Ductal Carcinoma In Situ. Cancer Res 2015;75:3980-90.
154. Thompson E, Taube JM, Elwood H, Sharma R, Meeker A, Warzecha HN, Argani P, Cimino-Mathews A, Emens LA. The immune microenvironment of breast ductal carcinoma in situ. Mod Pathol 2016;29:249-58.
155. Hernandez L, Wilkerson PM, Lambros MB, Campion-Flora A, Rodrigues DN, Gauthier A, Cabral C, Pawar V, Mackay A, A'Hern R, Marchio C, Palacios J, Natrajan R, Weigelt B, Reis-Filho JS. Genomic and mutational profiling of ductal carcinomas in situ and matched adjacent invasive breast cancers reveals intra-tumour genetic heterogeneity and clonal selection. J Pathol 2012;227:42-52.
156. Kim SY, Jung SH, Kim MS, Baek IP, Lee SH, Kim TM, Chung YJ, Lee SH. Genomic differences between pure ductal carcinoma in situ and synchronous ductal carcinoma in situ with invasive breast cancer. Oncotarget 2015;6:7597-607.
157. Sentman CL, Meehan KR. NKG2D CARs as cell therapy for cancer. Cancer J 2014;20:156-9.
158. Bassani-Sternberg M, Coukos G. Mass spectrometry-based antigen discovery for cancer immunotherapy. Curr Opin Immunol 2016;41:9-17.
159. Larkin J, Chiarion-Sileni V, Gonzalez R, Grob JJ, Cowey CL, Lao CD, Schadendorf D, Dummer R, Smylie M, Rutkowski P, Ferrucci PF, Hill A, Wagstaff J, Carlino MS, Haanen JB, Maio M, Marquez-Rodas I, McArthur GA, Ascierto PA, Long GV, Callahan MK, Postow MA, Grossmann K, Sznol M, Dreno B, Bastholt L, Yang A, Rollin LM, Horak C, Hodi FS, Wolchok JD. Combined Nivolumab and Ipilimumab or Monotherapy in Untreated Melanoma. N Engl J Med 2015;373:23-34.
160. Tran E, Turcotte S, Gros A, Robbins PF, Lu YC, Dudley ME, Wunderlich JR, Somerville RP, Hogan K, Hinrichs CS, Parkhurst MR, Yang JC, Rosenberg SA.

Cancer immunotherapy based on mutation-specific CD4+ T cells in a patient with epithelial cancer. Science 2014;344:641-5.
161. Rosenberg SA, Yang JC, Sherry RM, Kammula US, Hughes MS, Phan GQ, Citrin DE, Restifo NP, Robbins PF, Wunderlich JR, Morton KE, Laurencot CM, Steinberg SM, White DE, Dudley ME. Durable complete responses in heavily pretreated patients with metastatic melanoma using T-cell transfer immunotherapy. Clin Cancer Res 2011;17:4550-7.
162. Romero P, Banchereau J, Bhardwaj N, Cockett M, Disis ML, Dranoff G, Gilboa E, Hammond SA, Hershberg R, Korman AJ, Kvistborg P, Melief C, Mellman I, Palucka AK, Redchenko I, Robins H, Sallusto F, Schenkelberg T, Schoenberger S, Sosman J, Tureci O, Van den Eynde B, Koff W, Coukos G. The Human Vaccines Project: A roadmap for cancer vaccine development. Sci Transl Med 2016;8:334ps9.
163. Carreno BM, Magrini V, Becker-Hapak M, Kaabinejadian S, Hundal J, Petti AA, Ly A, Lie WR, Hildebrand WH, Mardis ER, Linette GP. Cancer immunotherapy. A dendritic cell vaccine increases the breadth and diversity of melanoma neoantigen-specific T cells. Science 2015;348:803-608.
164. Overwijk WW, Wang E, Marincola FM, Rammensee HG, Restifo NP. Mining the mutanome: developing highly personalized Immunotherapies based on mutational analysis of tumors. J Immunother Cancer 2013;1:11.
165. Wilgenhof S, Corthals J, Heirman C, van Baren N, Lucas S, Kvistborg P, Thielemans K, Neyns B. Phase II Study of Autologous Monocyte-Derived mRNA Electroporated Dendritic Cells (TriMixDC-MEL) Plus Ipilimumab in Patients With Pretreated Advanced Melanoma. J Clin Oncol 2016;34:1330-8.
166. Dauber B, Wolff T. Activation of the Antiviral Kinase PKR and Viral Countermeasures. Viruses 2009;1:523-44.
167. Liu BL, Robinson M, Han ZQ, Branston RH, English C, Reay P, McGrath Y, Thomas SK, Thornton M, Bullock P, Love CA, Coffin RS. ICP34.5 deleted herpes simplex virus with enhanced oncolytic, immune stimulating, and anti-tumour properties. Gene Ther 2003;10:292-303.
168. Kohlhapp FJ, Kaufman HL. Molecular Pathways: Mechanism of Action for Talimogene Laherparepvec, a New Oncolytic Virus Immunotherapy. Clin Cancer Res 2016;22:1048-54.
169. Hill A, Jugovic P, York I, Russ G, Bennink J, Yewdell J, Ploegh H, Johnson D. Herpes simplex virus turns off the TAP to evade host immunity. Nature 1995;375:411-5.
170. Andtbacka RH, Kaufman HL, Collichio F, Amatruda T, Senzer N, Chesney J, Delman KA, Spitler LE, Puzanov I, Agarwala SS, Milhem M, Cranmer L, Curti B, Lewis K, Ross M, Guthrie T, Linette GP, Daniels GA, Harrington K, Middleton MR, Miller WH, Jr., Zager JS, Ye Y, Yao B, Li A, Doleman S, VanderWalde A,

Gansert J, Coffin RS. Talimogene Laherparepvec Improves Durable Response Rate in Patients With Advanced Melanoma. J Clin Oncol 2015;33:2780-8.
171. Rosenberg SA, Restifo NP. Adoptive cell transfer as personalized immunotherapy for human cancer. Science 2015;348:62-8.
172. Robbins PF, Morgan RA, Feldman SA, Yang JC, Sherry RM, Dudley ME, Wunderlich JR, Nahvi AV, Helman LJ, Mackall CL, Kammula US, Hughes MS, Restifo NP, Raffeld M, Lee CC, Levy CL, Li YF, El-Gamil M, Schwarz SL, Laurencot C, Rosenberg SA. Tumor regression in patients with metastatic synovial cell sarcoma and melanoma using genetically engineered lymphocytes reactive with NY-ESO-1. J Clin Oncol 2011;29:917-24.
173. Cameron BJ, Gerry AB, Dukes J, Harper JV, Kannan V, Bianchi FC, Grand F, Brewer JE, Gupta M, Plesa G, Bossi G, Vuidepot A, Powlesland AS, Legg A, Adams KJ, Bennett AD, Pumphrey NJ, Williams DD, Binder-Scholl G, Kulikovskaya I, Levine BL, Riley JL, Varela-Rohena A, Stadtmauer EA, Rapoport AP, Linette GP, June CH, Hassan NJ, Kalos M, Jakobsen BK. Identification of a Titin-derived HLA-A1-presented peptide as a cross-reactive target for engineered MAGE A3-directed T cells. Sci Transl Med 2013;5:197ra03.
174. Stronen E, Toebes M, Kelderman S, van Buuren MM, Yang W, van Rooij N, Donia M, Boschen ML, Lund-Johansen F, Olweus J, Schumacher TN. Targeting of cancer neoantigens with donor-derived T cell receptor repertoires. Science 2016;352:1337-41.
175. Jackson HJ, Rafiq S, Brentjens RJ. Driving CAR T-cells forward. Nat Rev Clin Oncol 2016;13:370-83.
176. Park JH, Geyer MB, Brentjens RJ. CD19-targeted CAR T-cell therapeutics for hematologic malignancies: interpreting clinical outcomes to date. Blood 2016;127:3312-20.
177. Warren RL, Freeman JD, Zeng T, Choe G, Munro S, Moore R, Webb JR, Holt RA. Exhaustive T-cell repertoire sequencing of human peripheral blood samples reveals signatures of antigen selection and a directly measured repertoire size of at least 1 million clonotypes. Genome Res 2011;21:790-7.
178. Brochet X, Lefranc MP, Giudicelli V. IMGT/V-QUEST: the highly customized and integrated system for IG and TR standardized V-J and V-D-J sequence analysis. Nucleic Acids Res 2008;36:W503-W8.
179. Yates A, Akanni W, Amode MR, Barrell D, Billis K, Carvalho-Silva D, Cummins C, Clapham P, Fitzgerald S, Gil L, Giron CG, Gordon L, Hourlier T, Hunt SE, Janacek SH, Johnson N, Juettemann T, Keenan S, Lavidas I, Martin FJ, Maurel T, McLaren W, Murphy DN, Nag R, Nuhn M, Parker A, Patricio M, Pignatelli M, Rahtz M, Riat HS, Sheppard D, Taylor K, Thormann A, Vullo A, Wilder SP, Zadissa A, Birney E, Harrow J, Muffato M, Perry E, Ruffier M, Spudich G, Trevanion SJ, Cunningham F, Aken BL, Zerbino DR, Flicek P. Ensembl 2016. Nucleic Acids Res 2016;44:D710-6.

180. Li H, Durbin R. Fast and accurate short read alignment with Burrows-Wheeler transform. Bioinformatics 2009;25:1754-60.
181. McKenna A, Hanna M, Banks E, Sivachenko A, Cibulskis K, Kernytsky A, Garimella K, Altshuler D, Gabriel S, Daly M, DePristo MA. The Genome Analysis Toolkit: a MapReduce framework for analyzing next-generation DNA sequencing data. Genome Res 2010;20:1297-303.
182. Langmead B, Salzberg SL. Fast gapped-read alignment with Bowtie 2. Nat Methods 2012;9:357-9.
183. Kim D, Pertea G, Trapnell C, Pimentel H, Kelley R, Salzberg SL. TopHat2: accurate alignment of transcriptomes in the presence of insertions, deletions and gene fusions. Genome Biol 2013;14:R36.
184. Trapnell C, Williams BA, Pertea G, Mortazavi A, Kwan G, van Baren MJ, Salzberg SL, Wold BJ, Pachter L. Transcript assembly and quantification by RNA-Seq reveals unannotated transcripts and isoform switching during cell differentiation. Nat Biotechnol 2010;28:511-5.
185. Li H, Handsaker B, Wysoker A, Fennell T, Ruan J, Homer N, Marth G, Abecasis G, Durbin R, Genome Project Data Processing S. The Sequence Alignment/Map format and SAMtools. Bioinformatics 2009;25:2078-9.
186. Li YM, Pan Y, Wei Y, Cheng X, Zhou BP, Tan M, Zhou X, Xia W, Hortobagyi GN, Yu D, Hung MC. Upregulation of CXCR4 is essential for HER2-mediated tumor metastasis. Cancer Cell 2004;6:459-69.
187. Liu C, Yang X, Duffy B, Mohanakumar T, Mitra RD, Zody MC, Pfeifer JD. ATHLATES: accurate typing of human leukocyte antigen through exome sequencing. Nucleic Acids Res 2013;41:e142.